UNCLASSIFIED

SECURITY CLASSIFICATION OF THIS PAGE (When Data Entered)

REPORT DOCUMENTATION PAGE		READ INSTRUCTIONS BEFORE COMPLETING FORM
1. REPORT NUMBER NAVENVPREDRSCHFAC Contractor Report CR 80-05	2. GOVT ACCESSION NO.	3. RECIPIENT'S CATALOG NUMBER
4. TITLE (and Subtitle) Satellite Wind-Profile Techniques		5. TYPE OF REPORT & PERIOD COVERED Final
		6. PERFORMING ORG. REPORT NUMBER SRI Project 8979
7. AUTHOR(s) Robert L. Mancuso and Roy M. Endlich		8. CONTRACT OR GRANT NUMBER(s) N00228-79-C-K890
9. PERFORMING ORGANIZATION NAME AND ADDRESS SRI International 333 Ravenswood Avenue Menlo Park, CA 94025		10. PROGRAM ELEMENT, PROJECT, TASK AREA & WORK UNIT NUMBERS PE 62759N PN 9F52551792 NEPRF WU 6.2-12
11. CONTROLLING OFFICE NAME AND ADDRESS Naval Air Systems Command Department of the Navy Washington, DC 20361		12. REPORT DATE December 1980
		13. NUMBER OF PAGES 70
14. MONITORING AGENCY NAME & ADDRESS(if different from Controlling Office) Naval Environmental Prediction Research Facility Monterey, CA 93940		15. SECURITY CLASS. (of this report) UNCLASSIFIED
		15a. DECLASSIFICATION/DOWNGRADING SCHEDULE

16. DISTRIBUTION STATEMENT (of this Report)

Approved for public release; distribution unlimited.

17. DISTRIBUTION STATEMENT (of the abstract entered in Block 20, if different from Report)

18. SUPPLEMENTARY NOTES

Performing organization report dated October 1980.

19. KEY WORDS (Continue on reverse side if necessary and identify by block number)

Wind profiles
Satellite data
Cloud motions
Temperature profiles

20. ABSTRACT (Continue on reverse side if necessary and identify by block number)

Satellite data that are currently available in numerical form for operational use include temperature profiles and cloud-motion measurements. In this study, several different techniques were tested for possible use in deriving wind profiles from these data. The eventual application of the wind profiles would be in objective analysis and numerical weather prediction. The techniques were tested using research data sets prepared by the National Environmental Satellite Service (NESS) at the University of Wisconsin. (Cont.)

DD FORM 1 JAN 73 1473 EDITION OF 1 NOV 65 IS OBSOLETE
S/N 0102-014-6601 |

UNCLASSIFIED

SECURITY CLASSIFICATION OF THIS PAGE (When Data Entered)

Block 20, Abstract, Continued

The satellite data consist of high-resolution TIROS-N temperature profiles and and GOES cloud-motion measurements. The evaluation of the techniques was based on comparisons with radiosonde observations over the United States.

Two of the techniques tested were found to give promising results: one, a technique based on the use of thermal winds to extrapolate wind values upward and downward from the cloud-motion level, and the other a technique based on eigenvector calculations. These two techniques, or similar ones, should be of current operational value over oceanic areas devoid of conventional data, provided that reliable height values for cloud motions and reasonably accurate estimates of surface winds can be provided.

AN (1) AD-A098 094
FG (2) 040200
CI (3) (U)
CA (5) SRI INTERNATIONAL MENLO PARK CA
TI (6) Satellite Wind-Profile Techniques.
TC (8) (U)
DN (9) Final rept.,
AU (10) Mancuso,Robert L.
AU (10) Endlich,Roy M.
RD (11) Dec 1980
PG (12) 68p
CT (15) N00228-79-C-K890
PJ (16) F52551
TN (17) WF52551792
RN (18) NEPRF-CR-80-05
RC (20) Unclassified report
DE (23) *Wind, Determination, Meteorological satellites, Optical images, Clouds, Motion, Atmospheric temperature, Profiles, Geostrophic wind, Eigenvectors, Meteorological data, Radiosondes, Comparison
DC (24) (U)
ID (25) *Wind profile measurement, LPN-SRI-8979, PE62759N, WU6212
IC (26) (U)
AB (27) Satellite data that are currently available in numerical form for operational use include temperature profiles and cloud-motion measurements. In this study, several different techniques were tested for possible use in deriving wind profiles from these data. The eventual application of the wind profiles would be in objective analysis and numerical weather prediction. The techniques were tested using research data sets prepared by the National Environmental Satellite Service (NESS) at the University of Wisconsin. The satellite data consist of high-resolution TIROS-N temperature profiles and GOES cloud-motion measurements. The evaluation of the techniques was based on comparisons with radiosonde observations over the United States. Two of the techniques tested were found to give promising results: one, a technique based on the use of thermal winds to extrapolate wind values upward and downward from the cloud-motion level, and the other a technique based on eigenvector calculations. These two techniques, or similar ones, should be of current operational value over oceanic areas devoid of conventional data, provided that reliable height values for cloud motions and reasonably accurate estimates of surface winds can be provided. (Author)
AC (28) (U)
DL (33) 01
SE (34) F

CC (35) 410281

ROUTINE REPLY, ENDORSEMENT, TRANSMITTAL OR INFORMATION SHEET

OPNAV 5216/158 (Rev. 7 78) *A WINDOW ENVELOPE MAY BE USED*
SN 0107 LF 052 1691 *Formerly NAVEXOS 3789*

CLASSIFICATION *(UNCLASSIFIED when detached from enclosures, unless otherwise indicated)* UNCLASSIFIED

FROM *(Show telephone number in addition to address)*
Commanding Officer, Naval Environmental Prediction Research Facility, Monterey, CA 93940 AVN 878-2928

DATE
2 MAR 1981

SUBJECT
NAVENVPREDRSCHFAC technical publications; forwarding of

SERIAL OR FILE NO.
NEPRF/SBB:sb 5600
SER: 106

TO:
Distribution
[See end pages, enclosures (1), (2)]

REFERENCE

ENCLOSURE
(1) NAVENVPREDRSCHFAC Technical Report TR 80-08: An Automatic Cloud Tracking System Based On The Cross-Covariance Method
(2) NAVENVPREDRSCHFAC Contractor Report CR 80-05: Satellite Wind-Profile Techniques

VIA:

ENDORSEMENT ON

XX FORWARDED ☐ RETURNED ☐ FOLLOW-UP, OR TRACER ☐ REQUEST ☐ SUBMIT ☐ CERTIFY ☐ MAIL ☐ FILE

GENERAL ADMINISTRATION	CONTRACT ADMINISTRATION	PERSONNEL
FOR APPROPRIATE ACTION	NAME & LOCATION OF SUPPLIER OF SUBJECT ITEMS	REPORTED TO THIS COMMAND:
UNDER YOUR COGNIZANCE	SUBCONTRACT NO. OF SUBJECT ITEM	
XX INFORMATION & retention	APPROPRIATION SYMBOL, SUBHEAD, AND CHARGEABLE ACTIVITY	DETACHED FROM THIS COMMAND
APPROVAL RECOMMENDED ☐ YES ☐ NO	SHIPPING AT GOVERNMENT EXPENSE ☐ YES ☐ NO	OTHER
☐ APPROVED ☐ DISAPPROVED	A CERTIFICATE, VICE BILL OF LADING	
COMMENT AND/OR CONCURRENCE	COPIES OF CHANGE ORDERS, AMENDMENT OR MODIFICATION	
CONCUR	CHANGE NOTICE TO SUPPLIER	
LOANED, RETURN BY:	STATUS OF MATERIAL ON PURCHASE DOCUMENT	
SIGN RECEIPT & RETURN		
REPLY TO THE ABOVE BY:		
REFERENCE NOT RECEIVED		
SUBJECT DOCUMENT FORWARDED TO		
SUBJECT DOCUMENT RETURNED FOR		
SUBJECT DOCUMENT HAS BEEN REQUESTED, AND WILL BE FORWARDED WHEN RECEIVED		
COPY OF THIS CORRESPONDENCE WITH YOUR REPLY		
ENCLOSURE NOT RECEIVED		
ENCLOSURE FORWARDED AS REQUESTED		
ENCLOSURE RETURNED FOR CORRECTION AS INDICATED		
CORRECTED ENCLOSURE AS REQUESTED		
REMOVE FROM DISTRIBUTION LIST		
REDUCE DISTRIBUTION AMOUNT TO		

REMARKS *(Continue on reverse)*

Enclosure (1) describes an automatic cloud tracking system based on the computation of the cross-covariance between satellite images, and gives examples of this system's application.

Enclosure (2) presents the results of a study to investigate techniques of deriving wind profiles from cloud motion vectors and satellite temperature soundings; a selected number of techniques are tested and compared.

SIGNATURE & TITLE
Commanding Officer

COPY TO:

CLASSIFICATION *(UNCLASSIFIED when detached from enclosures, unless otherwise indicated)* UNCLASSIFIED

★ G.P.O.: 1979-689-016/4281

NAVENVPREDRSCHFAC
CONTRACTOR REPORT
CR 80-05

NAVENVPREDRSCHFAC CR 80-05

SATELLITE WIND-PROFILE TECHNIQUES

Prepared By:

Robert L. Mancuso and Roy M. Endlich
SRI International
Menlo Park, California 94025

Contract No. N00228-79-C-K890

DECEMBER 1980

Prepared For:
NAVAL ENVIRONMENTAL PREDICTION RESEARCH FACILITY
MONTEREY, CALIFORNIA 93940

CONTENTS

ILLUSTRATIONS

TABLES

I INTRODUCTION

Meteorological satellite systems are now supplying large amounts of valuable data that were previously unattainable. The temperature profile data from the recent TIROS-N cover the globe and provide reasonably accurate descriptions of large-scale temperature structure (Smith et al, 1979).* Despite some remaining undesirable characteristics, these data are being used by the National Meteorological Center (NMC) to fill-in oceanic data-sparse areas (Phillips et al., 1979). Numerous studies have shown that cloud-motion measurements are valid if the cloud heights are known with reasonable accuracy (e.g., Hasler et al., 1979), which can be achieved using infrared observations. Improved sensors and processing procedures will permit more accurate depictions in the future, particularly of small-scale phenomena. Other types of meteorological data that may become available routinely from satellites include measurements of surface winds over the oceans (from microwave instruments like those used on SEASAT) and constant-level balloon observations of high-altitude conditions.

The various types of satellite data currently available do not in themselves give a complete description of the air flow of the atmosphere. However, they provide sufficient information for estimating wind profiles, the most obvious method being to use thermal winds derived from the satellite temperature profiles to build upward or downward from known wind values. The known wind values can be radiosonde winds, cloud-motion measurements, aircraft measurements, surface data, or some combination of these.

In this study by SRI International (SRI) for the Naval Environmental Prediction Research Facility (NEPRF), four different techniques were tested for deriving wind profiles from satellite cloud-motion measurements and retrieved temperature profiles. The testing was done using recent satellite data for 1979: The temperature retrievals were from the TIROS-N polar orbiting satellite, and the cloud motions were derived from GOES geosynchronous satellite imagery. The temperature profiles and cloud motions, which are of relatively high-spatial resolution, were provided by the National Environmental Satellite Service (NESS) at the Space Science Center, University of Wisconsin.

In Section II of this report, we describe the approach and the four different techniques that were tested. Section III gives a description of the data sources that were used, and presents computer flow charts that

*References are provided in full at the end of this report.

pertain both to the data processing and the testing of the techniques. In Section IV, the results for the three test cases are presented, and a discussion is given of the errors, particularly the inaccuracies in cloud-height estimates and their effects on the results. Section V provides a summary with concluding remarks. Appendix A is included as a comparison between analyses of conventional radiosonde observations and of Atmospheric Variability Experiment (AVE) data.

II BASIC PROCEDURE AND TECHNIQUES

In collaboration with NEPRF personnel, four different techniques were selected for determining wind profiles from satellite data. The basic approach adopted for applying and testing the techniques was as follows:

- Step 1: Make horizontal grid-point analyses of temperature from the satellite data at the levels 850-, 700-, 500-, 400-, 300-, 250-, and 200 mb, and then calculate thermal winds. This produces a set of temperature and thermal-wind profiles at each vertical column of the three-dimensional mesh. [Thermal winds could also be derived directly from the radiance data--see Fleming (1979).]

- Step 2: Use the thermal-wind vectors at grid points to build geostrophic wind profiles upward from some given low-level wind. In this study, gradient-wind profiles computed in this manner were provided by NESS for the same locations as the temperature-profile data. (The gradient wind is similar to the geostrophic wind, but has curvature corrections for speed.) Thus, it was only necessary to analyze grid-point values of these gradient winds in conjunction with the temperature-profile values.

- Step 3: Construct an improved wind field at a selected level by analyzing the available cloud-motion data at this level using the gradient wind as a first guess. In this study, the 300-mb level was selected because the cloud-motion data for the test cases were principally at this level.

- Step 4: Apply one of the techniques to obtain improved wind fields at all the other levels, and thus improve the wind profiles at each horizontal location of the vertical columns of the mesh.

The wind-profile techniques that were tested in this study are described below.

Technique T1--In this technique, after cloud motions are analyzed for a selected height (h), a complete wind profile is derived for each grid point using a procedure based on a characteristic profile concept, which is as follows:

- The analyzed cloud motions provide the winds at the height h.
- The thermal-wind profiles, which are derived from the satellite temperature-profile data, are used to determine the height at which the thermal wind reverses direction--this is assumed to be the height of the maximum wind level (MWL). A reversal in thermal

wind is defined to take place at a certain height if the dot product of the thermal-wind vector below and above this height has a large negative value. Above 500 mb, the level having the largest negative dot product is assumed to be the MWL.

- The wind-speed profile is then built upward and downward from the cloud-motion level (h) using relationships between speed and shear that were developed by Endlich and McLean (1960). At the MWL, the direction of the shear reverses. Wind directions are held constant with height.

Technique T2--In this technique, the improved wind analysis at the cloud-motion height (h) is first made nondivergent using the wind-altering method developed by Endlich (1967). In this method, the grid-point winds are altered in a systematic manner until the divergence of the wind field has been eliminated without changing the rotational properties of the flow. Based on previous studies (Viezee et al., 1972; 1977), eliminating divergence appears to be desirable because it eliminates a large part of the random measurement error. After the wind field at height h is made nondivergent, the satellite thermal-wind fields are used to directly extrapolate wind values both upward and downward to produce improved wind profiles at each vertical column of the three-dimensional mesh. If there were no cloud motions at height h in the vicinity of the location of a vertical column of the mesh, then the wind profile calculated for that location would essentially be the same as the original gradient wind profile.

Technique T3--This technique is a modification of T2; the modification is intended to account for the differences between geostrophic and nondivergent winds, as expressed by the balance equation. These differences can be as large as 10 to 20 percent of the geostrophic speeds in high-speed curved flow such as jet streams. In moderate or weak flow, the differences may be small and difficult to detect. Unfortunately, the wind speeds in the cases available for this study were mostly weak or moderate. The T3 technique operates as follows: After an improved wind field is analyzed at the cloud-motion height h and is made nondivergent as in T2, it is converted to a geostrophic-wind field, using the wind-altering technique applied to the balance equation; that is

$$f\zeta_g - \beta u_g = f\zeta - \beta u + 2J(u,v) \qquad (1)$$

where u and v are the wind components, f is the Coriolis parameter, $\beta = \partial f/\partial y$, ζ is the relative vorticity, $J(u,v) = (\partial u/\partial x)(\partial v/\partial y) - (\partial u/\partial y)(\partial v/\partial x)$, and the subscript g denotes geostrophic values.

The right-hand side of the equation is calculated only once and held fixed, while the u_g and v_g values on the left side are successively altered until they satisfy Equation (1) and

$$\partial u_g/\partial x + \partial v_g/\partial y = -(\beta/f)v_g \qquad (2)$$

After this computation is made, the satellite thermal winds are used to extrapolate geostrophic winds vertically. The geostrophic wind fields at each level are then converted to nondivergent winds, again using the wind-altering technique applied to the balance equation [Eq. (1)] in a reverse direction. This procedure is analogous to the standard solution of the balance equation that begins with height values at grid points and obtains a stream function. The above two applications of the wind-altering method are described in detail in literature (Endlich, 1968; 1970). The resulting nondivergent winds should be a better approximation to the real winds than the geostrophic winds in regions of strong winds.

Technique T4--This technique follows the approach described by Kalb (1979), which is based on calculating eigenvectors for the satellite geostrophic- (or gradient-) wind profiles. Only the first eigenvector for a profile is used, since it explains most of the variance of the profile, and a cloud-motion wind is used to estimate the coefficient of this first eigenvector. Since the coefficient applys at all levels, it is in turn used with the first eigenvector to compute the entire wind profile. A more detailed explanation follows.

By the use of linear transformations based on the eigenvectors of the covariance matrix, the number of variables can be reduced while still retaining most of the information in the original data set. Lorenz (1956) has given a description of the method as applied to temperature and pressure observations; others, such as Holmström (1963), have used the eigenvector method for representing wind profiles.

A profile of any scalar quantity can be represented as a linear combination of a set or orthonormal eigenvectors, and the value of q for any profile (n) and for any level (ℓ) would be given by:

$$q(n,\ell) = \overline{q(\ell)} + \sum_{k=1}^{K} \left[c(n,k) \cdot e(\ell,k)\right] \qquad (3)$$

where $\overline{q(\ell)}$ is the average value of q at the ℓ^{th} level, i.e., $\sum_{n=1}^{N} q(n,\ell)/N$

$c(n,k)$ is the coefficient associated with n^{th} profile and k^{th} eigenvector element (independent of the level).

$e(\ell,k)$ is the element for the ℓ^{th} level of the k^{th} eigenvector; thus, the k = 1 column of elements $[e(1,1), e(2,1), \ldots e(\ell,1)]$ is the first eigenvector.

K is the total number of eigenvectors, which is equal to the total number of levels (L).

N is the total number of profiles (in our application, the total number of vertical columns in the mesh that are used in the evaluation).

The coefficients c(n,k) are inner products of the input data vector and the eigenvector, and can be calculated by:

$$c(n,k) = \sum_{\ell=1}^{L} \left[q(n,\ell) \cdot \overline{q(\ell)}\right] \quad e(\ell,k) \qquad (4)$$

The normal procedure would thus consist of calculating first the eigenvector* and then the coefficients of the original data set. One thus replaces the NxL observations with L^2 eigenvector elements and NxL coefficients. The principal value of this procedure is that the first eigenvector explains most of the variance, and each additional eigenvector explains a successively smaller part of the remaining variance. If all the eigenvectors are used, the profile is reconstructed exactly. Kalb (1979) found in his study that the first eigenvector explains over 80 percent of either the u or v wind-profile variance.

In Kalb's application, the u and v wind components are treated independently and each has its own set of eigenvectors. The u_g component of the geostrophic (or gradient) wind is first used in place of q in Eq. (3) to calculate a set of eigenvectors. An estimate of the $c(n,\ell)$ values are then obtained from the cloud motion u values at the cloud level, say $\ell = 5$, by:

$$c(n,1) \approx \left[u(n,5) - \overline{u_g(5)}\right]/e(5,1) \qquad (4)$$

Estimates of the u wind component at all levels are then made by:

$$u(n,\ell) \approx \overline{u_g(\ell)} + c(n,1)\cdot e(\ell,1) \qquad (5)$$

The v component profiles, $v(n,\ell)$, are then calculated similarly. [The u and v components can also be calculated simultaneously as done by Ludwig and Byrd (1980), which would be more efficient.]

---

*Determining the eigenvector matrix E is a standard problem. It first requires determining the covariance matrix A of the data set, which is defined as:

$$A = QQ^T$$

In this application, the matrix Q would be an LxN matrix, where L is the number of levels and N is the number of gradient-wind profiles. Each element in Q is the difference between the actual data $q(n,\ell)$ value and the mean for the level over all N profiles $\left[\overline{q(\ell)}\right]$. The matrix Q^T is the NxL transpose of Q. The eigenvector matrix E is defined as the matrix that satsifies:

$$EE^T = I \text{ and } EAE^T = D$$

where I is the identity matrix and D is the diagonal matrix of eigenvalues. In this application, the International Mathematical and Statistical Library (IMSL) subroutines BECOVN and EIGRS were used. BECOVN is also used to evaluate the mean u_g and v_g values for each level.

In summary, the satellite gradient-wind data are first used to calculate a set of eigenvectors (one for each layer) for both the u and v components. The cloud-motion winds are then used to estimate the coefficients that are used with the first eigenvectors of both the u and v wind-components profiles. Since these coefficients also apply at each level with different elements of the first eigenvector, and since the first eigenvector explains most of the variation in the wind profile, it is possible to estimate u and v wind components at all levels. If more than one cloud-motion (or other wind) measurement is available, a more accurate estimate can be made by using the first and the second eigenvectors.

It should be noted that this technique is based on the use of an initial gradient-wind profile that is built upward from given surface winds, and that these initial profiles play a significant role, since they are used for calculating the eigenvectors and the $\overline{u_g}$ and $\overline{v_g}$ values used in Eq. (4) and (5).

III TEST CASE SELECTION AND COMPUTER FLOW CHARTS

The three test cases that were selected are special satellite data sets that were provided by NESS. These data sets contain TIROS-N temperature-profile data and cloud-motion measurements based on GOES cloud imagery. The temperature-profile data were processed using the McIDAS interactive system at the University of Wisconsin. This type of processing permits the generation of a dense network of soundings (Smith et al., 1979). The cloud-motion measurements were also made with the McIDAS system (Smith, 1975). The accuracies of the cloud-motion measurements are quite good; Wilson and Houghton (1979) estimate the error to be ~ 4.7 ms^{-1}. However, the estimation of the cloud heights are based on simplified emissivity assumptions and the use of standard atmospheric values (Mosher, 1976). The data sets also contain gradient-wind profiles; gradient or geostrophic wind profiles are calculated with the McIDAS system from pressure values built-up from the surface (see Kalb, 1979).

The three test cases are for 10 April, 14 March, and 2 May 1979, and the regions covered in these test cases are shown in Figure 1. All three cases are over the United States, where there are ample conventional radiosonde data to use in judging the techniques: the first two cases (10 April, 14 March) are over the central-eastern United States, and the third case (2 May) is over the western United States. All of the cases occurred during the spring of 1979, but are distinctly different. The 14 March case contains a jet stream over the northeastern United States, and the 10 April case involved an intense squall-line situation.

Conventional U.S. radiosonde data for these test cases were obtained from the National Climatic Center (NCC) for use as ground-truth data. Also, Atmospheric Variability Experiment (AVE) three-hourly radiosonde data were obtained from the National Aeronautics and Space Administration (NASA)* for the 10 April case.

The flowcharts for computer software used in this study are shown in Figures 2 and 3. The conventional radiosonde data are analyzed using the AEROMAT program (Figure 2) that was previously developed at SRI (Mancuso and Endlich, 1979; Jones and Mancuso, 1979). Programs were also developed for processing the NESS satellite data (Figure 3): the processing consists of decoding and selecting the data for use in testing and evaluating the four candidate techniques for estimating wind profiles from satellite data. The main testing program, TESTECH (Figure 3), is used to test the various techniques by successively replacing the subroutine that implements each of the techniques. The VALDAT (Figure 3) program provides quantitative comparisons of the technique's results with the radiosonde winds.

---

*These data were made available to SRI by the NASA Marshall Space Flight Center.

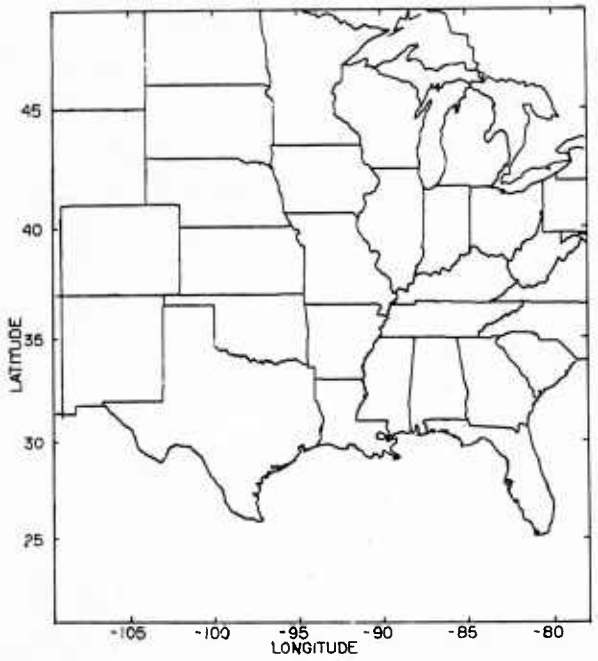

(a) TEST CASE I: 10 APRIL 1979

(b) TEST CASE II: 14 MARCH 1979

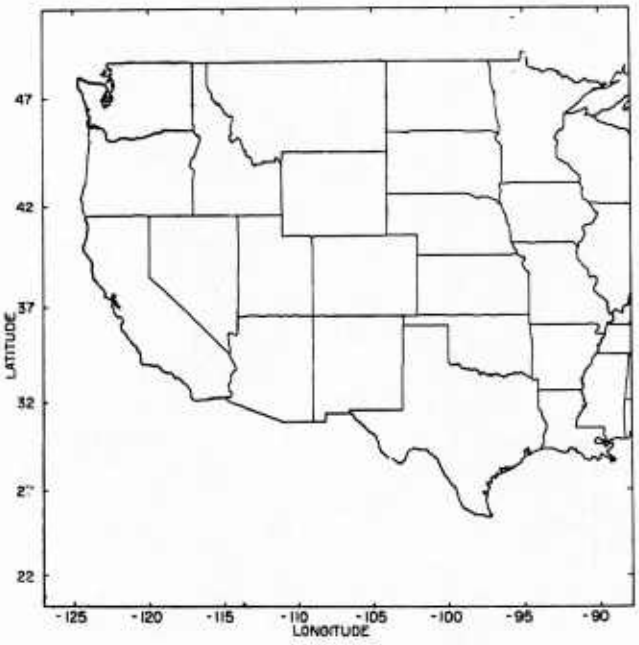

(c) TEST CASE III: 2 MAY 1979

FIGURE 1 REGIONS COVERED BY THE THREE TEST CASES USED IN THE STUDY

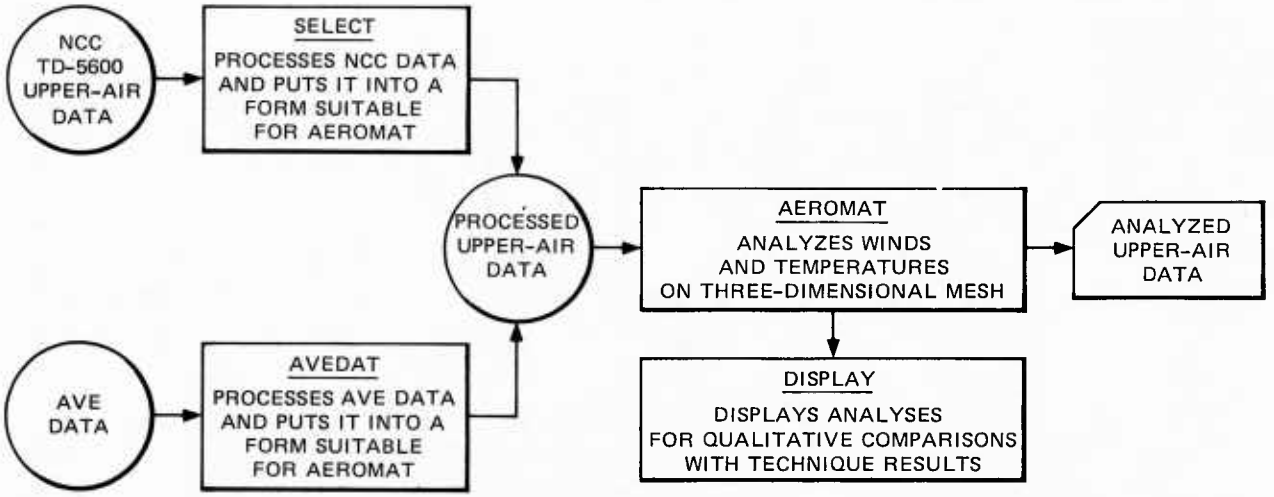

FIGURE 2 PROCESSING AND ANALYSIS OF UPPER-AIR RADIOSONDE DATA USING SRI PROGRAM AEROMAT

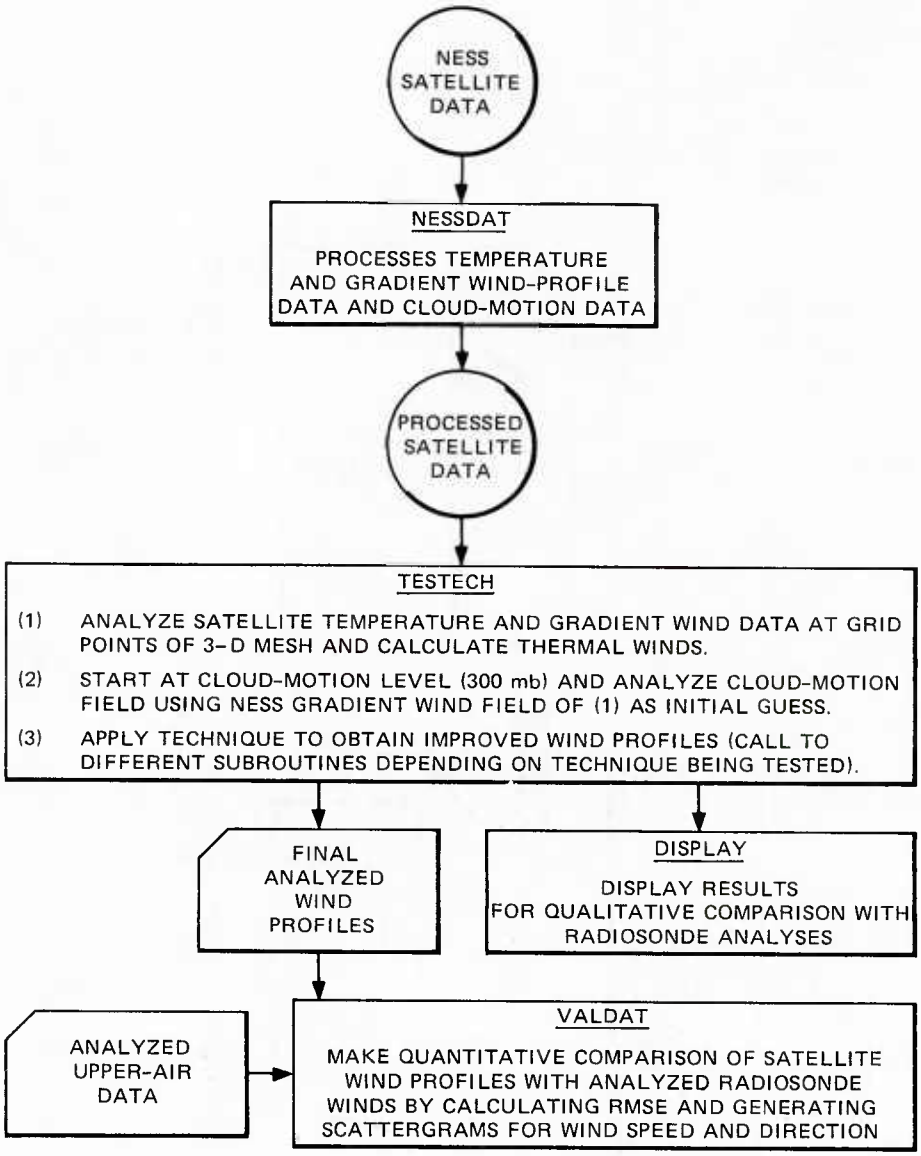

FIGURE 3 FLOW DIAGRAM SHOWING PROCESSING OF NESS DATA AND WIND-PROFILE TECHNIQUE TESTING AND EVALUATION

IV RESULTS

A. Test Case 1: 10 April 1979

Figure 4 shows the gradient winds, cloud motions, and radiosonde data at the 300-mb level for the 10 April 1979 case. The gradient-wind and cloud-motion data do not completely cover the analysis region, but show considerable overlap. The conventional radiosonde data provide a relatively complete and reasonably dense coverage, although they are for 0000 GMT 11 April, four hours after the satellite data time (2000 GMT 10 April). The area enclosed by dashed lines shows a subregion that contains a complete coverage of both the gradient-wind and radiosonde data, and that was used for evaluating the results (it was not made a requirement that this subregion contain cloud-motion data). In this test case, the gradient winds show a number of inconsistencies, such as at 89°W and 35°N. Ideally, these data should be edited; however we believed that this would introduce a personal bias into the results of the study.

Figure 5 shows grid-point analyses of the three data sets of Figure 1. The gradient-wind analysis [Figure 5(a)] was used as a first guess for the cloud-motion analysis [Figure 5(b)]. Figure 5(c) is a time interpolation for 2000 GMT made from three separate analyses of radiosonde data at 1200 GMT 10 April, 0000 GMT 11 April, and 1200 GMT 11 April. The interpolated analyses give reasonably good results, as shown by comparisons with AVE data that were available for the 2000 GMT 10 April 1979 (see Appendix). The grid-point analysis of the gradient wind shows features that differ considerably in detail from the radiosonde analysis, partially due to the use of unedited gradient winds. The cloud-motion analysis [Figure 5(b)] also shows a somewhat different pattern than the radiosonde wind analysis [Figure 5(c)]. For reasons given later, it appears that this is mainly caused by inaccuracies in cloud-height determination and the assignment of the cloud motions to unrepresentative pressure levels.

The TIROS-N temperature and thermal-wind analysis for the 300-mb level at 2000 GMT 10 April, shown in Figure 6(a), are based on temperature data given at the same locations as those shown for the gradient winds of Figure 4(a). The temperature and thermal-wind analysis, which as based on the radiosonde data for the same level and time, is shown in Figure 6(b). (This result was also interpolated from three separate analyses of radiosonde data at the times 1200 GMT 10 April, 0000 GMT 11 April, and 1200 GMT 11 April 1979). The 300-mb patterns of both types of data are similar; however, they differ in detail as shown by the thermal-wind vectors, and the radiosonde temperature are about 2° colder. Differences between these two types of data should be expected since one (radiosonde) is a point measurement, while the other (satellite) represents a volume measurement.

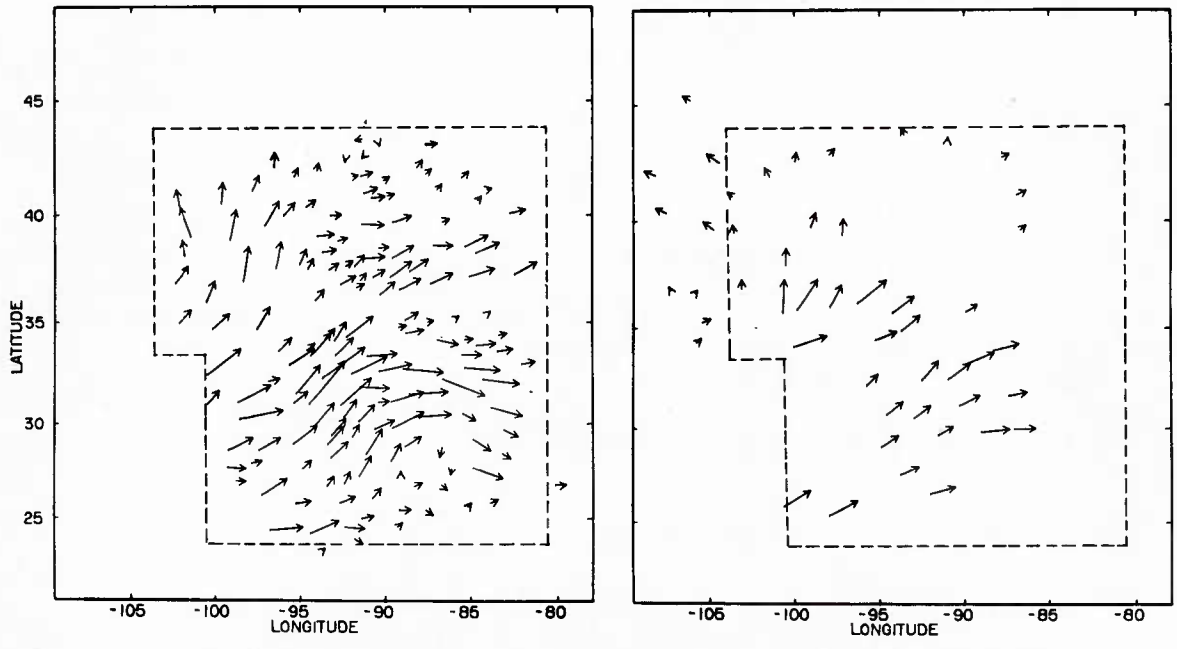

(a) GRADIENT WINDS (TIROS-N)

(b) CLOUD MOTIONS (GOES-EAST)

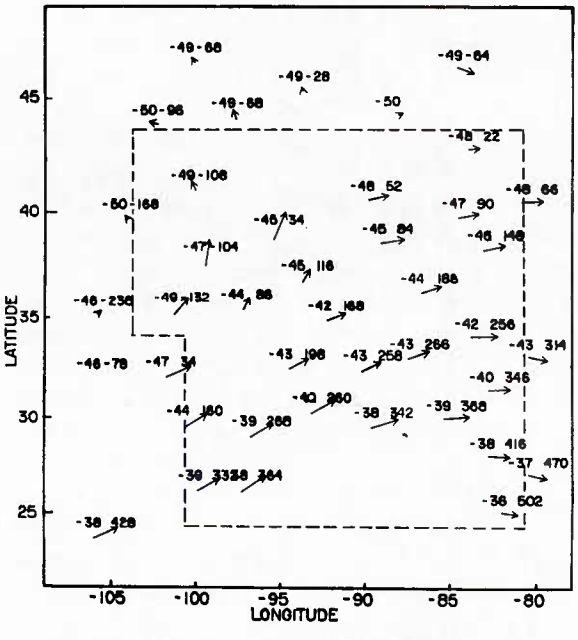

(c) RADIOSONDE DATA (0000 GMT 11 APRIL)

FIGURE 4 AVAILABLE DATA FOR THE 300-mb LEVEL OF TEST CASE I, 2000 GMT 10 APRIL 1979

Satellite gradient-wind and cloud-motion data provided by NESS.

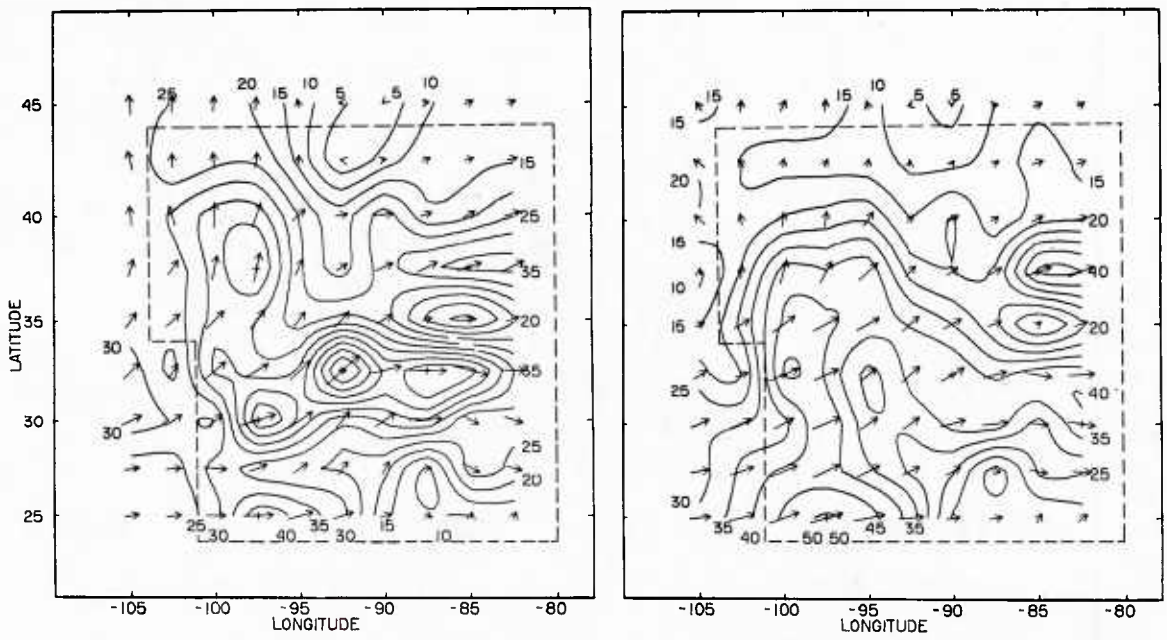

(a) GRADIENT WINDS

(b) CLOUD MOTIONS AND GRADIENT WINDS

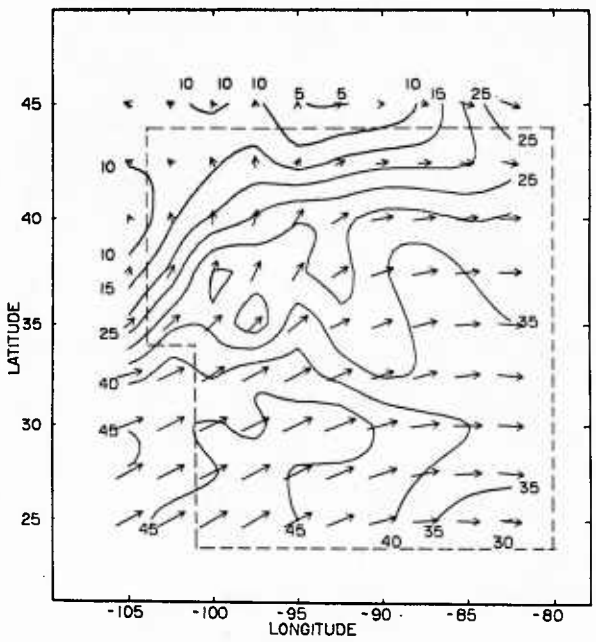

(c) RADIOSONDE WINDS

FIGURE 5 GRID-POINT ANALYSES FOR THE 300-mb LEVEL OF TEST CASE I, 2000 GMT 10 APRIL 1979

Wind speeds shown by isotachs in ms^{-1}.

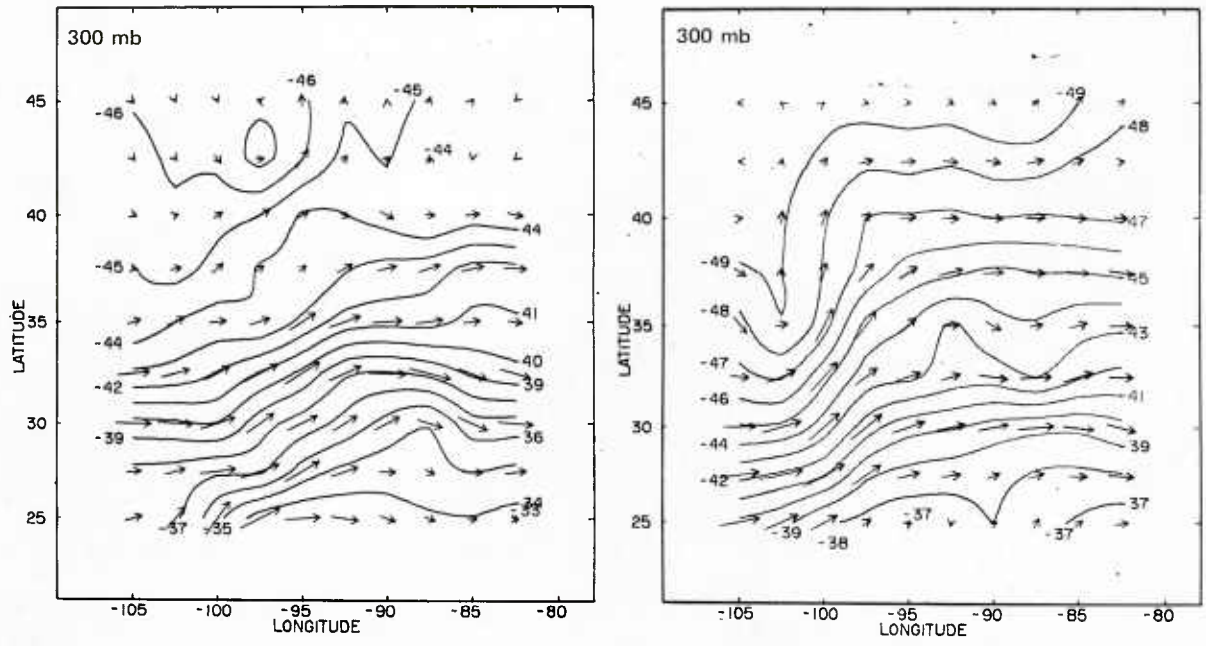

(a) BASED ON TIROS-N DATA

(b) BASED ON RADIOSONDE DATA

FIGURE 6 TEMPERATURE (°C) AND THERMAL-WIND ANALYSES FOR 2000 GMT 10 APRIL 1979

Figure 7 shows the GOES-EAST satellite infrared (IR) image for 2000 GMT 10 April 1979. It reveals a deep, low-pressure system over the southwestern U.S. and an associated high-cloud mass lying to the east, over northwestern Texas and southern Oklahoma. This weather system, which produced numerous tornadoes at this time along the Texas/Oklahoma border, is discussed in detail by Williams et al. (1980). The image also shows a typical jet extending along the Gulf coast. Generally, high clouds (brightest areas) exist in all areas where 300-mb cloud motions are shown in Figure 4(b). There is a cluster of high clouds over the eastern Kentucky/Tennessee area; however, for this case there were no cloud-motions measurements made east of 85°W longitude. The clear area extending from southeastern Missouri to Georgia is also the area where weak gradient-wind speeds are shown in Figure 4(a). These weak gradient-wind speeds do not appear to be very consistent with either the cloud motions or radiosonde winds.

The 850-, 500-, 300- and 200-mb wind analyses for 2000 GMT 10 April 1979 that were based on radiosonde data are shown in Figure 8. [The 300-mb analysis is the same as that shown in Figure 5(c).] A southwesterly diffluent flow pattern generally persisted throughout the troposphere at this time, with wind speeds increasing with altitude and reaching values above 60 ms^{-1} at the 200-mb level. At the 850-mb level, the wind speeds were strongest in the western center of the region. From the 500-mb level and up, the wind speeds were strongest in the southwest of the region. As mentioned previously, this case was associated with severe weather near 99°W and 34°N.

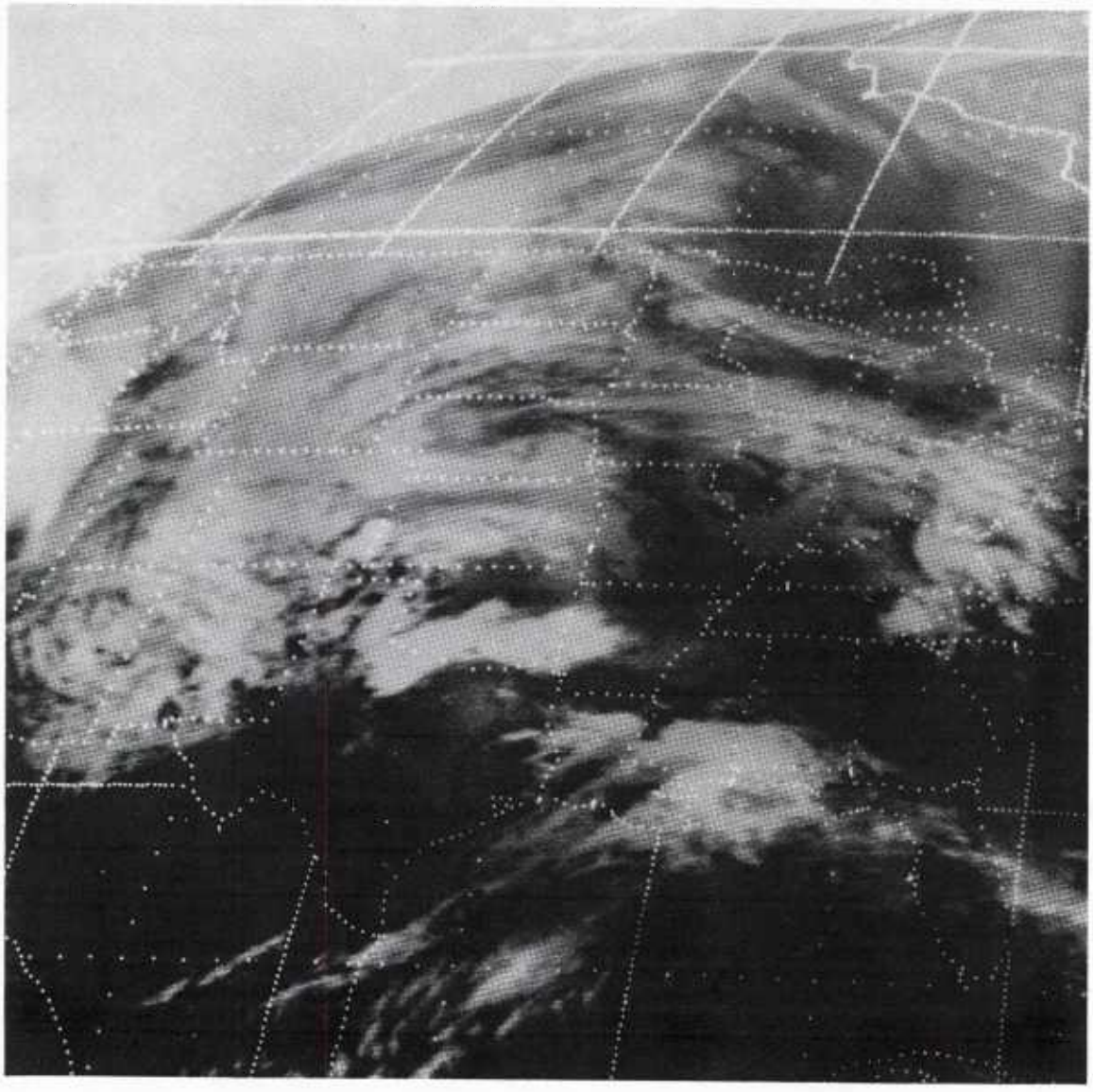

FIGURE 7 GOES-EAST INFRARED IMAGE FOR 2000 GMT 10 APRIL 1979

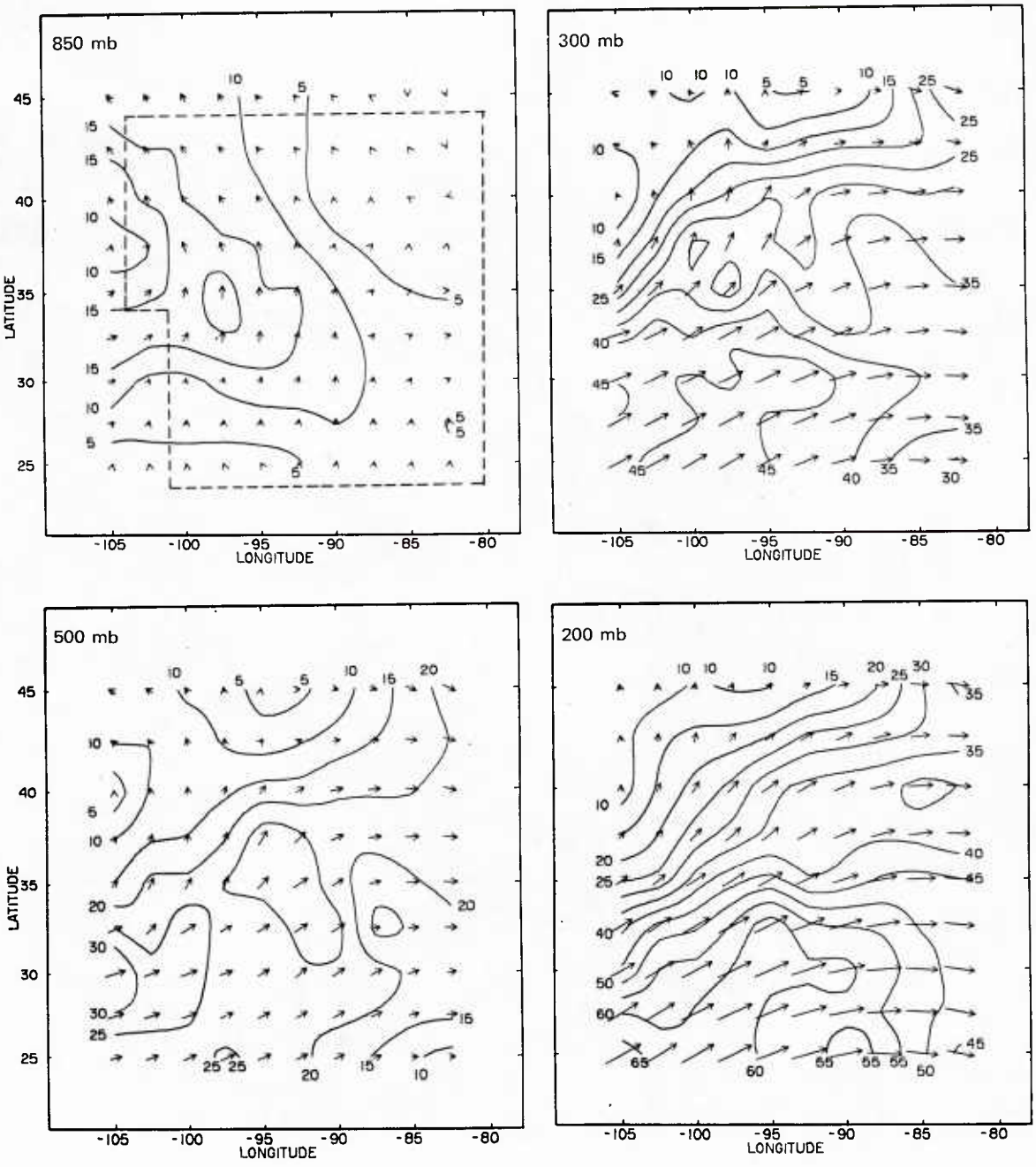

FIGURE 8 WIND FIELDS FOR 2000 GMT 10 APRIL 1979 ANALYZED FROM RADIOSONDE DATA AT 1200 GMT 10 APRIL, 0000 GMT 11 APRIL, AND 1200 GMT 11 APRIL

Isotachs in ms^{-1}.

The graphical results obtained for each of the four techniques are shown in Figures 9-12. The discussion of the results for each of the four techniques is given below.

1. Technique T1 Results

The results for the characteristic profile technique (T1) are shown in Figure 9. In this technique, a downward extrapolation was made from the 300-mb cloud-motion level to 500 mb, giving weaker winds at all points; however, the general pattern at 300 mb was retained. The upward extrapolation to 200 mb was based on knowing the height of the maximum-wind level (MWL), which was determined as described in Section II. The speeds were increased to the MWL and then decreased at higher levels, thereby giving a peaked wind profile. The MWL computed from the thermal-wind reversal varied considerably in height from point to point, between 300 and 200 mb. Thus, the resulting 200-mb wind speeds (Figure 9) also show considerable small-scale variability. Although such variability could be real, it is greater than that analyzed from radiosonde winds (Figure 8) and it therefore appears to be unacceptable.

2. Technique T2 Results

The results for technique T2, which uses the thermal winds to build upward and downward from the cloud-motion level, are shown in Figure 10. The 300-mb cloud-motion field [nondivergent form of Figure 5 (b)] is similar to that shown for the radiosonde analysis in Figure 8, except that the wind speeds are generally lower. The difference appears to be principally attributable to the cloud motions being more representative of a lower level, as will be discussed later. Consistent with this, technique T2 also appears to have made winds at both 500 mb and 200 mb too light in comparison with Figure 8, and to have distorted the winds at the 850-mb level (extrapolated from the 300-mb wind field using the satellite thermal winds).

3. Technique T3 Results

The results for technique T3, which is based on use of the balance equation, are shown in Figure 11. These results are similar to those of technique T2 (Figure 10), except that some of the jet-stream winds are stronger, as would be desired. However, this improvement is noticeable only in the high-speed areas.

4. Technique T4 Results

The results for the eigenvector technique (T4) are shown in Figure 12. [The 300-mb analysis is identical to that of Figure 5(b).] The 500-mb and 200-mb results are fairly similar to those for the radiosonde analyses shown in Figure 8; however, the 850-mb result appears

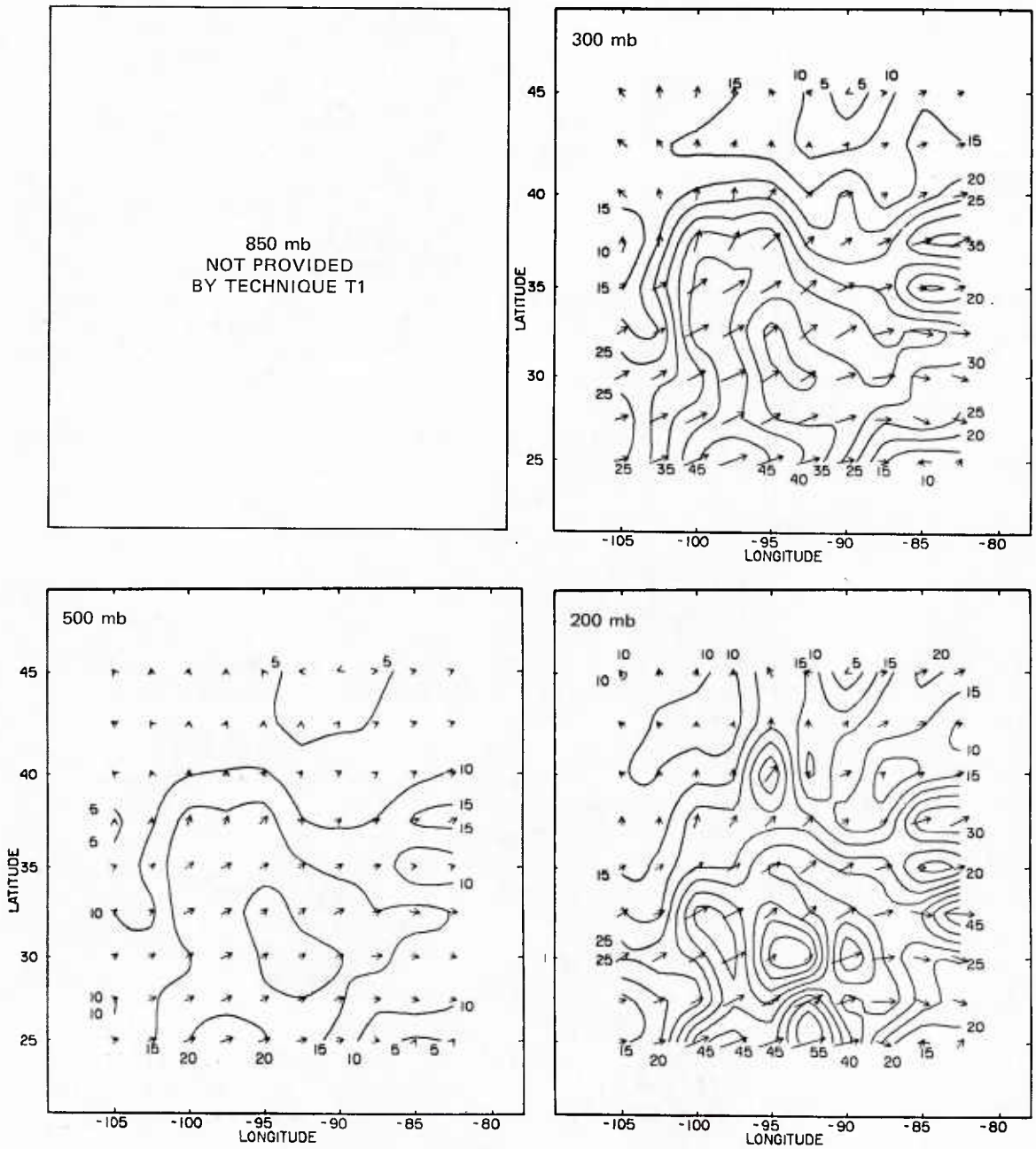

FIGURE 9 WIND FIELDS FOR 2000 GMT 10 APRIL DERIVED USING TECHNIQUE T1

Isotachs in ms^{-1}.

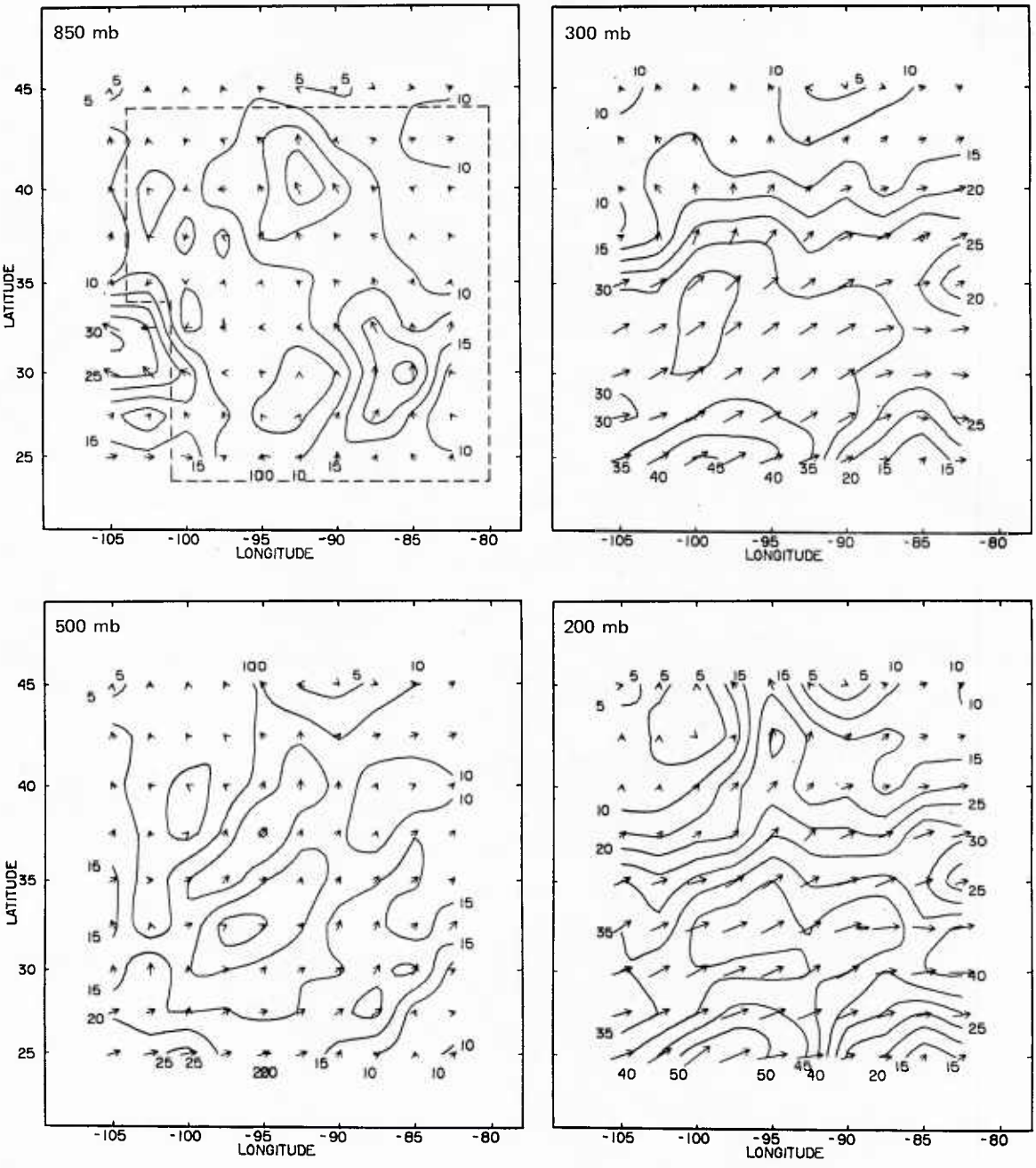

FIGURE 10 WIND FIELDS FOR 2000 GMT 10 APRIL 1979 DERIVED USING TECHNIQUE T2
Isotachs in ms^{-1}.

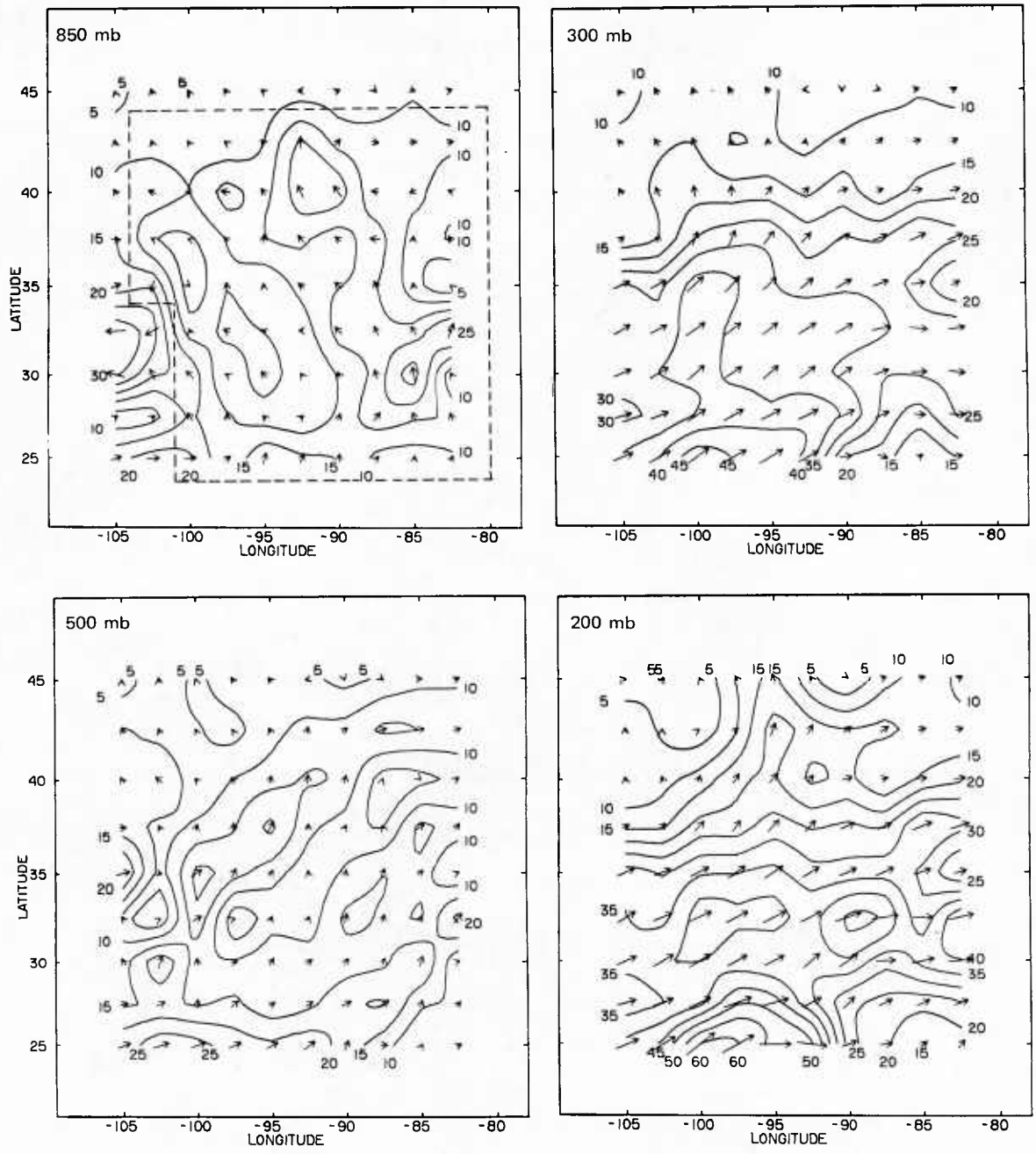

FIGURE 11 WIND FIELDS FOR 2000 GMT 10 APRIL 1979 DERIVED USING TECHNIQUE T3
Isotachs in ms^{-1}.

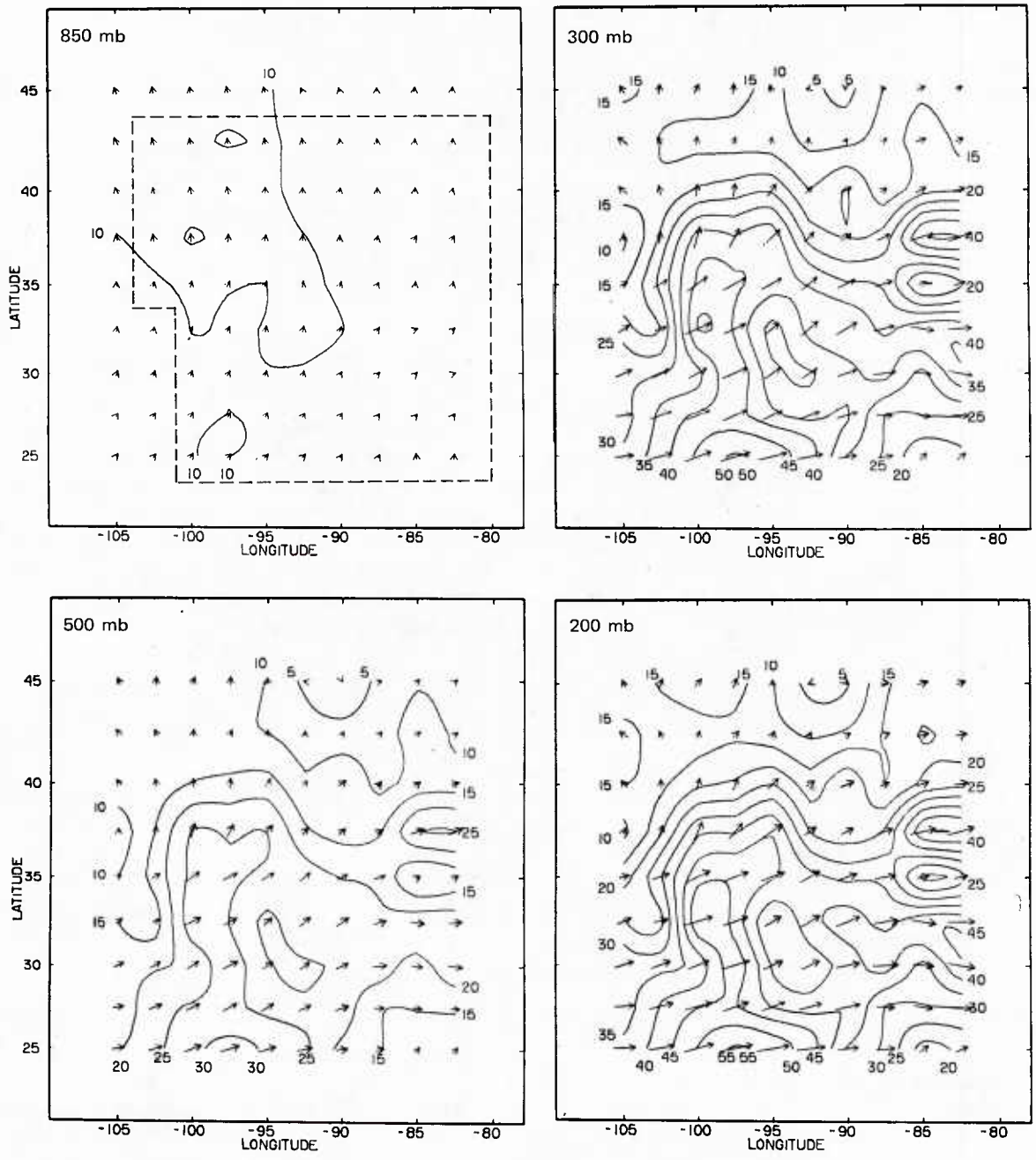

FIGURE 12 WIND FIELDS FOR 2000 GMT 10 APRIL 1979 DERIVED USING TECHNIQUE T4
Isotachs in ms^{-1}.

rather flat. Overall, technique T4 appears to have performed reasonably well, and might be further improved.

5. Summary

In this test case, techniques T2 and T4 performed best, giving a reasonable representation of the winds, although not as good as would be desired. (Technique T2 did not perform very well near the surface.) All of the techniques appear to have been adversely affected by probable errors in the heights of cloud-motion vectors. Also, in this case, there were discrepancies between the temperature fields of the TIROS-N sounding data and radiosonde data that have adversely affected the results.

B. Test Case II: 14 March 1979

Figure 13 shows the gradient winds, cloud motions, and radiosonde data at the 300-mb level for the 14 March 1979 case. The satellite gradient-wind data give a good coverage of the region, except in the mid-south and northeast. These satellite gradient winds (and the satellite temperature data) show more internal consistency than did those for Test Case I [Figure 4(a).] The 300-mb cloud motions give only a sparse coverage, but tend to fill-in the data-void areas of the gradient winds. The radiosonde data provide a relatively complete data set covering most of the region. They are for 1200 GMT 14 March 1979 which is only two hours later than the time of the satellite data (1000 GMT). The area enclosed by the dashed line in Figure 13 shows the area used for evaluating the results.

The GOES-EAST satellite infrared image for the Test Case II region for 1000 GMT 14 March 1979 is shown in Figure 14. The 300-mb cloud motions of Figure 13(b) generally lie in areas where Figure 14 depicts high clouds (brightest cloud areas); a large part of the region appears to be clear of high clouds. Although this picture is not of high quality, it reveals the general flow structure (compare with Figure 13) and a frontal system over the eastern U.S.

The 850-, 500-, 300-, and 200-mb wind analyses for the radiosonde data of 1200 GMT 14 March 1979 are shown in Figure 15. At this time, a trough centered over eastern Canada extends south into the eastern United States. At the higher altitudes over the eastern United States, a southern jet merges with a northern jet, with the southern jet appearing to dominate at 200 mb. The wind speeds are generally low over the northeastern and western parts of the region, with high speeds exceeding 55 ms^{-1} at higher altitudes in the north and southeast of the region.

A discussion of the results obtained for each of the four techniques is given below.

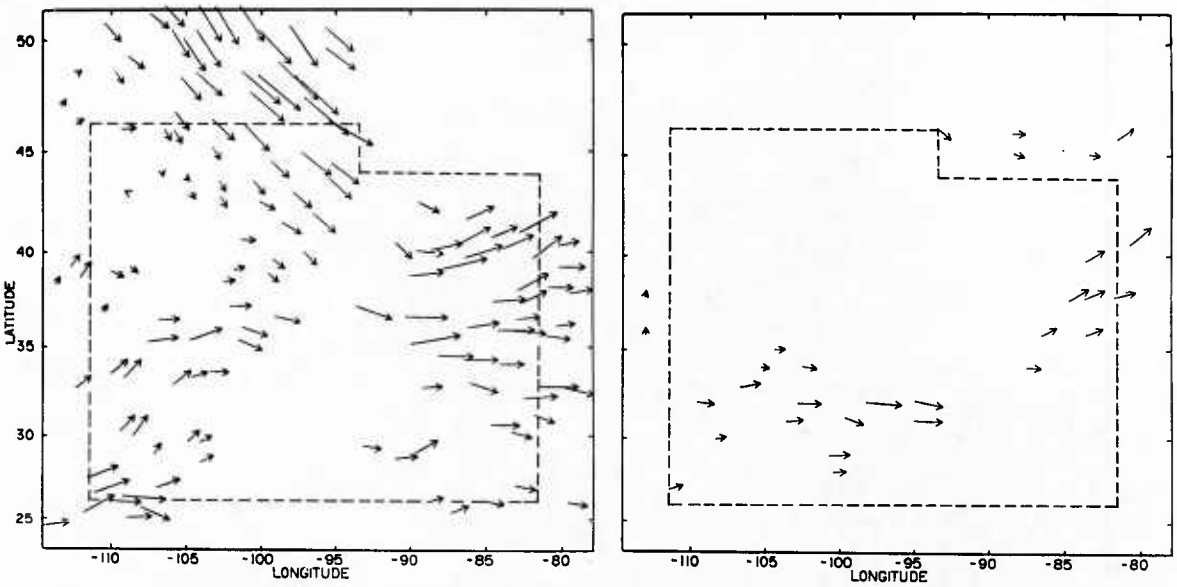

(a) GRADIENT WINDS

(b) CLOUD MOTIONS

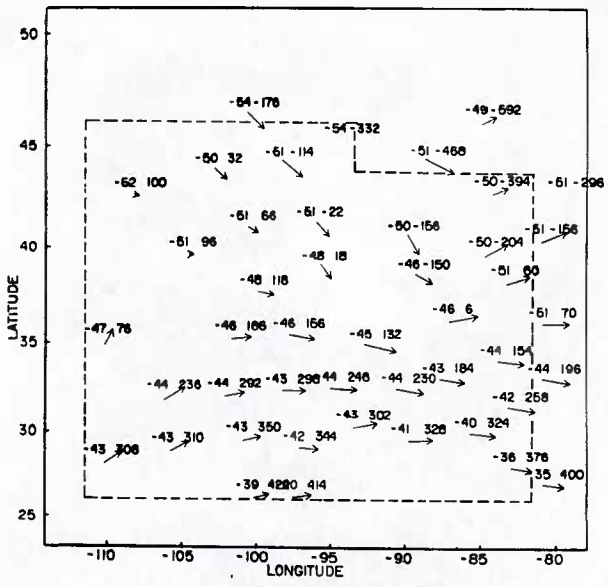

(c) RADIOSONDE DATA (1200 GMT)

FIGURE 13 AVAILABLE DATA AT THE 300-mb LEVEL OF TEST CASE II, 1000 GMT 14 MARCH 1979

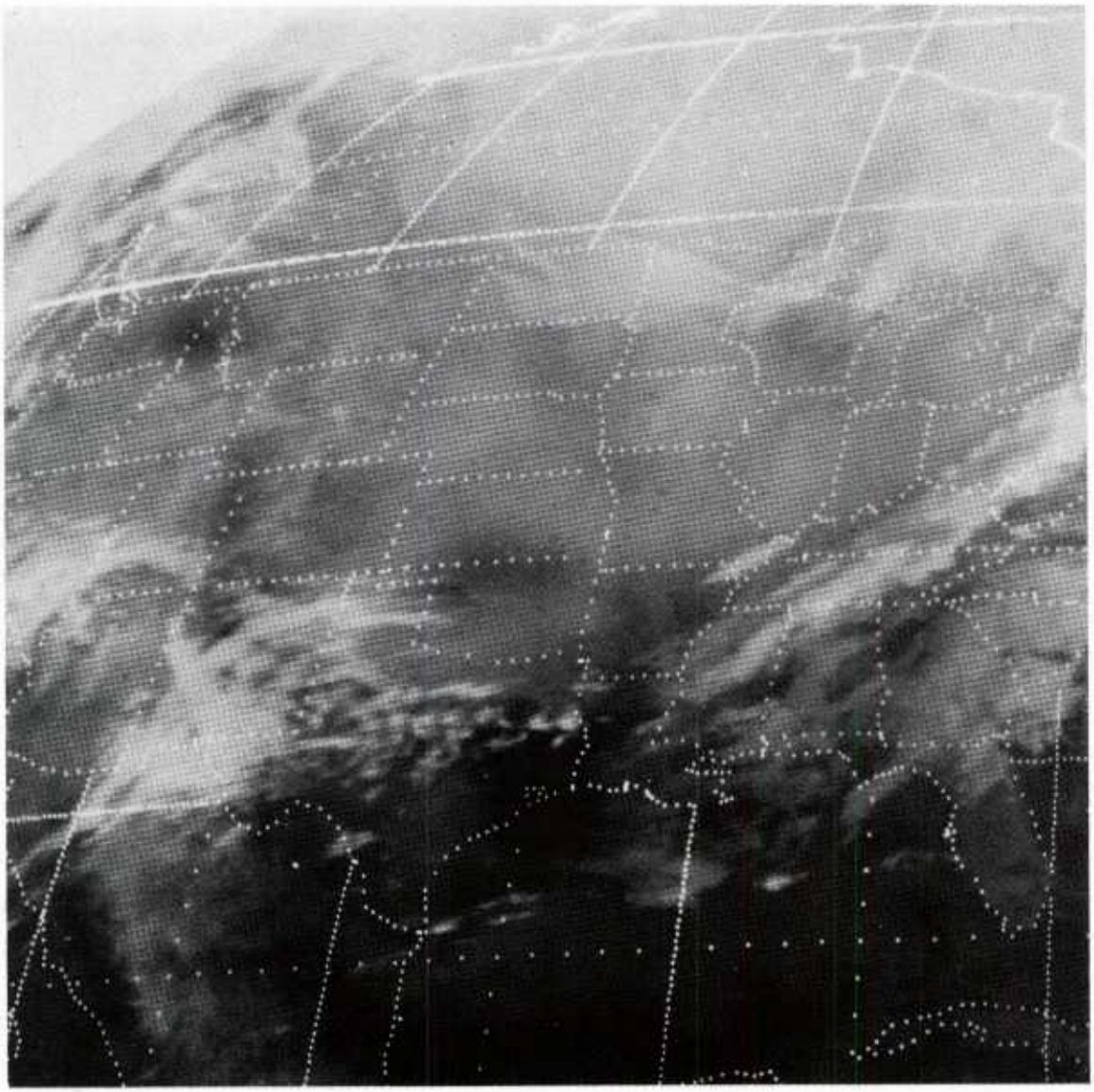

FIGURE 14 GOES-EAST INFRARED IMAGE FOR 1000 GMT 14 MARCH 1979

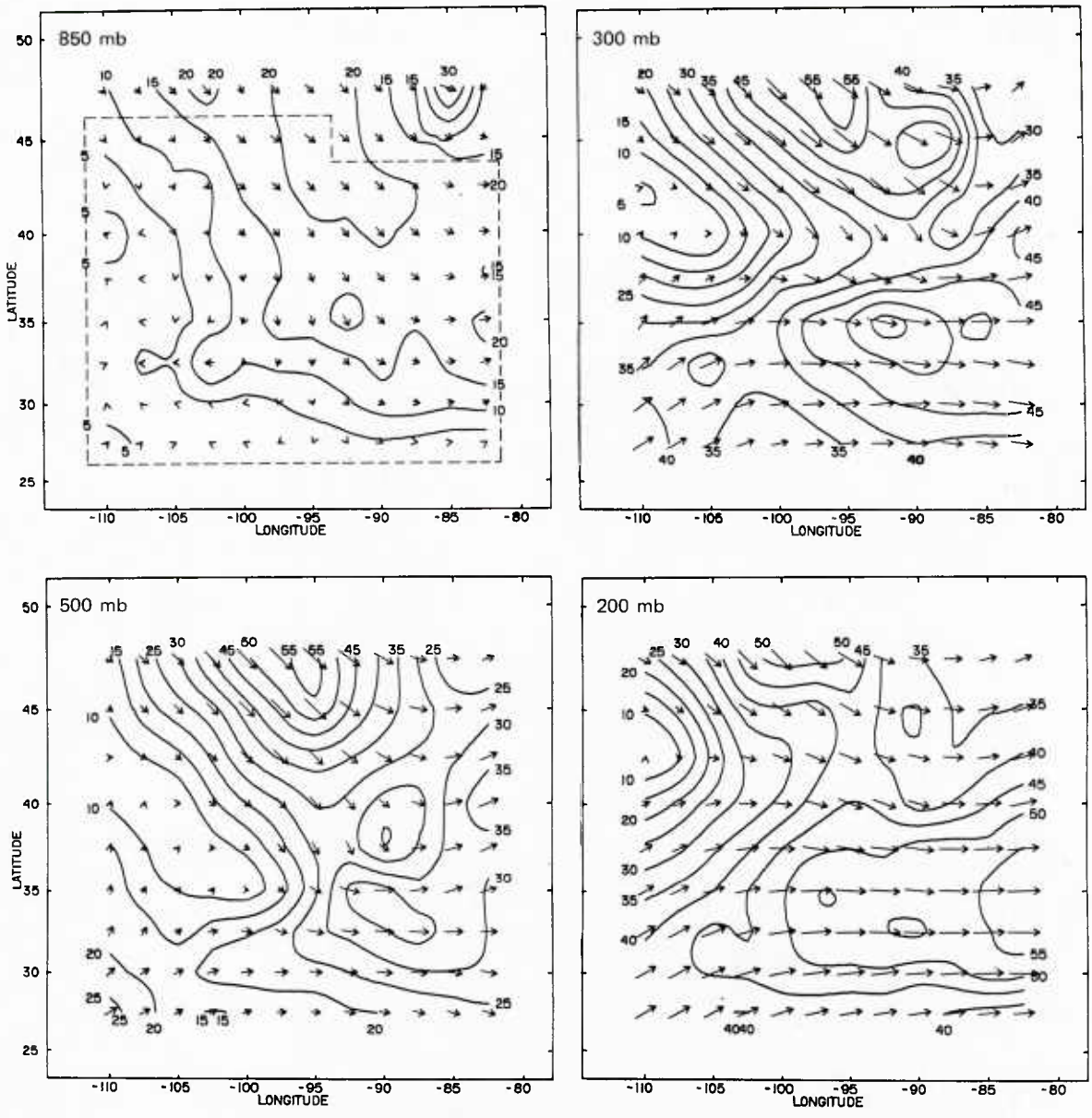

FIGURE 15 WIND FIELDS FOR 1000 GMT 14 MARCH 1979 ANALYZED FROM RADIOSONDE DATA FOR 1200 GMT 14 MARCH 1979

Isotachs in ms^{-1}.

1. Technique T1 Results

As in the 10 April case, technique T1 gave erratic heights for the MWL. Thus, the wind results (not shown) were also very erratic for levels above 300 mb. This method, which is based on an application of characteristic jet-stream profiles, does not appear to be satisfactory in its present form for use in deriving wind profiles from satellite data. Improved results may be possible with this type of approach but would require the development of a family of characteristic wind profiles based on more extensive three-dimensional wind profile information than is currently available.

2. Technique T2 Results

The results for technique T2 are shown in Figure 16. The 300-mb field, which is a nondivergent analysis of the cloud motions of Figure 13(b), is similar to that of the 300-mb radiosonde analysis shown in Figure 15. However, it is even more similar to the 500-mb radiosonde analysis of Figure 15, again suggesting that the cloud motions should have been assigned to a height lower than 300-mb. Consistent with this is the fact that the 500- and 850-mb wind fields for technique T2 in Figure 16 show patterns that appear to be somewhat distorted, and the 200-mb field does not show the broad southern jet of the radiosonde wind field. It appears that the results might have been more satisfactory had the cloud heights been determined more accurately.

3. Technique T3 Results

The results for the balance technique (T3) are not shown. As in Test Case I, they were very similar to the T2 results but with stronger maximum winds, particularly at higher altitudes. Use of the balance relationship appears to give a slight improvement in the high-speed areas, but does not justify the additional computations at this stage of development.

4. Technique T4 Results

The results for the eigenvector technique (T4) are shown in Figure 17. There are no 200-mb results because the gradient-wind data were not available above 250 mb. In this case, technique T4 results appear to be in better agreement with the radiosonde winds at lower levels than are the technique T2 results.

5. Summary

The March test case had few cloud-motion measurements. However, the results were similar to those for the 10 April case. Techniques T2

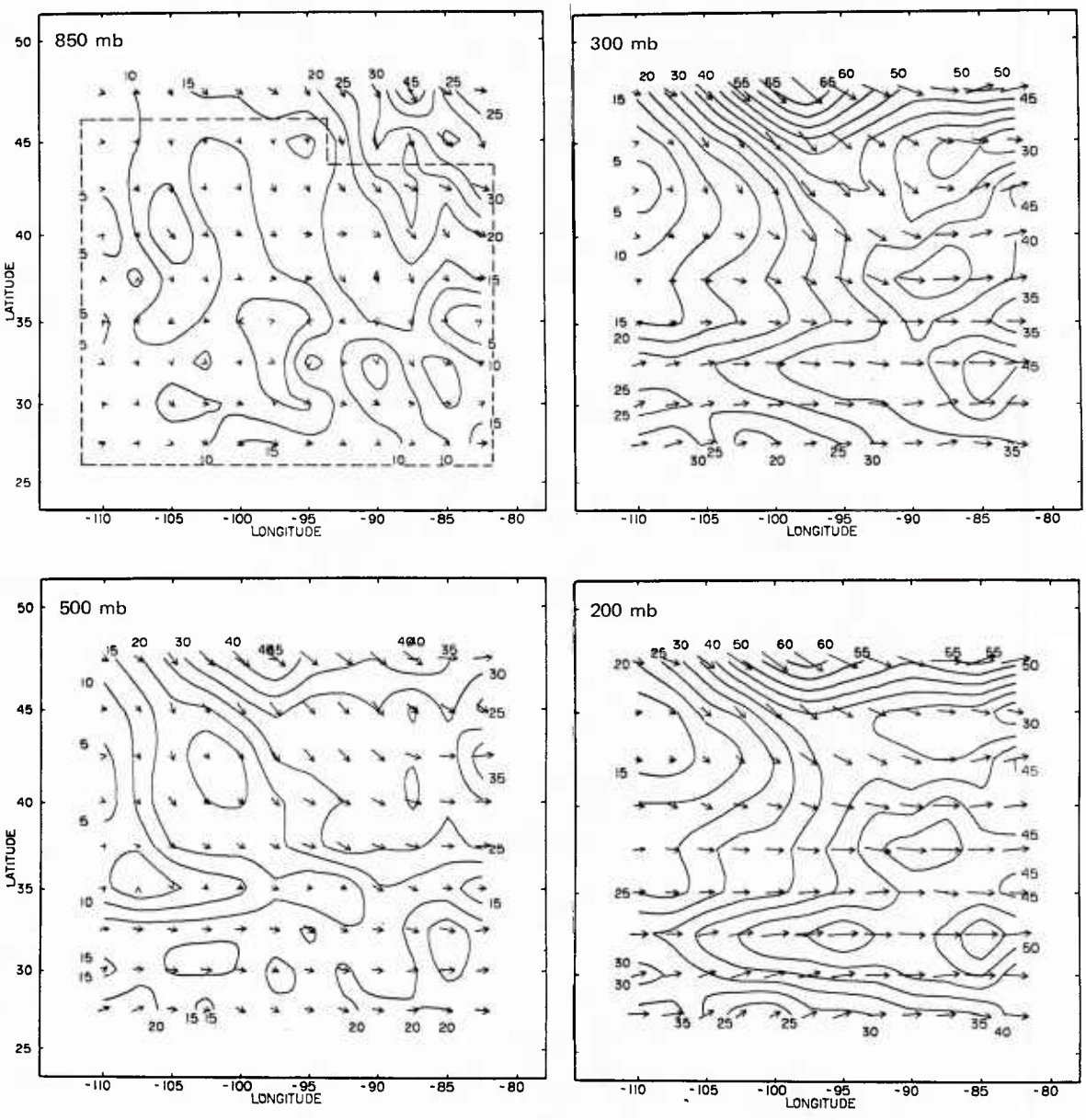

FIGURE 16 WIND FIELDS FOR 1000 GMT 14 MARCH 1979 DERIVED USING TECHNIQUE T2
Isotachs in ms^{-1}.

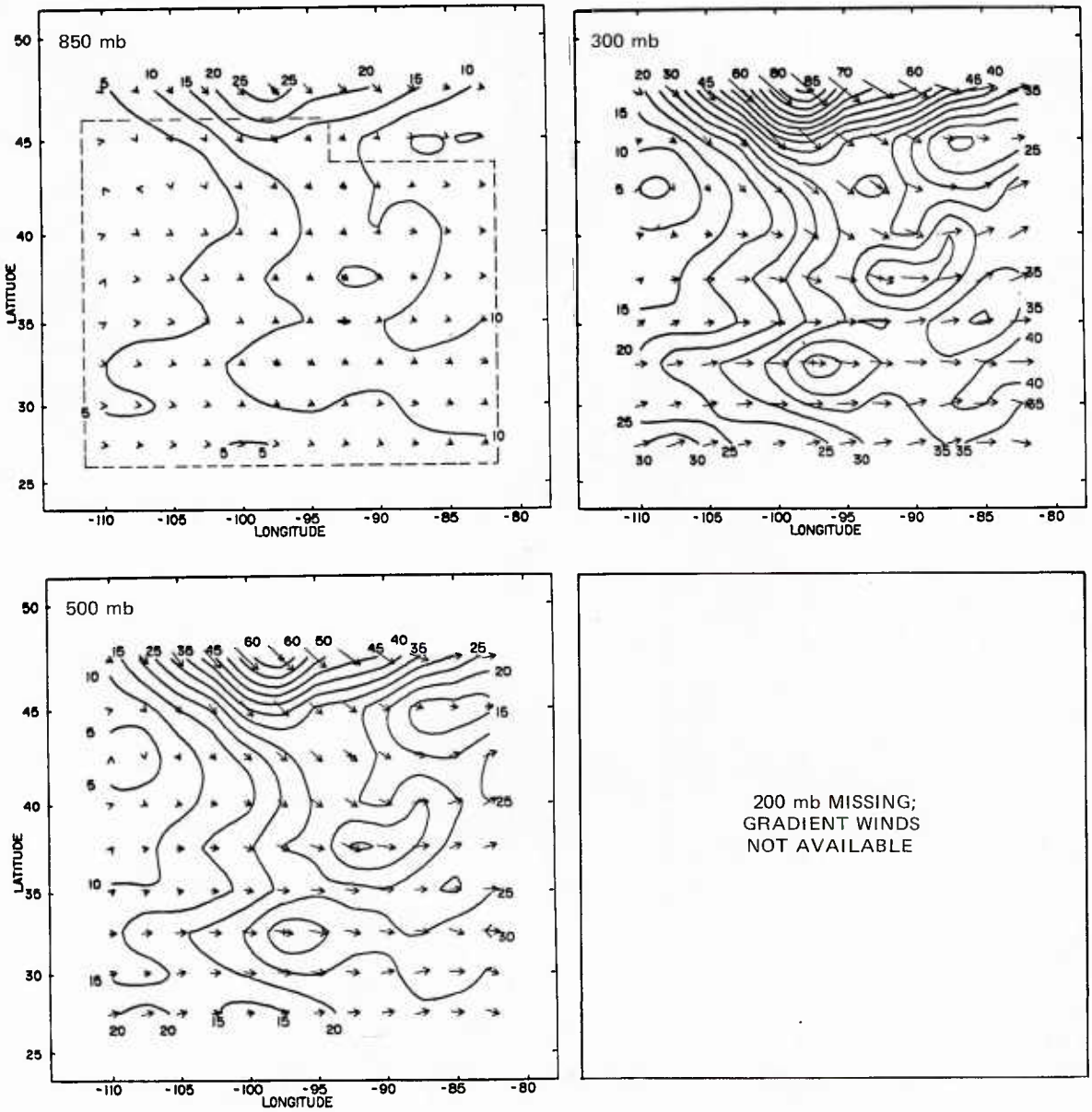

FIGURE 17 WIND FIELDS FOR 1000 GMT 14 MARCH 1979 DERIVED USING TECHNIQUE T4
Isotachs in ms^{-1}.

and T4 performed the best and gave fair agreement with the radiosonde-wind profiles. The analyses again appeared to be adversely affected by the assigned cloud-motion heights.

C. Test Case III: 2 May 1979

Figure 18 shows the gradient winds, cloud motions and radiosonde data at the 300-mb level for the 2 May 1979 test case. In this test case, both the gradient winds and cloud motions give reasonably good coverage of the region. There are no gradient winds in the south and the southeast of the region, and no cloud motions in the north and west of the region (except for a cluster in the northwest corner). However, the cloud motions and gradient winds tend to complement each other at the 300-mb level. The radiosonde data are for 1200 GMT 2 May 1979, which is only two hours later than satellite data (1000 GMT). The area enclosed within the dashed line was used for evaluating the results.

The GOES-WEST satellite infrared image for the Test Case III region and for 1015 GMT 2 May 1979 is shown in Figure 19. The cloud features reveal a southwesterly flow of high-level air from the Pacific into northwestern Mexico, and a strong development within the center of the trough over Arizona and Colorado. The high-cloud areas are consistent with the 300-mb cloud motions of Figure 18.

The 700-,* 500-, 300-, and 200-mb wind analyses of the radiosonde data for 1200 GMT 2 May 1979 are shown in Figure 20. A fairly deep trough was situated over the westernmost U.S. with very light winds extending up through the atmosphere at the center of the trough over northern Colorado. Strong northerly winds existed just off the west coast and strong westerly winds across the southern border of the country, with speeds reaching up to 45 ms^{-1} at higher altitudes. The wind field is fairly uniform throughout the upper troposphere (above 500 mb). The analyses in the southwest corner of the analysis region are extrapolated values and are not very meaningful [see Figure 18(a)].

Only techniques T2 and T4 were tested with this Test Case III; a discussion is given below.

1. Technique T2 Results

The results for technique T2, which are shown in Figure 21, are reasonably good--particularly for the upper two levels (300 and 200 mb). The technique has produced unrealistically strong winds in the southwest of the region at the lower two levels (700 and 500 mb); this area is at the boundary of the thermal-wind data. The high winds (>45 ms^{-1}) in the south of the region of the 300-mb radiosonde field (Figure 20) are stronger

*The 700-mb level is shown in this test case in place of the 850-mb because the 850-mb level was frequently below the level of the terrain.

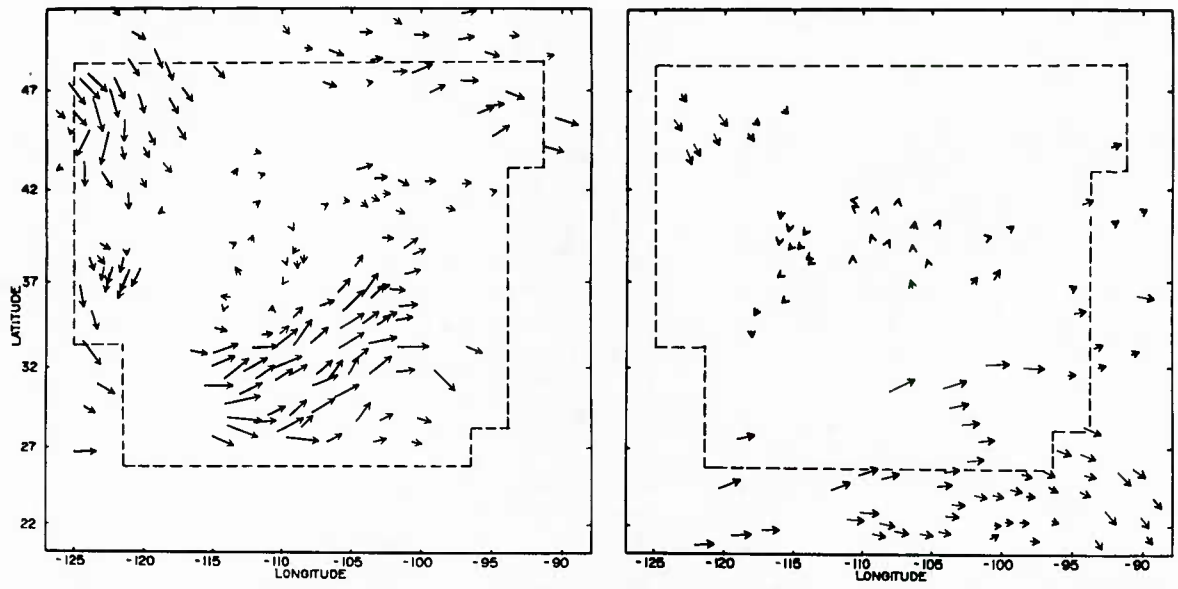

(a) GRADIENT WINDS

(b) CLOUD MOTIONS

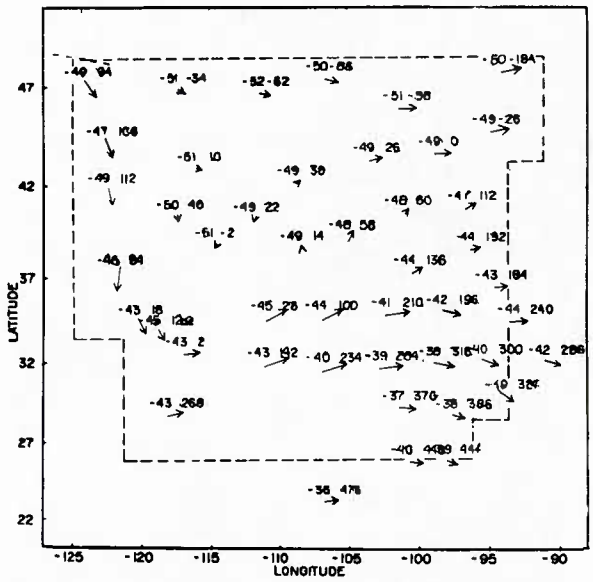

(c) RADIOSONDE DATA (1200 GMT)

FIGURE 18 AVAILABLE DATA AT THE 300-mb LEVEL, TEST CASE III, 1000 GMT 2 MAY 1979

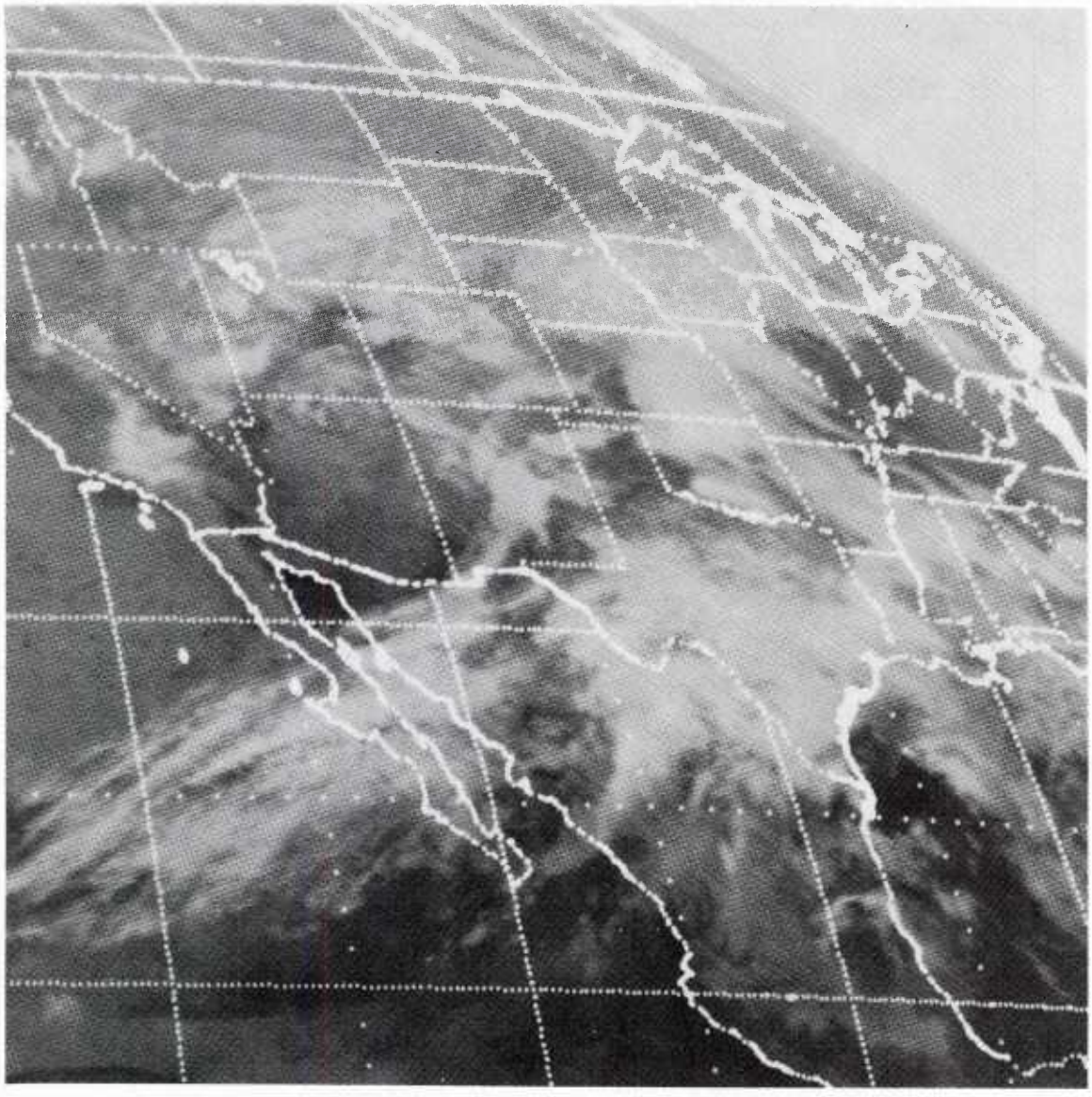

FIGURE 19 GOES-WEST INFRARED IMAGE FOR 1015 GMT 2 MAY 1979

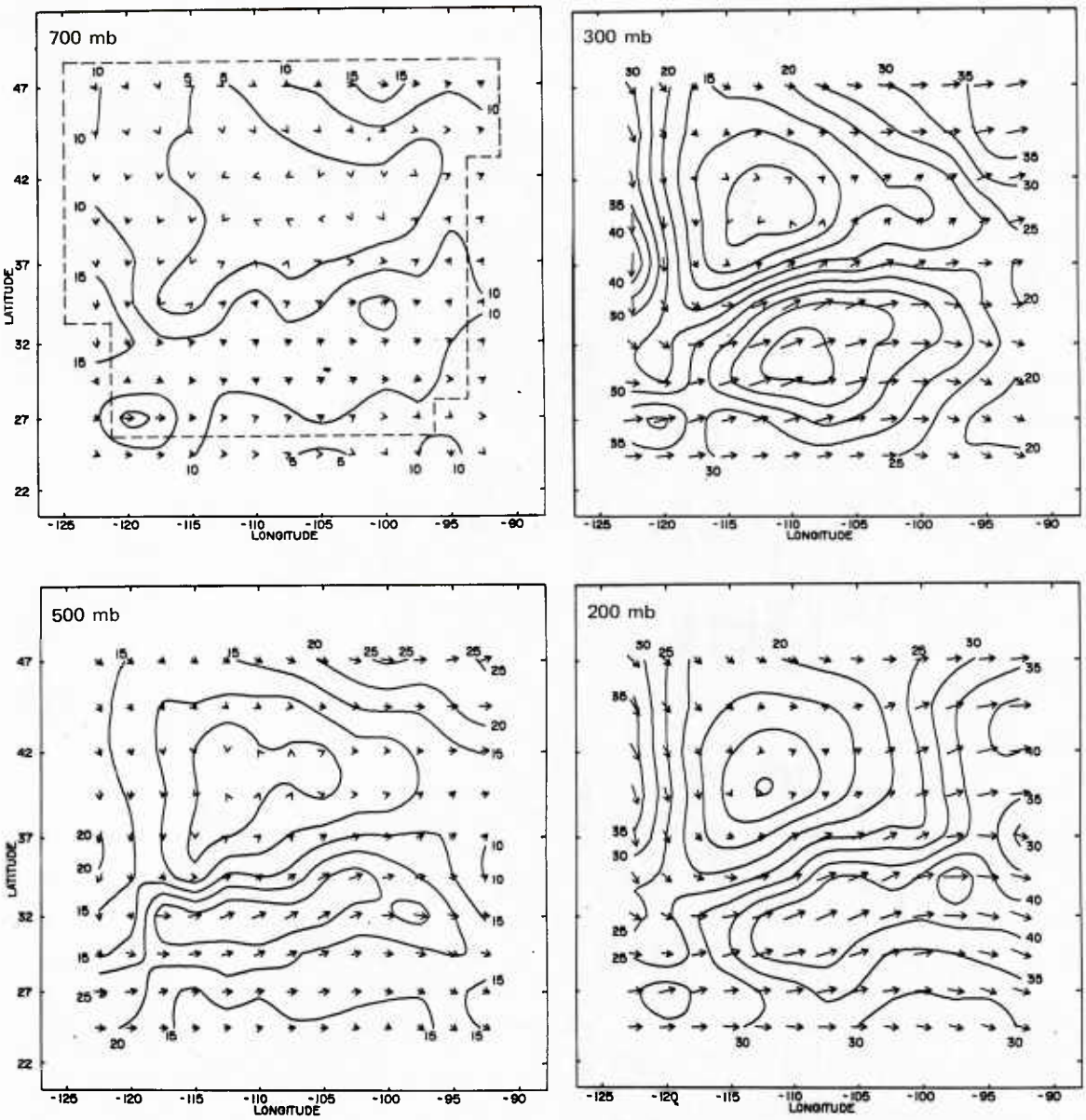

FIGURE 20 WIND FIELDS FOR 1000 GMT 2 MAY 1979 ANALYZED FROM RADIOSONDE DATA FOR 1200 GMT 2 MAY 1979

Isotachs in ms^{-1}.

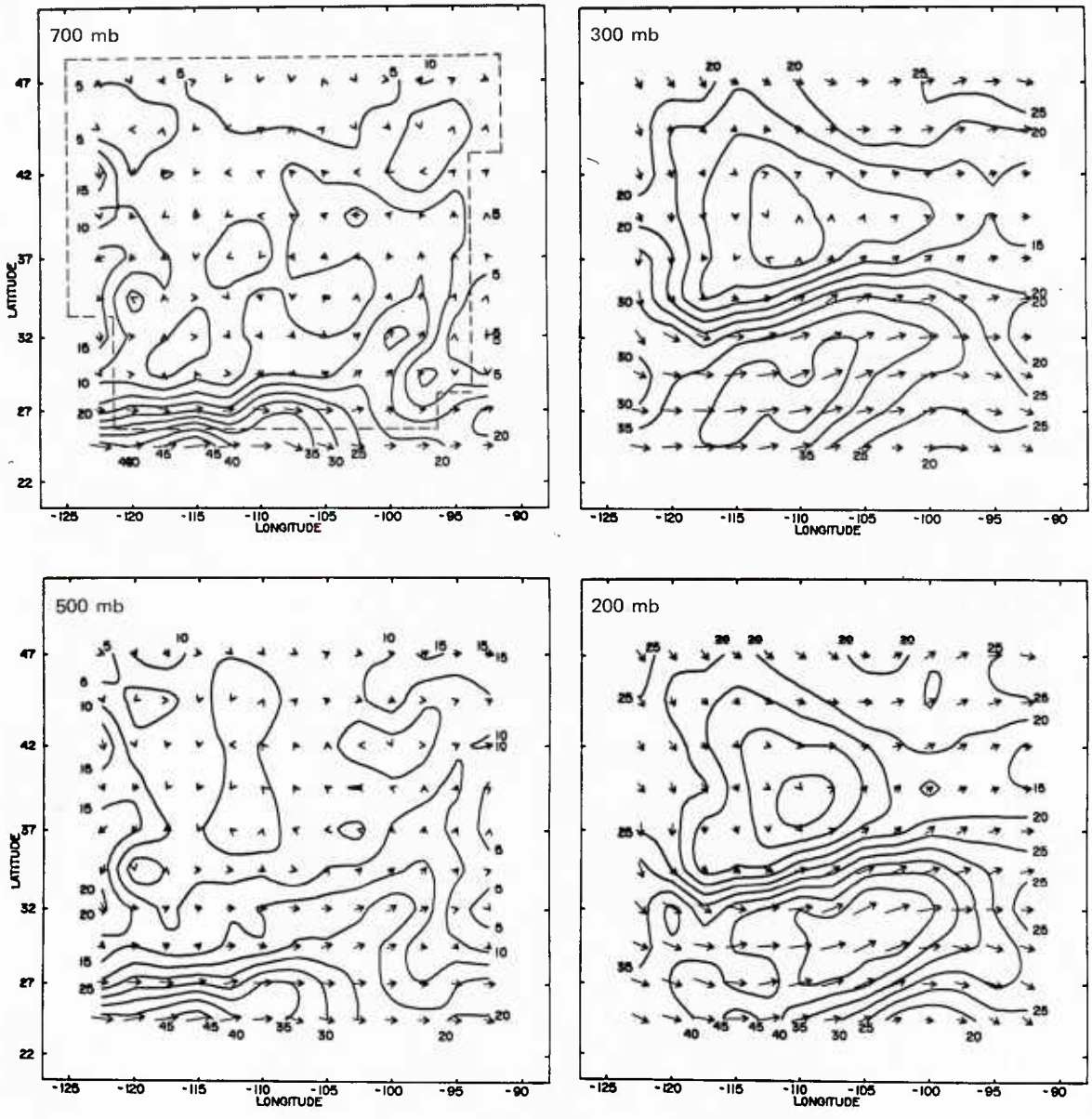

FIGURE 21 WIND FIELDS FOR 1000 GMT 2 MAY 1979 DERIVED USING TECHNIQUE T2

Isotachs in ms^{-1}.

than those (>40 ms^{-1}) for technique T2 (Figure 21); this could possibly be caused by a bias toward mid-range speeds associated with manual tracking of cloud motions (Leese et al., 1971).

2. Technique T4 Results

The results for technique T4, which are shown in Figure 22, are also relatively good. The results for the two higher levels (300 and 200 mb) are similar to those of technique T2; but the T4 results for the lower two levels are definitely superior, and are quite close to those of the radiosonde wind analyses.

3. Summary

In this case, only techniques T2 and T4 were tested. Good results were obtained, probably because of better satellite data than in the other cases and a closer agreement between the thermal winds and actual wind shear.

D. Root-Mean-Square Errors (rmse) and Scatter Diagrams

A summary of the results of the testing are shown in Table 1. This table lists the rmse values for each technique and for the gradient wind, and the values for the mean wind in each layer. The vector rmse values were calculated at each level using the formula:

$$\text{rmse} = \left(\sum_{n=1}^{N} \left| |M - \backslash V \right|^2 / N \right)^{1/2} \qquad (6)$$

where |M and \V are the technique estimated wind vector and the radiosonde wind vector at some grid point, and the summation is made over N grid points. The grid points used in the rmse calculations were those that fell within the areas that contained both satellite temperature profile data and radiosonde data (areas enclosed within dashed lines shown in preceding figures). As shown by this table, technique T1 did not perform well, particularly at 200 mb in the 10 April and 14 March cases, and its testing was discontinued. It apparently could not adequately delineate the radiosonde MWL, resulting in poor results above the cloud-motion level.

The rmse values for technique T3 are only slightly different from those for technique T2 and are actually slightly higher. Since the computations using the balance equation are extensive, use of technique T3 does not appear to be warranted at this time. Technique T3 was also not tested with the 2 May case.

The two remaining techniques, T2 and T4, appear to give reasonable rmse values. The eigenvector technique (T4) gives lower rmse values

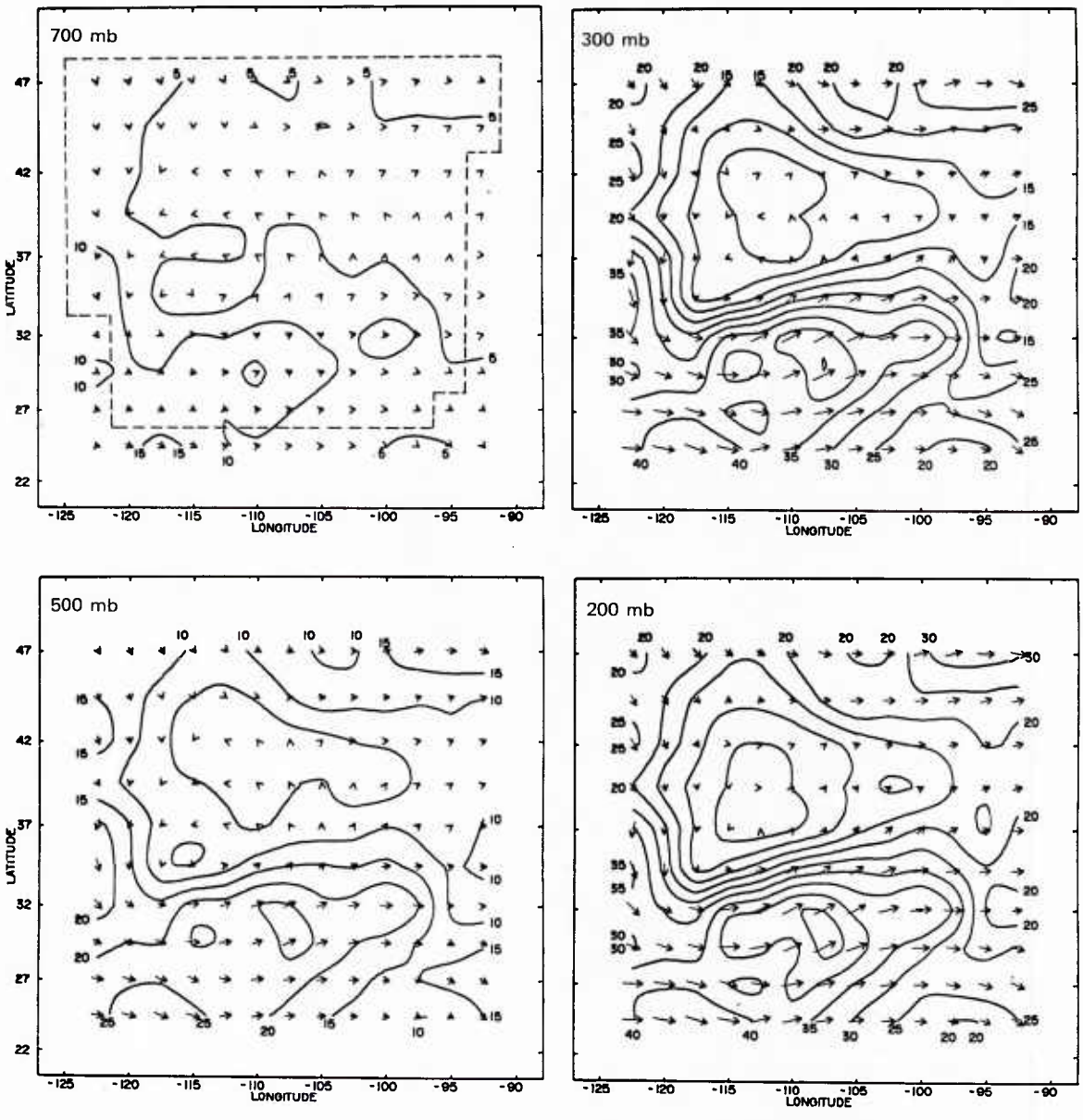

FIGURE 22 WIND FIELDS FOR 1000 GMT 2 MAY 1979 DERIVED USING TECHNIQUE T4
Isotachs in ms^{-1}.

Table 1

VECTOR RMSE OF WINDS DERIVED BY
TECHNIQUES T1, T2, T3, T4 COMPARED TO RADIOSONDE WINDS*
(All values in ms^{-1})

Case/Pressure	Mean Wind Speed	Vector Rmse				
		Gradient Wind	T1	T2	T3	T4
10 April 1979						
850 mb	10.7	5.9	--	12.4	12.9	6.0
500	19.2	10.0	9.0	12.4	13.1	7.9
300	33.4	17.3	11.4	11.4	11.6	11.8
200	43.4	22.5	22.7	17.4	19.0	18.0
14 March 1979						
850 mb	13.1	7.7	--	10.8	--	9.2
500	25.0	10.3	13.4	11.7	12.5	9.6
300	38.2	12.3	11.9	11.3	11.6	11.8
200	43.4	--	19.8	10.9	11.8	--
2 May 1979						
700 mb	9.8	6.5	+	10.9	+	5.3
500	17.0	8.6		11.2		7.2
300	28.1	13.0		9.4		10.2
200	29.6	13.2		10.9		11.1

*The radiosonde wind errors associated with high-wind conditions (or low elevation angles) are 3 ms^{-1} at 700 mb, 6 ms^{-1} at 500 mb, 8 ms^{-1} at 300 mb, and 11 ms^{-1} at 200 mb (NWS, 1967/1977).

+Testing discontinued: See text.

below the cloud-motion level (300 mb). This is reasonable, since these values are based not only on satellite cloud-motion and thermal-wind data, but also on known surface geostrophic-wind values. If technique T2 were modified to use the satellite thermal winds to interpolate wind values between the cloud motions and surface geostrophic winds, the results for T2 would probably be very similar to those for T4. Above the cloud-motion level, both techniques T2 and T4 give similar rmse values.

The calculated rmse values for the satellite gradient winds are also shown in Table 1. The values listed for the 500-mb level (10.0, 10.3 and 8.6 ms^{-1}) are very close to the rmse value (9.9 ms^{-1}) given by Thomasell and Shen (1980) for gradient winds derived from NIMBUS 6 microwave data. However, as shown for the 10 April case, the gradient wind errors can increase dramatically with height, indicating the importance of introducing the cloud-motion values at some high level, such as the 300-mb level.

The rmse values for the most promising techniques (T2 and T4) were based on comparisons with radiosonde measurements which can also contain large errors (listed in footnote of Table 1). The T2 and T4 results are superior to the use of purely gradient winds and their rmse values could probably be significantly reduced by the use of more accurately processed cloud-motion heights and thermal winds from satellite data.

Scatter diagrams for the most successful technique (T4) in its application to Test Cases I, II, and III are shown in Figures 23, 24, and 25. These figures compare both the wind speeds [part (a)] and directions [part (b)] computed by T4 with the corresponding radiosonde values. In the wind direction scatter diagrams, all points shown within the 0 to 360° range are duplicated at points outside this range for continuity purposes. The calculated rmse for the wind speeds and directions are also given in the figures, which are, of course, different from the vector rmse given in Table 1. Correlation coefficients (r) are also given for the wind speeds.

E. Cloud-Motion Height Errors

In this study all cloud motions used were those assigned a cloud height of 300 mb. However, the cloud-motion measurements in these test cases had been simply set at a mandatory level that was nearest to the height estimated from the infrared radiance value.

The graphical displays of the results generated for all of the test cases (Section IV-A to IV-C) indicated that the cloud motions had generally been assigned to a level too high in the atmosphere. To assess this more objectively, calculations were made to determine the level of best fit; that is, the level at which the cloud motions are in best agreement with the radiosonde wind field. Figure 26 shows the rmse that were obtained when the 300-mb cloud motions were compared to the radiosonde winds at different

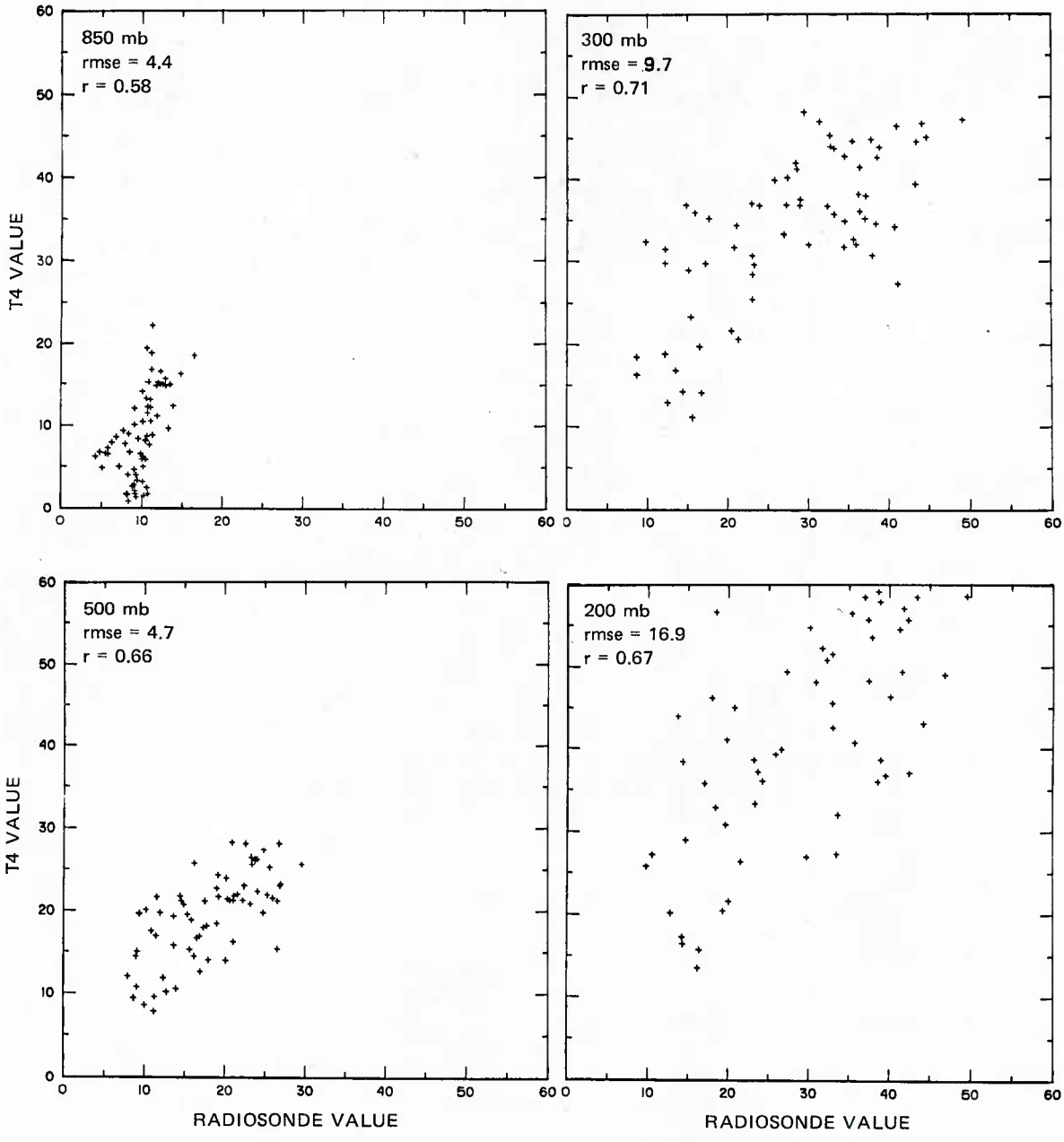

(a) WIND SPEEDS — ms^{-1}

FIGURE 23 SCATTERGRAM SHOWING T4 CALCULATED VALUES AS A FUNCTION OF RADIOSONDE VALUES FOR TEST CASE I, 10 APRIL 1979

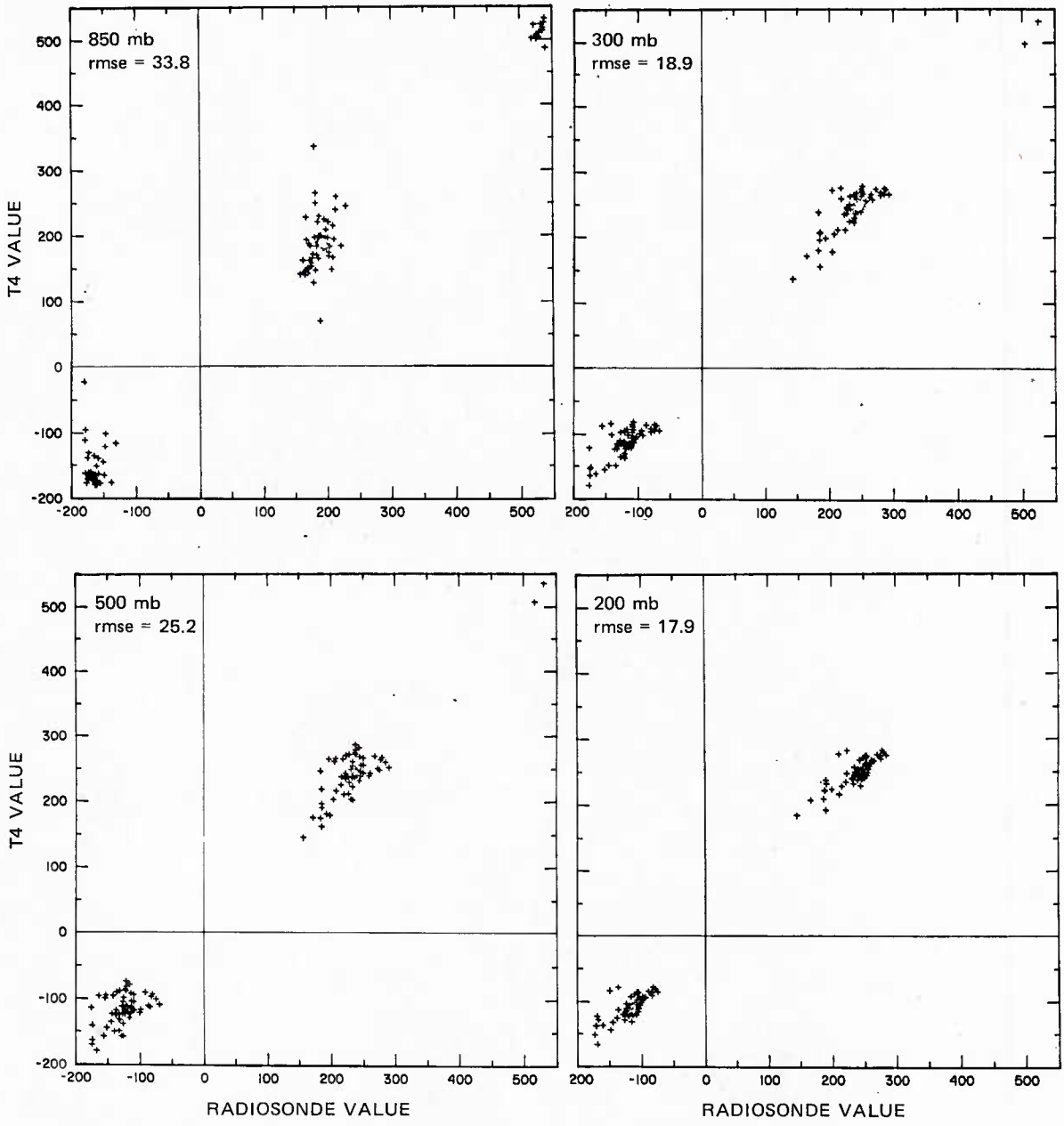

(b) WIND DIRECTION — degrees

FIGURE 23 SCATTERGRAM SHOWING T4 CALCULATED VALUES AS A FUNCTION OF RADIOSONDE VALUES FOR TEST CASE I, 10 APRIL 1979 (Concluded)

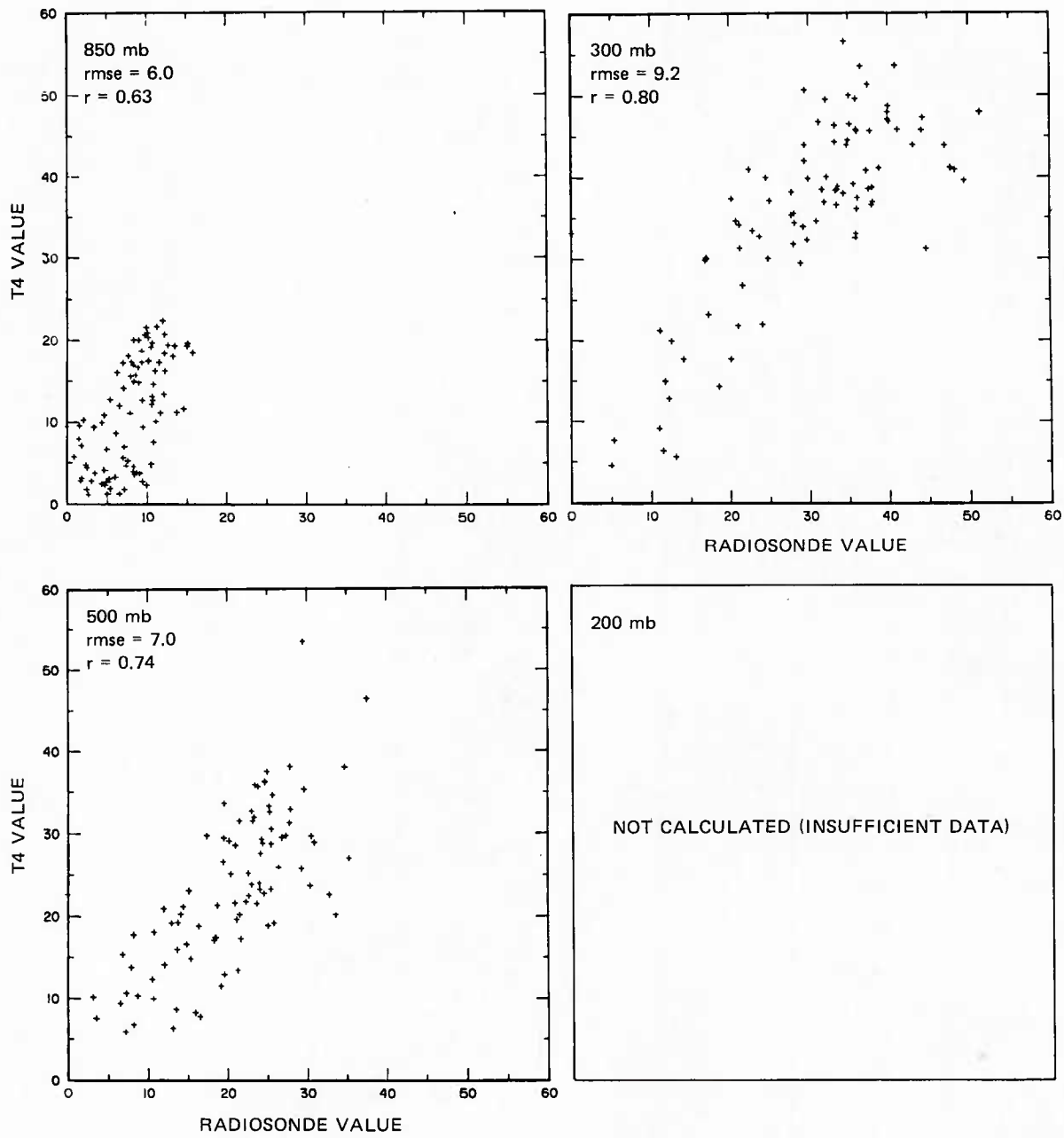

(a) WIND SPEEDS — ms^{-1}

FIGURE 24 SCATTERGRAM SHOWING T4 CALCULATED VALUES AS A FUNCTION OF RADIOSONDE VALUES FOR TEST CASE II, 14 MARCH 1979

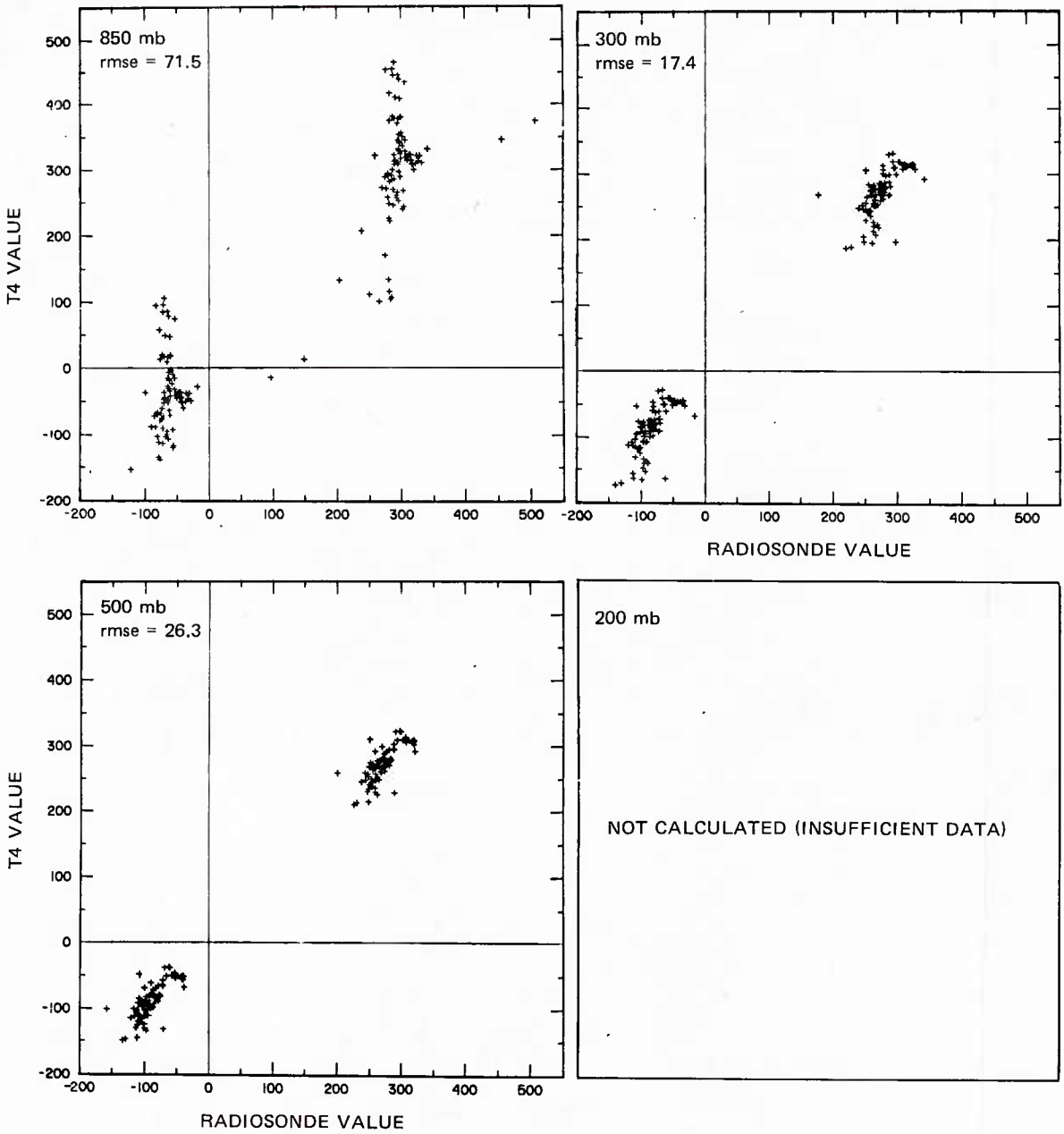

(b) WIND DIRECTIONS — degrees

FIGURE 24 SCATTERGRAM SHOWING T4 CALCULATED VALUES AS A FUNCTION OF RADIOSONDE VALUES FOR TEST CASE II, 14 MARCH 1979 (Concluded)

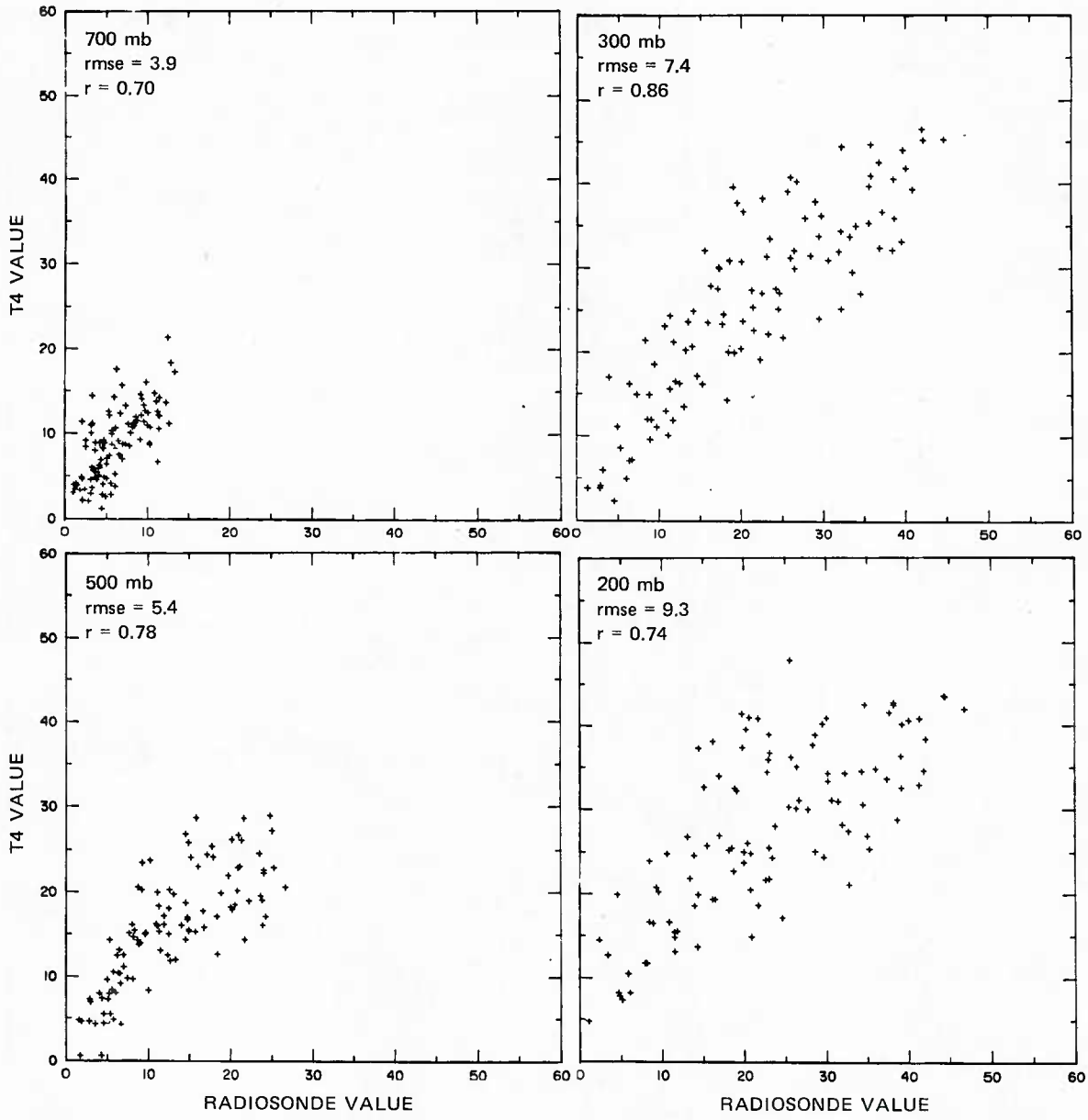

FIGURE 25 SCATTERGRAM SHOWING T4 CALCULATED VALUES AS A FUNCTION OF RADIOSONDE VALUES FOR TEST CASE III, 2 MAY 1979

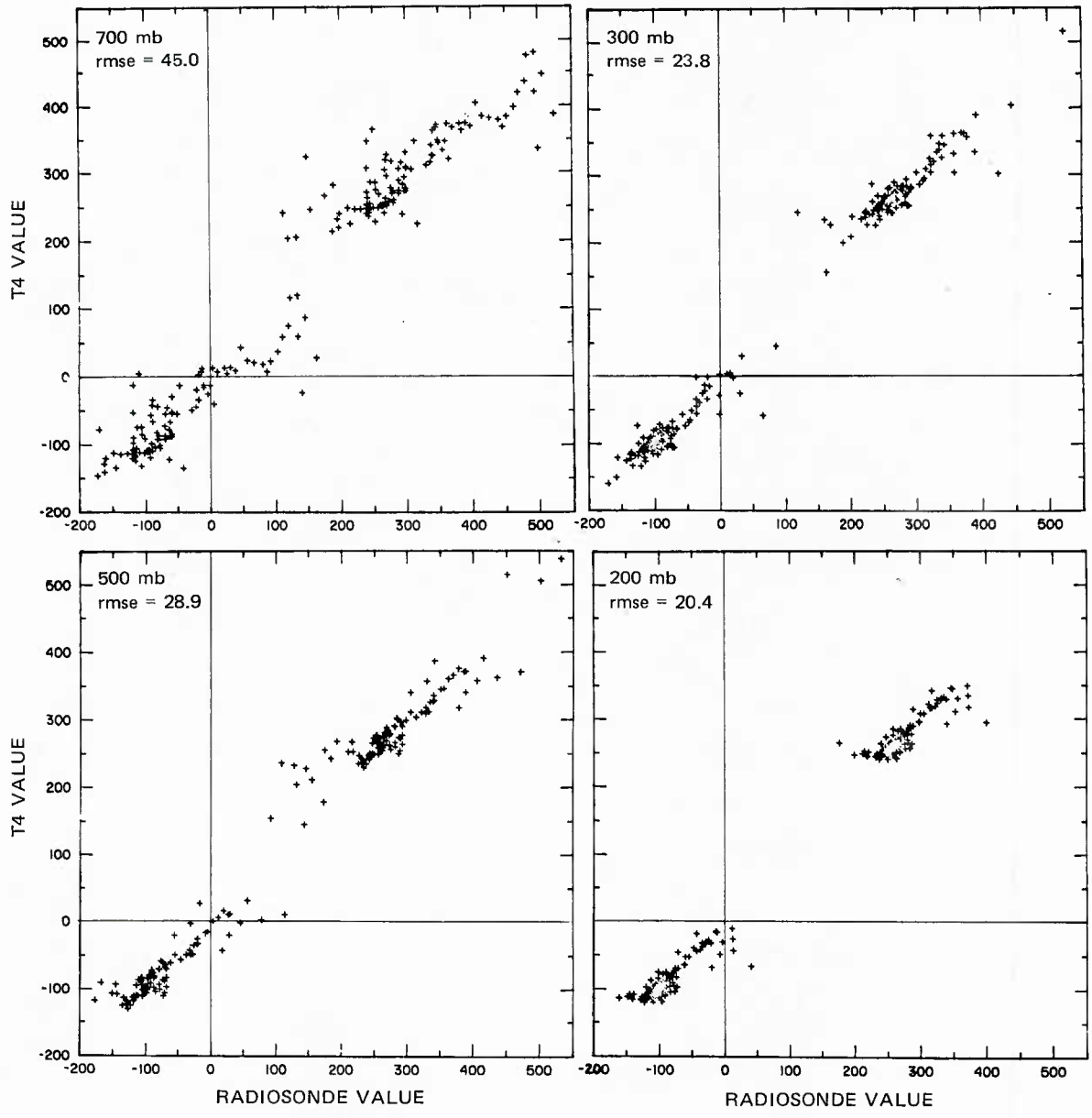

(b) WIND DIRECTIONS — degrees

FIGURE 25 SCATTERGRAM SHOWING T4 CALCULATED VALUES AS A FUNCTION OF RADIOSONDE VALUES FOR TEST CASE III, 2 MAY 1979 (Concluded)

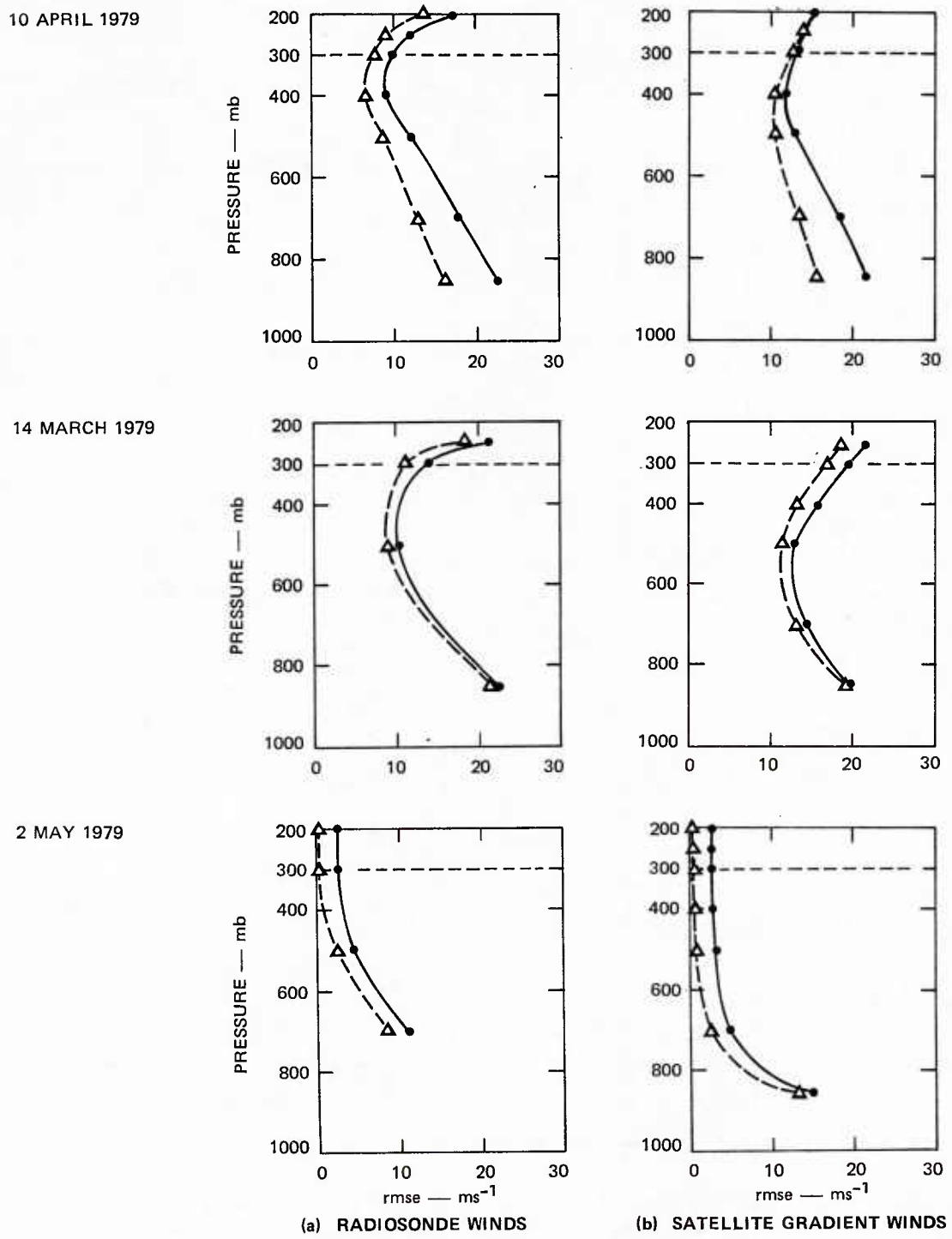

FIGURE 26 ROOT-MEAN-SQUARE ERROR PROFILES FOR CLOUD MOTIONS COMPARED WITH RADIOSONDE WINDS AND SATELLITE GRADIENT WINDS

Dashed lines show results obtained when cloud motions are first made nondivergent.

levels (solid lines in the left column of Figure 26). These rmse values were calculated at each level using the formula given in Eq. (6), but where |M and \V are now the analyzed cloud-motion vector and the analyzed radiosonde wind vector at some grid point. The summation is again made over N grid points, but the grid points used in this rmse calculations were those that fell within the areas that contained all three types of data (cloud motion, satellite temperature profile, and radiosonde).* The best fit (lowest rmse) for the first two test cases occurs at some level noticeably lower than the 300-mb level. In the 10 April case it appears to occur at, or slightly above 400 mb; and in the 14 March case between the 500- and 400-mb levels. The rmse curves for the 2 May case do not clearly depict any level of best fit, because the wind field was relatively similar at all levels above 500 mb.

Rmse profile values for the cloud motions were also calculated by comparing the cloud motions with the satellite gradient winds, rather than the radiosonde winds--the resulting rmse profiles are also shown in Figure 26 (solid lines in right column). The level of best fit now tends to occur somewhat lower: between 500 and 400 mb for the 10 April case and between 600 and 500 mb for the 14 March case.

The dashed lines in Figure 26 show the rmse that were obtained when the cloud motions were first made nondivergent. The effect was to decrease all the rmse values which is reasonable since a large part of the random error in the cloud-motion measurement is eliminated when the divergent component is eliminated. However, both the solid and dashed rmse curves give about the same result for the level of best fit.

The effects of applying the cloud motions to a level approximately 100-mb too high would be significant for the 10 April and 14 March cases. This is particularly true for technique T2, which does not have any control mechanism to ensure that the values are reasonable near the surface.

F. Modified Results For Test Case II: 14 March 1979

To illustrate the significance of the possible errors in the cloud-motion height assignment, a repeat calculation was made for Test Case II using technique T2. Test Case II was selected because it showed the greatest discrepancy between the height (300 mb) assigned to the cloud motions and the height of best fit (500 to 400 mb). Technique T2 was used because it would be more affected by incorrect cloud-motion heights than would T4. In the repeat calculation the following was performed:

---

* In the rmse calculations shown in Table 1, the grid points used were required to only lie within areas that contained satellite temperature profile data and radiosonde data.

- The cloud motions, originally assigned to 300 mb, were assumed instead to apply to both the 500- and 400-mb levels, because the best-fit level fell in between. Thus, nondivergent cloud-motion analyses were made for both of these levels using the same cloud motions but different gradient-wind first-guess fields.
- The wind fields below 500 mb and above 400 mb were then derived using the thermal wind to approximate the change of wind with height; that is technique T2 was applied below 500 mb and above 400 mb.

The graphical display of the wind fields obtained in this T2 calculation for Test Case II are shown in Figure 27. These results show a better agreement with the radiosonde analyses (Figure 15) than did the previous T2 analyses for this case (Figure 16), as would be expected. Scatter diagrams comparing the wind speeds and directions of this modified T2 analyses with those of the radiosonde analyses are shown in parts (a) and (b) of Figure 28. The scatter diagram results for Test Case II are comparable to those shown for T4 in Figure 24 although an improved agreement would also be achieved for T4 if reassigned cloud-motion heights were used in its application.

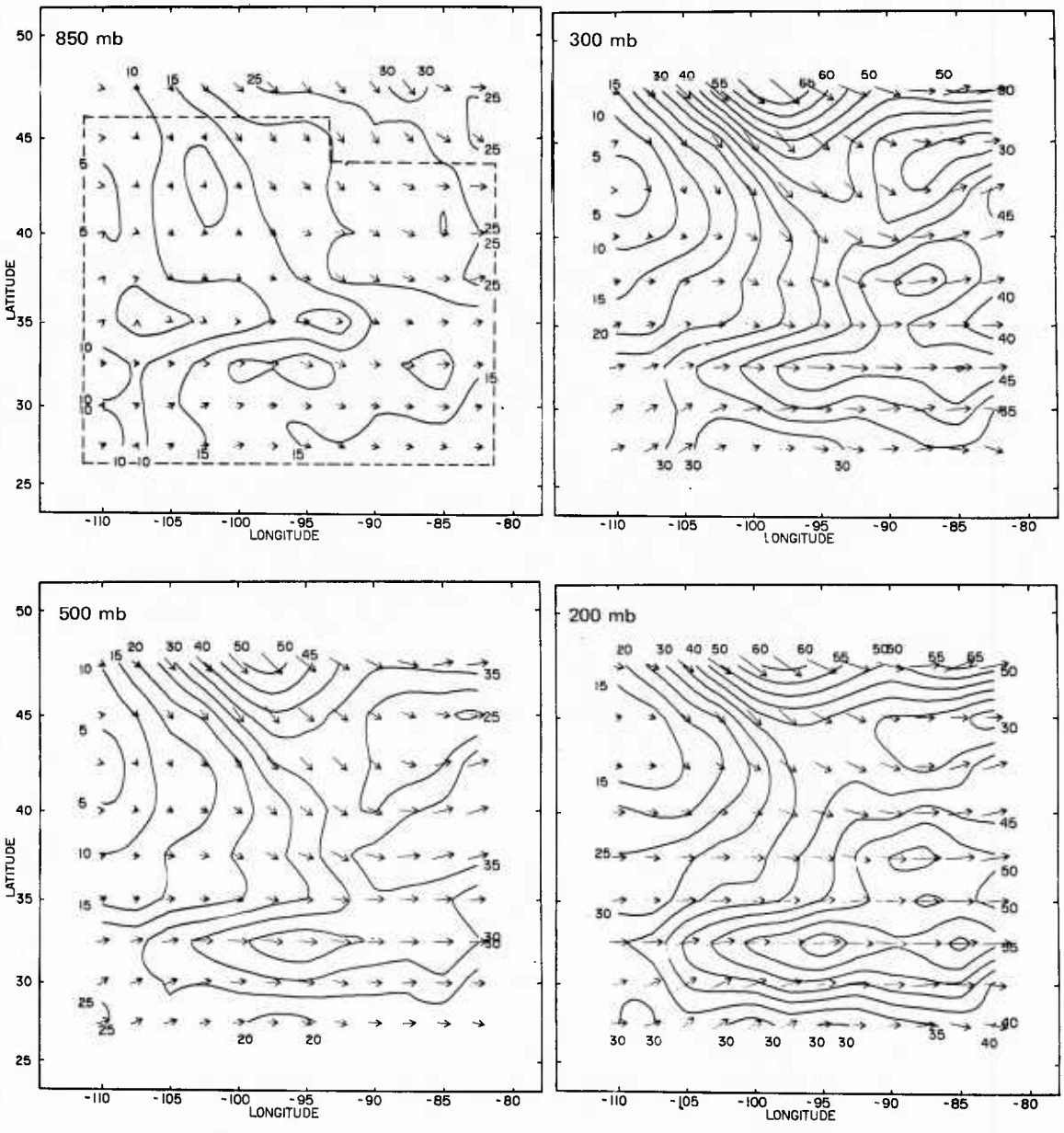

FIGURE 27 WIND FIELDS FOR 1000 GMT 14 MARCH 1979 DERIVED USING TECHNIQUE T2 AND MODIFIED CLOUD-MOTION HEIGHT ASSIGNMENT

Isotachs in ms^{-1}.

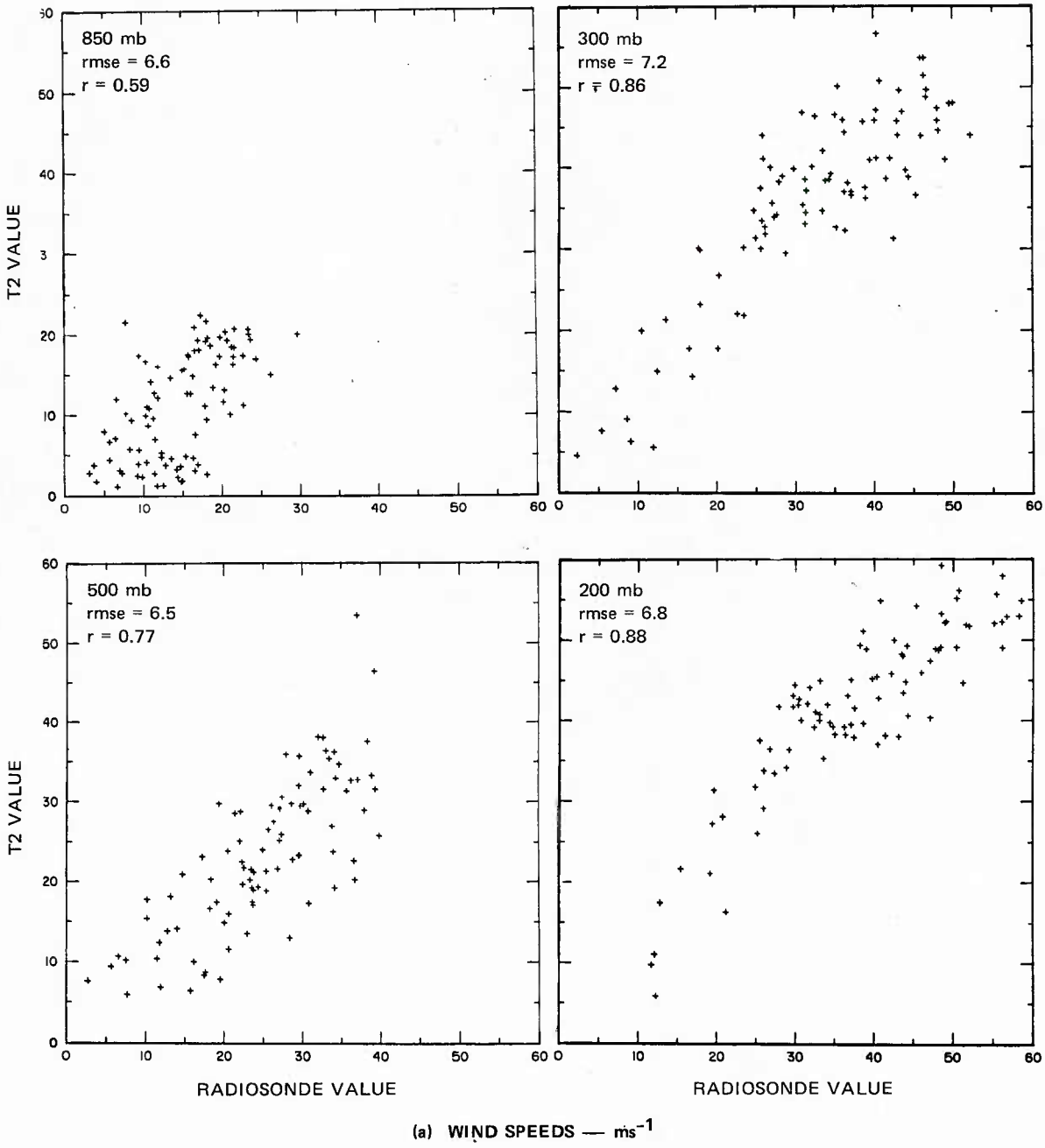

FIGURE 28 SCATTERGRAM SHOWING MODIFIED T2 CALCULATED VALUES AS A FUNCTION OF RADIOSONDE VALUES FOR TEST CASE II, 14 MARCH 1979

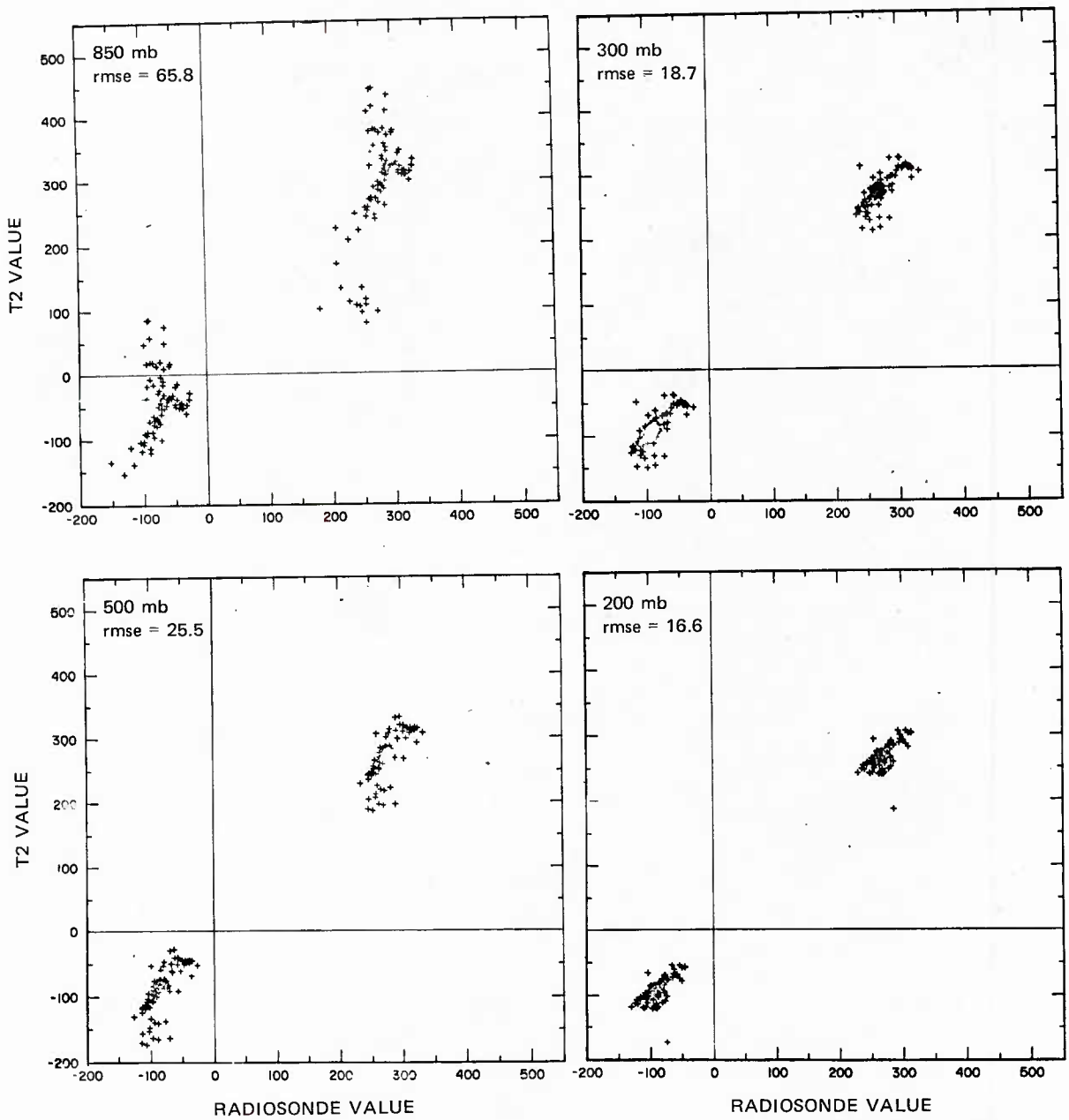

(b) WIND DIRECTIONS — degrees

FIGURE 28 SCATTERGRAM SHOWING MODIFIED T2 CALCULATED VALUES AS A FUNCTION OF RADIOSONDE VALUES FOR TEST CASE II, 14 MARCH 1979 (Concluded)

V SUMMARY AND CONCLUSIONS

In this study, four different techniques were tested for constructing wind profiles from satellite cloud-motion and temperature-profile data. The techniques were tested on three cases with TIROS-N temperature profile and GOES cloud-motion measurements. The four techniques are:

- T1--which is based on an attempt to locate the maximum wind level from the temperature structure characteristics. This technique was not successful because of the difficulty of accurately identifying the maximum wind level and because the cases did not have the classical features of jet streams upon which the concept was based.
- T2--which uses the thermal wind to build upward and downward from the cloud-motion level. This technique gave good results close to the cloud-motion level, but poorer results elsewhere, particularly near the surface.
- T3--which attempts to improve upon T2 by the introduction of the balance relationship. This technique gave some improvements in high-speed flow but did not result in any overall improvement over T2.
- T4--which is based on an eigenvector approach. This technique gave the best results principally because the surface geostrophic wind is used in its application--thus producing better results near the surface.

All the techniques gave definitely improved wind values at the cloud-motion level as compared with a geostrophic or gradient wind buildup from the surface. The differences between the calculated winds of the techniques and the radiosonde winds were caused by:

- Errors in the cloud-height estimates. These errors might be satisfactorily reduced by the use of more accurate algorithms based on satellite temperature sounding data or by the use of a cloud-motion level that gives the best fit with the satellite gradient wind profile.
- Errors and inconsistency in the satellite temperature-profile data. A combination of improved retrieval procedures and data editing should improve on the reliability and quality of these data.
- Differences between the geostrophic and actual winds. However, no significant improvement in the results was obtained by the use of the balance relationship.

- The errors of radiosonde data and the inconsistency between the spatial representatives of satellite temperature data and of radiosonde temperature data. These types of problems present basic limitations upon the techniques which can only be partially removed by smoothing.

Although the errors associated with the techniques are greater than would be desired, the results from this study are promising, particularly for application to data-sparse regions and for studying the detailed evolution of events using geosynchronous-type satellite data. Further investigations that would be of value are:

- Refinement of techniques T2 and T4. Technique T2, which has the advantage of being simpler, should be tested using surface data to permit a better comparison with T4. Technique T4 has the advantage that it can be applied directly to each cloud-motion measurement for deriving wind profiles at that point. (These profiles could then be analyzed onto the three-dimensional mesh.)
- Use of the geostationary VAS satellite data. This satellite is now in operation and will be providing continuous temperature sounding data for the global area within its view. Combined TIROS-N and VAS data sets, which should be available in the near future, will provide a good basis for further testing of the techniques.
- Use of additional data types, such as the recent high-quality automated aircraft reports, constant-level balloon measurements, and SEASAT winds. The SEASAT winds would be particularly valuable, since they would provide surface values over oceanic areas for use in calculating wind profiles. Some SEASAT data are available that may coincide with available temperature sounding data, so that this idea could be tested.
- Testing the techniques over tropical areas. In the equatorial zones, the geostrophic and thermal-wind approximations are not generally valid; however, they may still present a suitable guide for interpolating between a surface wind and a cloud motion. The winter MONEX data for the Malaysia area could provide cases for study.
- Testing other types of techniques, possibly based on statistical profile relationships similar to that attempted in technique T1. Use of eigenvectors would probably be useful in such an attempt, since the number of variables between which relationships would need to be derived could be significantly reduced. This type of investigation would require processing of large amounts of data.

REFERENCES

Endlich, R.M., 1967: "An Iterative Technique for Altering the Kinematic Properties of Wind Fields," J. Appl. Meteor., Vol. 6, pp. 837-844.

Endlich, R.M., 1968: "Direct Computation of Geostrophic Winds from Observed Winds Using the Balance Equation," J. Appl. Meteor., Vol. 7, pp. 994-1003.

Endlich, R.M., 1970: "A Method for Solving the Balance Equation Using Vector Alterations to Geostrophic Winds," Tellus, Vol. 6, pp. 620-626.

Endlich, R.M. and G.S. McLean, 1960: "Analyzing and Forecasting Meteorological Conditions in the Upper Troposphere and Lower Stratosphere," Air Force Surveys in Geophysics, No. 121, 40 pp. (April).

Fleming, H.E., 1979: "Determination of Vertical Wind Shear from Linear Combinations of Satellite Radiance Gradients: A Theoretical Study," Technical Report, NPS63-79-004, U.S. Naval Post Graduate School, Monterey, California.

Hasler, A.F., W.C. Skillman, W.E. Shenk and J. Steranka, 1979: "In Situ Aircraft Verification of the Quality of Satellite Clouds Winds Over Oceanic Regions," J. Appl. Meteor., Vol. 18, pp. 1481-1489.

Hill, K., G.S. Wilson, and R.E Turner, 1979: "NASA's Participation in the AVE-SESAME 79 Program," Bull. Am. Meteor. Soc., Vol. 60, pp. 1323-1329.

Holmström, I., 1963: "On a Method for Parametric Representation of the State of the Atmosphere," Tellus, Vol. 2, pp. 127-149.

Jones, L., and R.L. Mancuso, 1979: "Aeronautical Mesoscale Analysis Techniques (AEROMAT), "User's Manual, Contract NAS4-2520, SRI International, Menlo Park, California.

Kalb, M.W., 1979: "A Technique for Utilizing Satellite Derived Geostrophic Winds," Masters Thesis, University of Wisconsin, Madison, Wisconsin.

Leese, J.A., C.S. Novak, and B.B. Clark, 1971: "An Automated Technique for Obtaining Cloud Motions from Geosynchronous Satellite Data Using Cross Corrections," J. Appl. Meteor., Vol. 10, pp. 118-132.

Lorenz, E.N., 1956: "Empirical Orthogonal Functions and Statistical Weather Prediction," Scientific Report, 1, Statistical Forecasting Project, Massachusetts Institute of Technology, Cambridge, Mass.

Ludwig, F.L. and G. Byrd, 1980: "An Efficient Method for Deriving Mass Consistent Flow Fields from Wind Observations in Rough Terrain," Atmos. Environ., Vol. 14.

Mancuso, R.L. and R.M. Endlich, 1979: "Objective Techniques of Mesoscale Analysis for the Aeronautical Flight-Test Environment," Final Report, Contract NAS4-2520, SRI International, Menlo Park, California.

Mosher, F.R., 1976: "Cloud Height Determination," Proc. Symp. Meteor. Observations from Space--Contributions to FGGE, pp. 201-204.

NWS, 1967/1977: "Draft Copy of Standards for Weather Bureau Field Program," National Weather Service, Washington, D.C. (wind accuracies updated in 1977).

Phillips, N., L. McMillin, A. Gruber, and D. Wark, 1979: "An Evaluation of Early Operational Temperature Soundings from TIROS-N," Bull. Amer. Meteor. Soc., Vol. 60, pp. 1188-1197.

Smith, E.A., 1975: "The McIDAS System," IEEE Transaction of Geoscience Electronics, GE-13, No. 3, pp. 123-136.

Smith, W.L., H.M. Woolf, C.M. Hayden, D.Q. Wark and L.M. McMillin, 1979: "The TIROS-N Operational Vertical Sounder," Bull. Amer. Meteor. Soc., Vol. 60, pp. 1177-1187.

Viezee, W., S.M. Serebreny and R.L. Mancuso, 1972: A Sample Computation of Kinematic Properties from Cloud Motion Vectors," J. Appl. Meteor., Vol. 11, pp. 731-741.

Viezee, W., D.E. Wolf, and R.M. Endlich, 1977: "Evaluation of the FIB Methodology for Application to Cloud Motion Wind Data," Technical Report TR-77-08 (SRI), Contract NOO228-76-C-3182, SRI International Menlo Park, California.

Williams, S.F., J.R. Scoggins, N. Horvath and K. Hill, 1980: "A Preliminary Look at AVE-SESAMET Conducted on April 10-11, 1979," NASA Technical Memorandum 78262, Marshall Space Flight Center, Alabama.

Wilson, T.A. and D.D. Houghton, 1979: "Mesoscale Wind Fields for a Severe Storm Situation Determined from SMS Cloud Observations." Mon. Wea Rev., Vol. 109, pp. 1198-1209.

Appendix A

ANALYSES FOR 2000 GMT 10 APRIL 1979 BASED ON AVE RADIOSONDE DATA

Appendix A

ANALYSES FOR 2000 GMT 10 APRIL 1979 BASED ON AVE RADIOSONDE DATA

AVE radiosonde data at 300 mb for 2000 GMT 10 April 1979 are shown in Figure A-1(a). These data much more densely spaced than the standard radiosonde data, are for the same time as the satellite data of Test Case I. Wind and temperature/thermal-wind analyses of these data are shown in Figure A-1 (b) and (c). These analyses may be compared with those made for the standard data [see Figures 4(c), 5(c), and 6(b) of text].

Although the AVE data analyses show more detail, they are basically consistent with those based on the standard observations, and the time interpolation procedure used in the study to produce the 2000 GMT analyses [such as Figure 5(c)] appears to be justified. The differences between satellite and radiosonde analyses would, therefore, have to be attributable to either the current inaccuracies of satellite-data or the inconsistencies between the two types of measurement; that is, a radiosonde temperature measurement is essentially for a point location, but a satellite measurement is for a large volume of both considerable vertical thickness and horizontal size.

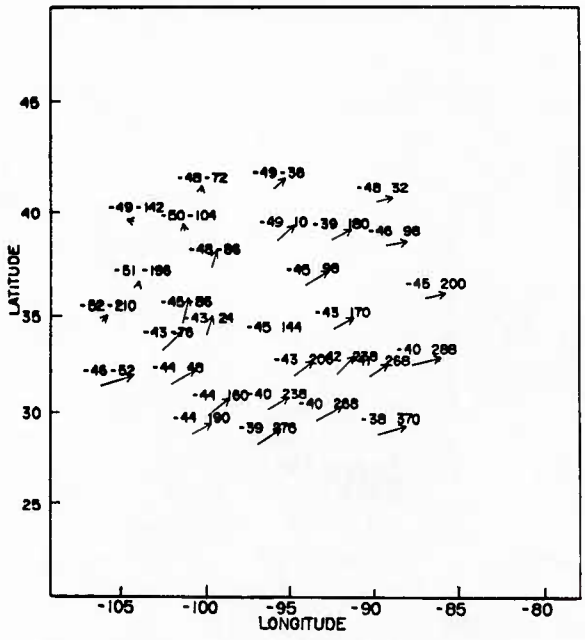

(a) OBSERVED VALUES

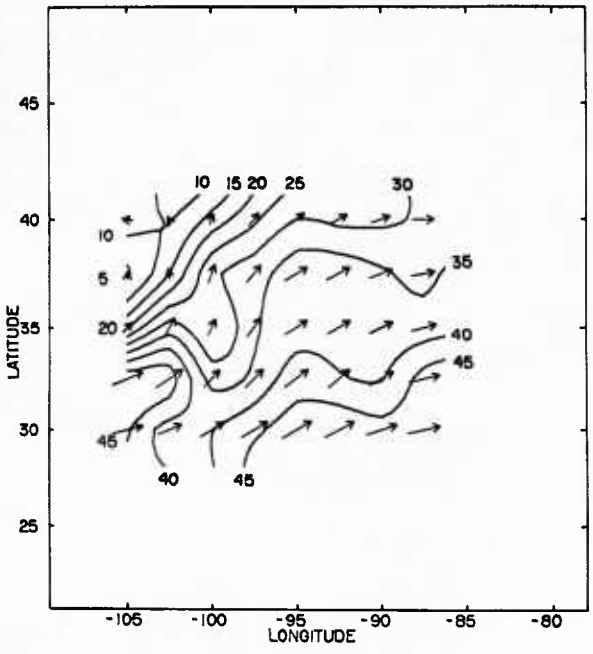

(b) WIND ANALYSES

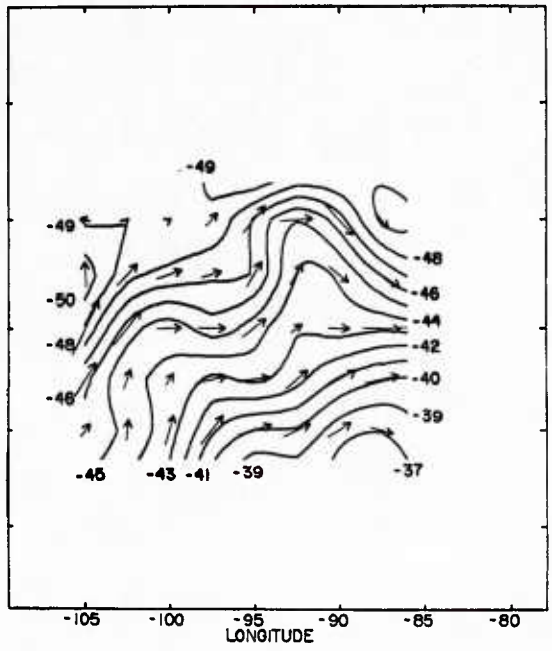

(c) TEMPERATURE ANALYSES

FIGURE A-1 AVE WIND AND TEMPERATURE VALUES AT 300mb FOR 2000 GMT 10 APRIL 1979

DISTRIBUTION

COMMANDER IN CHIEF
U.S. PACIFIC FLEET
PEARL HARBOR, HI 96860

COMMANDER
SEVENTH FLEET (N30W)
ATTN: FLEET METEOROLOGIST
FPO SAN FRANCISCO 96601

COMMANDER
NAVAL SURFACE FORCE
U.S. PACIFIC FLEET
CODE N331A
NAVAL AMPHIBIOUS BASE
SAN DIEGO, CA 92155

COMMANDER
AMPHIBIOUS GROUP 1
ATTN: METEOROLOGICAL OFFICER
FPO SAN FRANCISCO 96601

OFFICER IN CHARGE
OPERATIONAL TEST & EVALUATION
FORCE, SUNNYVALE
NAVAL AIR STATION
MOFFETT FIELD, CA 94035

COMMANDER
U.S. NAVAL SUPPORT FORCE
ANTARCTICA
FPO SAN FRANCISCO 96601

COMMANDER
SURFACE WARFARE DEVELOPMENT GRP
NAVAL AMPHIBIOUS BASE, LITTLE CREEK
NORFOLK, VA 23521

COMMANDER NAVAL SURFACE GROUP
WESTERN PACIFIC
FPO SAN FRANCISCO 96601

COMMANDING OFFICER
USS FORRESTAL (CV-59)
ATTN: METEOROLOGICAL OFFICER
FPO MIAMI 34080

COMMANDING OFFICER
USS INDEPENDENCE (CV-62)
ATTN: METEOROLOGICAL OFFICER
FPO NEW YORK 09537

COMMANDING OFFICER
USS NIMITZ (CVN-68)
ATTN: METEOROLOGICAL OFFICER
FPO NEW YORK 09542

COMMANDING OFFICER
USS CONSTELLATION (CV-64)
ATTN: METEOROLOGICAL OFFICER
FPO SAN FRANCISCO 96635

COMMANDING OFFICER
USS ENTERPRISE (CVN-65)
ATTN: METEOROLOGICAL OFFICER
FPO SAN FRANCISCO 96636

COMMANDING OFFICER
USS KITTY HAWK (CV-63)
ATTN: METEOROLOGICAL OFFICER
FPO SAN FRANCISCO 96634

COMMANDING OFFICER
USS MIDWAY (CV-41)
ATTN: METEOROLOGICAL OFFICER
FPO SAN FRANCISCO 96631

COMMANDING OFFICER
SARATOGA NUCLEUS CREW
ATTN: METEOROLOGICAL OFFICER
FPO NEW YORK 09501

COORDINATOR
NATIONAL ATMOSPHERIC RSCH PROGRAM
INSTITUTE OF PHYSICS
ACADEMIA SINICA
TAIPEI, TAIWAN

COMMANDING OFFICER
USS GUADALCANAL (LPH-7)
ATTN: METEOROLOGICAL OFFICER
FPO NEW YORK 09562

COMMANDING OFFICER
USS GUAM (LPH-9)
ATTN: METEOROLOGICAL OFFICER
FPO NEW YORK 09563

COMMANDING OFFICER
USS INCHON (LPH-12)
ATTN: METEOROLOGICAL OFFICER
FPO NEW YORK 09529

COMMANDING OFFICER
USS IWO JIMA (LPH-2)
ATTN: METEOROLOGICAL OFFICER
FPO NEW YORK 09561

COMMANDING OFFICER
USS NEW ORLEANS (LPH-11)
ATTN: METEOROLOGICAL OFFICER
FPO SAN FRANCISCO 96627

COMMANDING OFFICER
USS LEXINGTON (AVT-16)
FPO MIAMI 34088

AVIATION SUPPORT DEPT. OFFICER
NSFA, DETACHMENT CHRISTCHURCH
ANTARCTIC DEV. SQUADRON 6-VXE-6
FPO SAN FRANCISCO 96690

SACLANT
ASW RESEARCH CENTER
APO NEW YORK 09019

SPECIAL ASST. TO THE ASST.
SECRETARY OF THE NAVY (R&D)
ROOM 4E741
THE PENTAGON
WASHINGTON, DC 20350

CHIEF OF NAVAL RESEARCH
LIBRARY SERVICES (CODE 734)
RM 633, BALLSTON TOWER #1
800 QUINCY STREET
ARLINGTON, VA 22217

OFFICE OF NAVAL RESEARCH
CODE 465
ARLINGTON, VA 22217

DR. R. W. JAMES
OPNAV 952D1
U.S. NAVAL OBSERVATORY
34th & MASSACHUSETTS AVE, N.W.
WASHINGTON, DC 20390

CHIEF OF NAVAL MATERIAL
(MAT-034)
NAVY DEPARTMENT
WASHINGTON, DC 22332

NAVAL DEPUTY TO THE
ADMINISTRATOR, NOAA
ROOM 200, PAGE BLDG. #1
3300 WHITEHAVEN ST. NW
WASHINGTON, DC 20235

OFFICER IN CHARGE
NAVOCEANCOMDET
NAVAL STATION
FPO SEATTLE 98791

OFFICER IN CHARGE
US NAVOCEANCOMDET
BOX 81
U.S NAVAL AIR STATION
FPO SAN FRANCISCO 96637

CENTRAL WX BUREAU
64, KUNG YUAN RD
TAIPEI, TAIWAN 100

DEPARTMENT OF ATMOS. SCIENCE
NATIONAL TAIWAN UNIVERSITY
TAIPEI, TAIWAN 107

OFFICER IN CHARGE
NAVOCEANCOMDET
U.S. NAVAL AIR FACILITY
FPO SEATTLE 98767

CHIEF PETTY OFFICER IN CHARGE
NAVOCEANCOMDET
CHASE FIELD
BEEVILLE, TX 78103

OFFICER IN CHARGE
NAVOCEANCOMDET
NAVAL AIR STATION
CORPUS CHRISTI, TX 78419

OFFICER IN CHARGE
US NAVOCEANCOMDET
BOX 63
U.S. NAVAL AIR STATION
FPO SAN FRANCISCO 96654

OFFICER IN CHARGE
NAVOCEANCOMDET
BOX 9048
NAVAL AIR STATION
KEY WEST, FL 33040

CHIEF PETTY OFFICER IN CHARGE
NAVOCEANCOMDET
NAVAL AIR STATION
KINGSVILLE, TX 78363

OFFICER IN CHARGE
NAVOCEANCOMDET
NAVAL AIR STATION
WHITING FIELD
MILTON, FL 32570

OFFICER IN CHARGE
NAVOCEANCOMDET
NAVAL AIR STATION
MERIDIAN, MS 39301

OFFICER IN CHARGE
NAVOCEANCOMDET
NAVAL AIR STATION
MOFFETT FIELD, CA 94035

OFFICER IN CHARGE
US NAVOCEANCOMDET
NAPLES, BOX 23
FPO NEW YORK 09520

OFFICER IN CHARGE
NAVOCEANCOMDET
AFGWC
OFFUTT AFB, NE 68113

OFFICER IN CHARGE
NAVOCEANCOMDET
NAVAL AIR STATION
PATUXENT RIVER, MD 20670

OFFICER IN CHARGE
NAVOCEANCOMDET
U.S. NAVAL STATION
FPO MIAMI 34051

OFFICER IN CHARGE
NAVOCEANCOMDET
U.S. NAVAL AIR FACILITY
FPO NEW YORK 09523

OFFICER IN CHARGE
NAVOCEANCOMDET
NAVAL AIR STATION, OCEANA
VIRGINIA BEACH, VA 23460

OFFICER IN CHARGE
NAVOCEANCOMDET
NAVAL AIR STATION
WILLOW GROVE, PA 19090

METEOROLOGICAL DEPT.
BOX 200 LUSAKA
ZAMBIA

METEOROLOGICAL SATELLITE
CENTER
235 NAKAKIYOT 3-CHROME
KIYOSE, TOKYO 180-04
JAPAN

OFFICER IN CHARGE
US NAVOCEANCOMDET
FPO SAN FRANCISCO 96685

OFFICER IN CHARGE
US NAVOCEANCOMDET
FLEET ACTIVITIES
FPO SEATTLE 98770

COMMANDING OFFICER
NAVAL RESEARCH LAB
ATTN: LIBRARY, CODE 2620
WASHINGTON, DC 20390

COMMANDING OFFICER
OFFICE OF NAVAL RESEARCH
1030 E. GREEN STREET
PASADENA, CA 91101

OFFICE OF NAVAL RESEARCH
SCRIPPS INSTITUTION OF
OCEANOGRAPHY
LA JOLLA, CA 92037

COMMANDING OFFICER
NORDA, CODE 101
NSTL STATION
BAY ST. LOUIS, MS 39529

COMMANDER
NAVAL OCEANOGRAPHY COMMAND
NSTL STATION
BAY ST. LOUIS, MS 39529

COMMANDING OFFICER
NAVAL OCEANOGRAPHIC OFFICE
NAVY LIBRARY
NSTL STATION
BAY ST. LOUIS, MS 39522

COMMANDING OFFICER
FLENUMOCEANCEN
MONTEREY, CA 93940

OFFICER IN CHARGE
NAVOCEANCOMDET
C/O FLENUMOCEANCEN
MONTEREY, CA 93940

COMMANDING OFFICER
NAVWESTOCEANCEN
BOX 113
PEARL HARBOR, HI 96860

COMMANDING OFFICER
NAVEASTOCEANCEN
MCADIE BLDG. (U-117)
NAVAL AIR STATION
NORFOLK, VA 23511

COMMANDING OFFICER
NAVPOLAROCEANCEN
NAVY DEPT.
4301 SUITLAND RD.
WASHINGTON, DC 20390

COMMANDING OFFICER
US NAVOCEANCOMCEN
BOX 12
COMNAVMARIANAS
FPO SAN FRANCISCO 96630

COMMANDING OFFICER
US NAVOCEANCOMCEN
BOX 31
FPO NEW YORK 09540

COMMANDING OFFICER
OCEANCOMFAC
P.O. BOX 85
NAVAL AIR STATION
JACKSONVILLE, FL 32212

COMMANDING OFFICER
OFFICE OF NAVAL RESEARCH
EASTERN/CENTRAL REGIONAL
OFFICE, BLDG 114 SECT. D
666 SUMMER ST.
BOSTON, MA 02210

COMMANDING OFFICER
NAVOCEANCOMFAC
NAVAL AIR STATION, NORTH ISLAND
SAN DIEGO, CA 92135

COMMANDING OFFICER
US NAVOCEANCOMFAC
FPO SEATTLE 98762

CHAIRMAN
OCEANOGRAPHY DEPT.
U.S. NAVAL ACADEMY
ANNAPOLIS, MD 21402

COMMANDER
NAVAIRSYSCOM
ATTN: LIBRARY (AIR-00D4)
WASHINGTON, DC 20361

COMMANDER
NAVAIRSYSCOM
AIR-370
WASHINGTON, DC 20361

COMMANDER
NAVAIRSYSCOM
METEOROLOGICAL SYSTEMS DIV.
AIR-553
WASHINGTON, DC 20360

COMMANDER
NAVAIRSYSCOM, AIR-03
ATTN: CAPT C.M. RIGSBEE
WASHINGTON, DC 20361

COMMANDER
ATTN: CODE 032
NAVFACENGCOM, RESEARCH DIV.
200 STOVALL ST.
ALEXANDRIA, VA 22332

COMMANDER
NAVAL OCEAN SYSTEMS CENTER
ATTN: CODE 4473
SAN DIEGO, CA 92152

COMMANDER
EARTH & PLANETARY SCIENCES
CODE 3918
NAVAL WEAPONS CENTER
CHINA LAKE, CA 93555

COMMANDER
NAVAL SHIP RSCH & DEV CENTER
CODE 5220
BETHESDA, MD 20084

COMMANDER
ATTN: DR. B. KATZ
WHITE OAKS LAB
NAVAL SURFACE WEAPONS CENTER
SILVER SPRING, MD 20910

NAVAL SPACE SYSTEMS ACTIVITY
CODE 60
P.O. BOX 92960
WORLDWAY POSTAL CENTER
LOS ANGELES, CA 90009

COMMANDER
PACIFIC MISSILE TEST CENTER
ATTN: GEOPHYSICS OFFICER
CODE 3250
PT. MUGU, CA 93042

DEPT. OF METEOROLOGY
NAVAL POSTGRADUATE SCHOOL
MONTEREY, CA 93940

DEPT. OF OCEANOGRAPHY
NAVAL POSTGRADUATE SCHOOL
MONTEREY, CA 93940

LIBRARY
NAVAL POSTGRADUATE SCHOOL
MONTEREY, CA 93940

COMMANDING OFFICER
ATTN: WEATHER SERVICE OFFICE
MARINE CORPS AIR STATION
KANEOHE BAY, HI 96863

COMMANDING GENERAL
ATTN: WEATHER SERVICE OFFICE
MARINE CORPS AIR STATION
EL TORO
SANTA ANA, CA 92709

COMMANDING OFFICER
ATTN: WEATHER SERVICE OFFICE
MARINE CORPS AIR STATION
YUMA, AZ 85364

COMMANDER
AWS/DN
SCOTT AFB, IL 62225

3350TH TECHNICAL
TRNG GROUP
TTGU-W/STOP 623
CHANUTE AFB, IL 61868

AFGL/LY
HANSCOM AFB, MA 01731

AFGWC/DAPL
OFFUTT AFB, NE 68113

AFGL/OPI
HANSCOM AFB, MA 01731

5WW/DN
LANGLEY AFB, VA 23665

OFFICER IN CHARGE
SERVICE SCHOOL COMMAND
DET. CHANUTE/STOP 62
CHANUTE AFB, IL 61868

1ST WEATHER WING (DON)
HICKAM AFB, HI 96853

DET 4 HQ AWS/CC
APO SAN FRANCISCO 96334

DET 8, 30 WS
APO SAN FRANCISCO 96239

AFOSR/NC
BOLLING AFB
WASHINGTON, DC 20312

OFFICE OF STAFF METEOROLOGY
WESTERN SPACE & MISSILE CENTER (WE)
VANDENBERG AFB, CA 93437

COMMANDER & DIRECTOR
ATTN: DELAS-DM-A
U.S. ARMY ATMOS. SCIENCES LAB
WHITE SANDS MISSILE RANGE
WHITE SANDS, NM 88002

COMMANDING OFFICER
U.S. ARMY RESEARCH OFFICE
ATTN: GEOPHYSICS DIV.
P.O. BOX 12211
RESEARCH TRIANGLE PARK, NC 27709

DIRECTOR
DEFENSE TECH. INFORMATION CENTER
CAMERON STATION
ALEXANDRIA, VA 22314

DIRECTOR
OFFICE OF ENV. & LIFE SCI.
OFFICE OF UNDERSECRETARY OF
DEFENSE FOR RSCH & ENG (E&LS)
ROOM 3D129, THE PENTAGON
WASHIGNTON, DC 20301

CHIEF
MARINE SCIENCE SECTION
U.S. COAST GUARD ACADEMY
NEW LONDON, CT 06320

COMMANDING OFFICER
U.S. COAST GUARD
OCEANOGRAPHIC UNIT
BLDG 159-E
WASHINGTON NAVY YARD
WASHINGTON, DC 20390

COMMANDING OFFICER
USCG RESEARCH & DEVELOPMENT CENTER
GROTON, CT 06340

DIRECTOR
SYSTEMS DEVELOPMENT
NWS/NOAA
ROOM 1216 - THE GRAMAX BLDG
8060 13TH STREET
SILVER SPRING, MD 20910

DEVELOPMENT DIVISION
NATIONAL METEOROLOGICAL CENTER
NWS/NOAA
WORLD WEATHER BLDG. W32, RM 204
WASHINGTON, DC 20233

DIRECTOR
NATIONAL EARTH SAT. SERV/SEL
FB-4, S321B
SUITLAND, MD 20233

ACQUISITIONS SECTION
IRDB-D823
LIBRARY & INFO. SERV. DIV.
NOAA, 6009 EXECUTIVE BLVD.
ROCKVILLE, MD 20852

FEDERAL COORDINATOR FOR
METEOR. SERV. & SUP. RSCH.
6010 EXECUTIVE BLVD
ROCKVILLE, MD 20852

DIRECTOR
OFFICE OF PROGRAMS RX3
NOAA RSCH LABS
BOULDER, CO 80302

DIRECTOR
NATIONAL HURRICANE CENTER
NOAA, UNIV. OF MIAMI BRANCH
CORAL GABLES, FL 33124

NATIONAL WEATHER SERVICE
WORLD WEATHER BLDG.
ROOM 307
5200 AUTH ROAD
CAMP SPRINGS, MD 20023

DIRECTOR
NATIONAL SEVERE STORMS LAB
1313 HALLEY CIRCLE
NORMAN, OK 73069

NATIONAL WEATHER SERVICE,
EASTERN REGION
ATTN: WFE3
585 STEWART AVE.
GARDEN CITY, NY 11530

CHIEF, SCIENTIFIC SERVICES
NWS, CENTRAL REGION
NOAA, ROOM 1836
601 EAST 12TH STREET
KANSAS CITY, MO 64106

CHIEF, SCIENTIFIC SERVICES
NWS, SOUTHERN REGION
NOAA, ROOM 10E09
819 TAYLOR STREET
FT. WORTH, TX 76102

CHIEF, SCIENTIFIC SERVICES
NWS, PACIFIC REGION
P.O. BOX 50027
HONOLULU, HI 96850

NOAA RESEARCH FACILITIES CENTER
P.O. BOX 520197
MIAMI, FL 33152

CHIEF, OPERATIONS BRANCH
AIR RESOURCES LAB, NOAA
P.O. BOX 14985 AEC
LAS VEGAS, NV 89114

DIRECTOR
ATLANTIC OCEANO & METEOR LABS
15 RICKENBACKER CAUSEWAY
VIRGINIA KEY
MIAMI, FL 33149

DIRECTOR
GEOPHYSICAL LUID DYNAMICS LAB
NOAA, PRINCETON UNIVERSITY
P.O. BOX 308
PRINCETON, NJ 08540

NATIONAL MARINE FISHERIES SERV.
OCEAN CLIMATOLOGY PROJECT
SOUTHWEST FISHERIES CENTER
P.O. BOX 271
LA JOLLA, CA 92037

DR. MICHAEL HELFERT
SF-NOAA LIAISON MANAGER
NASA-JOHNSON SPACE CENTER
HOUSTON, TX 77058

CHIEF
MESOSCALE APPLICATIONS BRANCH
NATIONAL EARTH SATELLITE SERV.
1225 WEST DAYTON
MADISON, WI 53562

HEAD, ATMOS. SCIENCES DIV.
NATIONAL SCIENCE FOUNDATION
1800 G. STREET, NW, Rm. 644
WASHINGTON, DC 20550

LABORATORY FOR ATMOS. SCI.
NASA GODDARD SPACE FLIGHT
CENTER
GREENBELT, MD 20771

PRELIMINARY SYSTEMS DESIGN
GROUP
NASA GODDARD SPACE FLIGHT
CENTER
GREENBELT, MD 20771

EXECUTIVE SECRETARY
CAO COMMITTEE ON ATMOS. SCI.
NATIONAL SCIENCE FOUNDATION
ROOM 510
1800 G STREET NW
WASHINGTON, DC 20550

NATIONAL CENTER FOR ATMOS. RSCH
LIBRARY ACQUISITIONS
P.O. BOX 1470
BOULDER, CO 80302

DEPT. OF ATMOSPHERIC SCIENCES
ATTN: LIBRARIAN
COLORADO STATE UNIVERSITY
FORT COLLINS, CO 80521

CHAIRMAN
DEPT. OF METEOROLOGY
PENNSYLVANIA STATE UNIVERSITY
503 DEIKE BLDG.
UNIVERSITY PARK, PA 16802

CHAIRMAN
DEPARTMENT OF METEOROLOGY
MASSACHUSETTS INSTITUTE OF
TECHNOLOGY
CAMBRIDGE, MA 02139

ATMOSPHERIC SCIENCES DEPT.
UNIVERSITY OF CHICAGO
1100 E. 57TH STREET
CHICAGO, IL 60637

DIRECTOR
INSTITUTE OF GEOPHYSICS
UNIV. OF CALIFORNIA AT
LOS ANGELES
LOS ANGELES, CA 90024

ATMOSPHERIC SCIENCES DEPT.
UNIVERSITY OF WASHINGTON
SEATTLE, WA 98195

CHAIRMAN
DEPT. OF METEOROLOGY &
OCEANOGRAPHY
4072 EAST ENGINEERING BLDG.
THE UNIVERSITY OF MICHIGAN
ANN ARBOR, MI 48104

CHAIRMAN
DEPARTMENT OF METEOROLOGY
UNIVERSITY OF WISCONSIN
METEOROLOGY & SPACE SCIENCE BLDG.
1225 WEST DAYTON STREET
MADISON, WI 53706

DIRECTOR
REMOTE SENSING LAB
P.O. BOX 248003
UNIVERSITY OF MIAMI
CORAL GABLES, FL 33124

ATMOSPHERIC SCIENCES DEPT.
OREGON STATE UNIVERSITY
CORVALLIS, OR 97331

CHAIRMAN
INSTITUTE OF ATMOS. PHYSICS
UNIVERSITY OF ARIZONA
TUSCON, AZ 85721

DEPT. OF METEOROLOGY
TEXAS A&M UNIVERSITY
COLLEGE STATION, TX 77843

DEAN OF THE COLLEGE OF SCIENCE
DREXEL INSTITUTE OF TECHNOLOGY
PHILADELPHIA, PA 19104

CHAIRMAN
DEPT. OF METEOROLOGY
UNIVERSITY OF OKLAHOMA
NORMAN, OK 73069

CHAIRMAN
DEPT. OF METEOROLOGY &
PHYSICAL OCEANO.
COOK COLLEGE,
P.O. BOX 231
RUTGERS UNIVERSITY
NEW BRUNSWICK, NJ 08903

CHAIRMAN
DEPT. OF ATMOSPHERIC SCIENCE
UNIV. OF MISSOURI, COLUMBIA
701 HITT STREET
COLUMBIA, MO 65211

DIRECTOR OF RESEARCH
INSTITUTE FOR STORM RSCH.
UNIVERSITY OF ST. THOMAS
3812 MONTROSE BLVD.
HOUSTON, TX 77006

CHAIRMAN
DEPARTMENT OF METEOROLOGY
CALIFORNIA STATE UNIV.
SAN JOSE, CA 95192

DOCUMENTS/REPORTS SECTION
LIBRARY
SCRIPPS INSTITUTE OF
OCEANOGRAPHY
LA JOLLA, CA 92037

LIBRARY
ATMOS SCIENCES DEPT.
STATE UNIV. OF NEW YORK
1400 WASHINGTON AVE.
ALBANY, NY 12222

DIRECTOR
CENTER FOR MARINE STUDIES
SAN DIEGO STATE UNIVERSITY
SAN DIEGO, CA 92182

R.S.M.A.S. LIBRARY
UNIVERSITY OF MIAMI
4600 RICKENBACKER CAUSEWAY
VIRGINIA KEY
MIAMI, FL 33149

HEAD
DEPT. OF ENVIRONMENTAL SCI.
UNIV. OF VIRGINIA, CLARK HALL
ATTN: R. PIELKE
CHARLOTTESVILLE, VA 22903

CHAIRMAN
DEPT. OF ATMOSPHERIC SCI.
UNIVERSITY OF VIRGINIA
CLARK HALL
CHARLOTTESVILLE, VA 22903

DEPT. OF GEOGRAPHY
GUSTAVUS ADOLPHUS COLLEGE
ST. PETER, MN 56082

ATMOSPHERIC SCIENCES DEPT.
UCLA
405 HILGARD AVE.
LOS ANGELES, CA 90024

DEPT. OF ATMOS. SCI. LIBRARY
COLORADO STATE UNIVERSITY
FOOTHILLS CAMPUS
FT. COLLINS, CO 80523

DEPT. OF METEOROLOGY
UNIVERSITY OF MARYLAND
COLLEGE PARK, MD 20742

SAINT LOUIS UNIVERSITY
DEPT. OF EARTH & ATMOS SCI.
P.O. BOX 8099 - LACLEDE STATION
ST. LOUIS, MO 63156

METEOROLOGY DEPT.
EASTERN AIR LINES, INC.
MIAMI INTERNATIONAL AIRPORT
MIAMI, FL 33148

WALTER A. BOHAN CO.
2026 OAKTON STREET
PARK RIDGE, IL 60068

METEOROLOGY INTERNATIONAL
2600 GARDEN RD.
MONTEREY, CA 93940

LIBRARY
THE RAND CORPORATION
1700 MAIN STREET
SANTA MONICA, CA 90406

DEPT. OF GEOPHYSICS & ASTRONOMY
THE RAND CORPORATION
1700 MAIN STREET
SANTA MONICA, CA 90406

METEOROLOGY DEPT.
UNITED AIR LINES
P.O. BOX 66100
CHICAGO, IL 60666

MANAGER
METEOROLOGICAL SERVICES
PAN AMERICAN AIRWAYS, HANGAR 14
JFK INTERNATIONAL AIRPORT
JAMAICA, NY 11430

CONTROL DATA CORP.
METEOROLOGY DEPT., RSCH DIV.
2800 E. OLD SHAKOPEE RD.
BOX 1249
MINNEAPOLIS, MN 55440

AEROSPACE CORPORATION
ATTN: METEOROLOGY SECTION
P.O. BOX 92957
LOS ANGELES, CA 90009

LFE ENVIRON. ANALYSIS LABS
2030 WRIGHT AVE.
RICHMOND, CA 94804

PRESIDENT
GEOATMOSPHERICS CORP.
BOX 177
LINCOLN, MA 01773

LABORATORY OF CLIMATOLOGY
ROUTE 1
CENTERTON
ELMER, NJ 08318

DIRECTOR OF METEOROLOGY
TRANS WORLD AIRLINES
HANGAR 12 - ROOM 235
J.F. KENNEDY INTERNATIONAL AIRPORT
JAMAICA, NY 11430

SECTION MANAGER
LIBRARY
MCDONNELL-DOUGLAS CO.
P.O. BOX 516
ST. LOUIS, MO 63166

LIBRARY
GULF COAST RESEARCH LAB
OCEAN SPRINGS, MS 39564

SEA USE COUNCIL
1101 SEATTLE TOWER
SEATTLE, WA 98101

ENVIRONMENTAL RESEARCH & TECHNOLOGY, INC.
696 VIRGINIA ROAD
CONCORD, MA 01742

OCEAN DATA SYSTEMS INC.
2460 GARDEN ROAD
MONTEREY, CA 93940

LEE W. PARKER, INC.
252 LEXINGTON RD.
CONCORD, MA 01742

LAGUNA RESEARCH LABS
21421 STANS LANE
LAGUNA BEACH, CA 92651

NAUTILUS PRESS, INC.
1056 NATIONAL PRESS BLDG.
WASHINGTON, DC 20045

UNIVERSAL MARINE, INC.
8222 TRAVELAIR ST.
HOUSTON, TX 77061

ATMOSPHERIC SCIENCE CENTER
SRI INTERNATIONAL
333 RAVENSWOOD AVE.
MENLO PARK, CA 94025

THE EXECUTIVE DIRECTOR
AMERICAN METEOROLOGICAL SOCIETY
45 BEACON STREET
BOSTON, MA 02108

AMERICAN MET. SOCIETY
METEOROLOGICAL & GEOASTROPHYSICAL ABSTRACTS
P.O. BOX 1736
WASHINGTON, DC 20013

WORLD METEOROLOGICAL ORGANIZATION
ATS DIVISION
ATTN: N. SUZUKI
CH-1211, GENEVA 20
SWITZERLAND

SERVICIO METEOROLOGICO
DE LA ARMADA
EDIFICIO LIBERTAD, PISO 15
COMODORO PY Y CORBETA URUGUAY (1104)
BUENOS AIRES
REPUBLICA ARGENTINA

DIRECTOR GENERAL
SERVICIO METEOROLOGICO NACIONAL
25 DE MAYO 658
BUENOS AIRES, ARGENTINA

LIBRARY, CSIRO DIV.
ATMOSPHERIC PHYSICS
STATION STREET
ASPENDALE, 3195
VICTORIA, AUSTRALIA

LIBRARIAN
METEOROLOGY DEPT.
UNIVERSITY OF MELBOURNE
PARKVILLE, VICTORIA 3052
AUSTRALIA

BUREAU OF METEOROLOGY
ATTN: LIBRARY
BOX 1289K, GPO
MELBOURNE, VIC, 3001
AUSTRALIA

AUSTRALIAN NUMERICAL METEOROLOGY RESEARCH CENTER
ATTN: DR. R. L. HUGHES
P.O. BOX 5089A
MELBOURNE VICTORIA, 3001
AUSTRALIA

DEPT. OF GEOGRAPHY
JAMES COOK UNIVERSITY OF NORTH QUEENSLAND
TOWNSVILLE Q4811
AUSTRALIA

RAN RESEARCH LABORATORY
ATTN: DR. IAN S.F. JONES
P.O. BOX 706
DARLINGHURST NSW 2010
AUSTRALIA

CHAIRMAN
DEPT. OF METEOROLOGY
MCGILL UNIVERSITY
805 SHERBROOKE ST. W.
MONTREAL, QUEBEC
CANADA H3A2K6

LIBRARY
ATMOS. ENVIRONMENT SERVICE
4905 DUFFERIN STREET
DOWNSVIEW M3H 5T4, ONTARIO
CANADA

DIRECTOR OF METEOROLOGY & OCEANOGRAPHY
NATIONAL DEFENSE HDQ
OTTAWA, ONTARIO, K1A 0K2
CANADA

INSTITUTE OF OCEANOGRAPHY
UNIV. OF BRITISH COLUMBIA
VANCOUVER BC, CANADA V6T-1W5

METOC CENTRE
MARITIME FORCES PACIFIC HDQ
FORCES MAIL OFFICE
VICTORIA, BRITISH COLUMBIA
V0S-1B0 CANADA

DEFENCE RSCH ESTABLISHMENT PACIFIC
ATTN: DIRECTOR-GENERAL
FORCES MAIL OFFICE
VICTORIA, BRITISH COLUMBIA
V0X 1B0, CANADA

PACIFIC BIOLOGICAL STATION
LIBRARY, FISHERIES & OCEANS
NAMAIMO, BRITISH COLUMBIA
CANADA V9R 5K6

INSTITUTE OF OCEANOGRAPHY
ATTN: DIRECTOR
DALHOUISE UNIVERSITY
HALIFAX, NOVA SCOTIA, B3H-4J1
CANADA

INSTITUT FOR TEORETISK
METEOROLOGI
HARALDSGADE 6
DK-2200 KOBENHAVN N
DENMARK

INTERNATIONAL COUNCIL FOR
SEA EXPLORATION
ATTN: GENERAL SECRETARY
CHARLOTTENLUND SLOT
DK-2920 CHARLOTTENLUND
DENMARK

METEOROLOGICAL OFFICE LIBRARY
LONDON ROAD
BRACKNELL, BERKSHIRE
RG 12 2SZ
ENGLAND

LIBRARY
INSTITUTE OF OCEANOGRAPHIC"SCI.
ATTN: DIRECTOR
WORMLEY, GODALMING
SURRY GU8 5UB, ENGLAND

DEPT. OF METEOROLOGY
UNIVERSITY OF READING
2 EARLYGATE, WHITEKNIGHTS
READING RG6 2AU
ENGLAND

EUROPEAN CENTRE FOR MEDIUM
RANGE WEATHER FORECASTS
SHINFIELD PARK, READING
BERKSHIRE RG29AX, ENGLAND

LIBRARY
FINNISH METEOROLOGICAL
INSTITUTE, BOX 503
SF-00101 HELSINKI 10
FINLAND

METEOROLOGIE NATIONALE
SMM/DOCUMENTATION
2, AVENUE RAPP
75340 PARIS CEDEX 07
FRANCE

SERVICE HYDROGRAPHIQUE ET
OCEANOGRAPHIQUE DE LA MARINE
ESTABLISSEMENT PRINCIPAL
CENTRE DE DOCUMENTATION
RUE DU CHATELLIER, B.P. 426
29275 - BREST CEDEX
FRANCE

EUROPEAN SPACE AGENCY
METEOROLOGICAL PROGRAM DEPT.
TOULOUSE, FRANCE
ATTN: DR. J. P. ANTIKIDES

DIRECTION DE LA METEOROLOGIE
ATTN: J. DETTWILLER
77 RUE DE SEVRES
92106 BOULOGNE-BILLANCOURT CEDEX
FRANCE

INSTITUT FUR MEERESKUNDE DER
UNIVERSITAT HAMBURG
ATTN: DIRECTOR
HEIMHUDERSTRASSE 71
2000 HAMBURG 13
FEDERAL REPUBLIC OF GERMANY

HEAD
DATA PROCESSING SECTION
GERMAN MILITARY GEOPHYSICAL OFFICE
MONT ROYAL, D-5580
TRABEAU-TRARBACH
FEDERAL REPUBLIC OF GERMANY

DEUTSCHER HYDROGRAPHISCHES INSTITUT
ATTN: DIRECTOR
TAUSCHSTELLE
POSTFACH 220
02000 HAMBURG 4
FEDERAL REPUBLIC OF GERMANY

EUROPEAN SPACE AGENCY
EUROPEAN SPACE OPERATIONS CEN.
ATTN: DR. JOHN MORGAN
DARMSTADT
FEDERAL REPUBLIC OF GERMANY

MAX PLANCK INSTITUT FUR CHEMIE
ATTN: DR. R. JAENICKE
POSTFACH 3060
D-65 MAINZ
SAARSTR 23
WEST GERMANY

CHIEF HYDROMETEOROLOGICAL OFFICER
HYDROMETEOROLOGICAL DIV.
MINISTRY OF WORKS & COMMUNICATIONS
P.O. BOX 26
GEORGETOWN, GUYANA
SOUTH AMERICA

DIRECTOR
ROYAL OBSERVATORY
NATHAN ROAD, KOWLOON
HONG KONG, B.C.C.

THE DIRECTOR
INDIAN INSTITUTE OF TROPICAL
METEOROLOGY
RAMDURG HOUSE
PUNE 411-005
INDIA

DEPT. OF METEOROLOGY
ANDHRA UNIVERSITY
WALTAIR, INDIA 530-003

DIRECTOR
METEOROLOGICAL & GEOPHY. SERV.
C/O DJALAN ARIEF RACHMAN HAKIM 3
DJAKARTA, INDONESIA

LIBRARY
IRISH METEOROLOGICAL SERVICE
GLASNEVIN HILL
DUBLIN 9, IRELAND

DIRECTOR
ISRAEL METEOROLOGICAL SERVICE
P.O. BOX 25
BET DAGEN 50200, ISRAEL

CONSIGLIO NAZIONALE DELLE RICERCHE
ISTITUTO TALASSOGRAFICO DI TRIESTE
VIALE R. GESSI 2 - 34123 TRIESTE
ITALY

ISTITUTO UNIVERSITARIO NAVALE
FACOLTA DI SCIENZE NAUTICHE
ISTITUTO DI METEOROLOGIA E
OCEANOGRAFIA
80133 NAPOLI - VIA AMM
ACTON, 38 ITALY

OCEAN RESEARCH INSTITUTE LIBRARY
UNIVERSITY OF TOKYO
15-1, 1-CHOME
MINAMIDAI, NAKANO-KU
TOKYO, JAPAN

MARITIME METEOROLOGY DIVISION
JAPAN METEOROLOGICAL AGENCY
OTE-MACHI 1-3-4 CHIYODA-KU
TOKYO, JAPAN

JAPAN METEOROLOGICAL AGENCY
3-4, OTEMACHI 1-CHOME, CHIYODA-KU
TOKYO 100, JAPAN

METEOROLOGICAL INSTITUTE
FACULTY OF SCIENCE
KYOTO UNIVERSITY
ATTN: DR. R. YAMAMOTO
SAKYO, KYOTO 606
JAPAN

DIRECTOR GENERAL
MALAYSIAN METEOROLOGICAL SERV.
JALAN SULTAN
PETALING JAYA
SELANGOR, WEST MALAYSIA

INSTITUTO DE GEOFISICA
U.N.A.M. BIBLIOTECA
TORRE DE CIENCIAS, 3ER PISO
CIUDAD UNIVERSITARIA
MEXICO 20, D.F.

KONINKLIJK NEDERLANDS
METEOROLOGISCH INSTITUUT
POSTBUS 201
3730 AE DEBILT, NETHERLANDS

PHYSICS LAB OF THE NATIONAL
DEFENCE RSCH ORGANIZATION TNO
P.O. BOX 96864
2509 JG
THE HAGUE, NETHERLANDS

BUREAU HYDROGRAFIE DER
KONINKLIJKE MARINE
AFD MILOC/METEO
BADHUISWEG 171
DEN HAAG, NETHERLANDS

THE LIBRARIAN
NEW ZEALAND OCEANOGRAPHIC
INSTITUTE
P.O. BOX 12-346
WELLINGTON NORTH, NEW ZEALAND

DEPT. OF METEOROLOGY
COLLEGE OF ARTS & SCIENCES
UNIV. OF THE PHILIPPINES
DILMAN, QUEZON CITY 3004
PHILIPPINES

THE LIBRARIAN
PHILIPPINE ATMOSPHERIC
GEOPHYSICAL & ASTRONOMICAL
SERVS. ADMIN (PAGASA)
1424 QUEZON AVE.
QUEZON CITY, PHILIPPINES

DIRECTOR
TYPHOON MODERATION RSCH &
DEVELOPMENT OFFICE PAGASA
MINISTRY OF NATIONAL DEFENSE
1424 QUEZON ave.
QUEZON CITY, PHILIPPINES

NATIONAL RESEARCH INSTITUTE
FOR OCEANOLOGY
COUNCIL FOR SCIENTIFIC &
INDUSTRIAL RESEARCH
P.O. BOX 17001
CONGELLA, 4013,
SOUTH AFRICA

INSTITUTE OF OCEANOGRAPHY
UNIVERSITY OF CAPE TOWN
RONDEBOSCH
CAPE TOWN, SOUTH AFRICA

INSTITUTE FOR MARITIME TECH
P.O. BOX 181
SIMONSTOWN, 7995
REPUBLIC OF AFRICA

LIBRARY
UNIV. OF STOCKHOLM
DEPT. OF METEOROLOGY
ARRHENIUS LABORATORY
S-106 91 STOCKHOLM, SWEDEN

DIRECTOR
SWEDISH METEOROLOGICAL &
HYDROLOGICAL INSTITUTE
P.O. BOX 923
S-601, 19 NORRKOPING
SWEDEN

CHIEF
ATMOSPHERIC SCIENCES DIV.
WORLD METEOROLOGICAL ORG.
P.O. BOX 5
GENEVA 20
SWITZERLAND